Lyza, A. W., R. Castro, E. Lenning, M. T. Friedlein, B. S. Borchardt, A. W. Clayton, and K. R. Knupp, 2019: Multi-platform reanalysis of the Kankakee Valley tornado cluster on 30 June 2014. *Electronic J. Severe Storms Meteor.*, **14** (3), 1–64.

Electronic Journal of
SEVERE STORMS METEOROLOGY

A Multi-Platform Reanalysis of the Kankakee Valley Tornado Cluster on 30 June 2014

ANTHONY W. LYZA[1], RICHARD CASTRO[2], ERIC LENNING[2], MATTHEW T. FRIEDLEIN[2], BRETT S. BORCHARDT[3], ADAM W. CLAYTON[1], AND KEVIN R. KNUPP[1]

[1]*Department of Atmospheric Science, Severe Weather Institute–Radar and Lightning Laboratories, University of Alabama in Huntsville, Huntsville, Alabama*

[2]*NOAA/National Weather Service, Romeoville, Illinois*

[3]*NOAA/National Weather Service, Grand Rapids, Michigan*

(Submitted 19 July 2018; in final form 21 August 2019)

ABSTRACT

Two derecho-producing quasi-linear convective systems moved across northeast Illinois and northwest Indiana on the evening of 30 June 2014. Both produced damage across a large area, including a concentrated cluster in the Kankakee River Valley associated with two long-lived and adjacent mesovortices in the second derecho. Post-event surveys of this region revealed a widespread, complex damage pattern and initially documented 14 tornadoes of EF1 rating on the Enhanced Fujita (EF) Scale, along with a swath of damaging nontornadic winds. Later, a number of uncertainties from the original surveys were examined in conjunction with high-resolution satellite imagery not available immediately after the event. Inconsistencies noted during this process led to an intensive reanalysis of the entire cluster using radar data, the original ground and aerial surveys, and the newly available satellite imagery. This new analysis concluded that at least 18 tornadoes impacted the Kankakee Valley, most with a path orientation different from the initial results. This paper details the reassessment process from initial motivation to final results, addresses potential sources of error, and discusses operational considerations stemming from such a prolifically tornadic event.

1. Introduction

Organized mesoscale convective systems (MCSs), including derecho-producing quasi-linear convective systems (QLCSs; Johns and Hirt 1987, Corfidi et al. 2016), are common during the summer months across the Midwestern United States (Smith et al. 2013). Guastini and Bosart (2016) identified southern Minnesota to the upper Ohio River Valley as the most climatologically favored region for progressive derecho events, with an absolute maximum across northern Illinois and northwest Indiana. This generally coincides with previous literature on derecho climatology (Johns and Hirt 1987; Coniglio and Stensrud 2004). Smith et al. (2012) also found the midwestern United States to be a common location for tornadoes associated with QLCSs, with most assigned EF0–EF1 rating on the Enhanced Fujita scale (WSEC 2006), but about 11% reaching EF2 rating or higher.

The most common sources of damage in an MCS are from bow echoes associated with descending rear-inflow jets (RIJs; Smull and Houze 1987; Weisman 1992, 1993; Przybylinski 1995) and from mesovortices (Trapp and Weisman 2003; Weisman and Trapp 2003; Wakimoto et al. 2006a,b; Atkins et al. 2004; Atkins et al. 2005; Wheatley et al. 2006; Atkins and St. Laurent 2009a,b; Lyza et al. 2017).

Corresponding author address: Anthony W. Lyza, Department of Atmospheric Science, University of Alabama in Huntsville, 4801 Bradford Dr., Huntsville, AL, 35805
Email: lyzaa@nsstc.uah.edu

RIJs are generally associated with damage that is nontornadic, though QLCSs (e.g., Trapp et al. 2005) and radar-observed mesovortices (e.g., Smith et al. 2012) can lead to both tornadic and nontornadic damage (e.g., Wakimoto et al. 2006a). In fact, the worst nontornadic damage found with QLCSs is frequently associated with mesovortices. This is particularly true when effects of the pressure-gradient force in a mesovortex are superimposed upon the momentum provided by the descending RIJ (Atkins and St. Laurent 2009a, Wakimoto et al. 2006b). This phenomenon typically occurs along the southern edge of a mesovortex. Damage from both tornadoes and nontornadic winds in an MCS, therefore, can be of similar magnitude and in close proximity to each other (e.g., Forbes and Wakimoto 1983). In some cases, multiple processes may be responsible for the damage at a given location. This poses considerable challenges to damage assessment efforts.

Given these challenges, ground-based surveys alone may be insufficient for deciphering the potentially complex origins of a damaging mesoscale convective system (MCS). In such cases, valuable information can be gleaned through manned and unmanned aerial surveys (Skow and Cogil 2017) as well as from high-resolution satellite imagery (Yuan et al. 2002, Jedlovec et al. 2006, Brown et al. 2012, Molthan et al. 2014, Lyza et al. 2016, Burow et al. 2017, Kingfield and de Beurs 2017). Additional context also can be obtained by close examination of radar data, including:

- Mid-altitude radial convergence (MARC) signatures (Eilts et al. 1996);
- Tornado vortex signatures (TVS; Brown et al. 1978);
- Polarimetric tornado debris signatures (TDS; Ryzhkov et al. 2005; Schultz et al. 2012a,b);
- Less formal debris "plumes," or radar signatures likely associated with debris that do not meet stringent TDS criteria (e.g., Clayton et al. 2016, Skow and Cogil 2017); and
- Enhanced spectrum width (σ_V) signatures (Spoden et al. 2012).

If no one source of information provides definitive evidence of how damage occurred at a location, information from multiple sources may provide the preponderance of evidence necessary to make a reasonable determination.

A particularly damaging pair of derecho-producing QLCSs occurred across the Midwestern United States on 30 June–1 July 2014. The first QLCS was responsible for 11 tornadoes across central and eastern Iowa, with wind damage extending from eastern Nebraska to the southern end of Lake Michigan. The second QLCS followed the first by only about 3 h, and ≈250 km. Initial documentation indicated that this second QLCS, despite moving largely over the remnant stable cold pool from the first QLCS, produced 29 tornadoes and widespread wind damage across northern Illinois and northern Indiana (NCEI 2018).

Given the scope of the event and the challenges previously discussed, there were concerns that not all tornado paths were identified or correctly documented. The paths submitted to *Storm Data* provided a reasonable summary of the information available at the time of publication, though several questions still had not been resolved. Later, after high resolution satellite imagery in Google Earth became available, a new examination revealed inconsistencies and even potential inaccuracies in some tornado tracks, especially those in the Kankakee River Valley where the most substantial damage occurred.

Lyza et al. (2017) provide an overview of the meteorological setup and evolution of the two QLCSs, as well as a detailed analysis of 38 mesovortices responsible for much of the tornado and wind damage from the second QLCS. The Kankakee River Valley region was associated with subvortices[1] G-1 and G-2 of mesovortex "G" as described in Lyza et al. (2017; Fig. 1). Of the 29 tornadoes initially listed in *Storm Data* from the second QLCS, 14 were documented in this region. Eight were associated with G-1 and six were associated with G-2. Additionally, a widespread swath of nontornadic wind damage was analyzed along the southern periphery of G-1.

This study reanalyzes the widespread damage in the Kankakee Valley associated with G-1 and G-2 in the second 30 June–1 July 2014 QLCS. It first reviews the initial survey results and explains the inconsistencies and inaccuracies that motivated this reanalysis effort. It then presents a new summary of the Kankakee Valley tornado cluster based on an integration of the original ground and aerial surveys,

[1] In Lyza et al. (2017), these features are referenced as "subvortices" to emphasize their evolution from mesovortex "G". From henceforth in this manuscript, they are referenced as "mesovortices" to match the most common nomenclature applied to these phenomena.

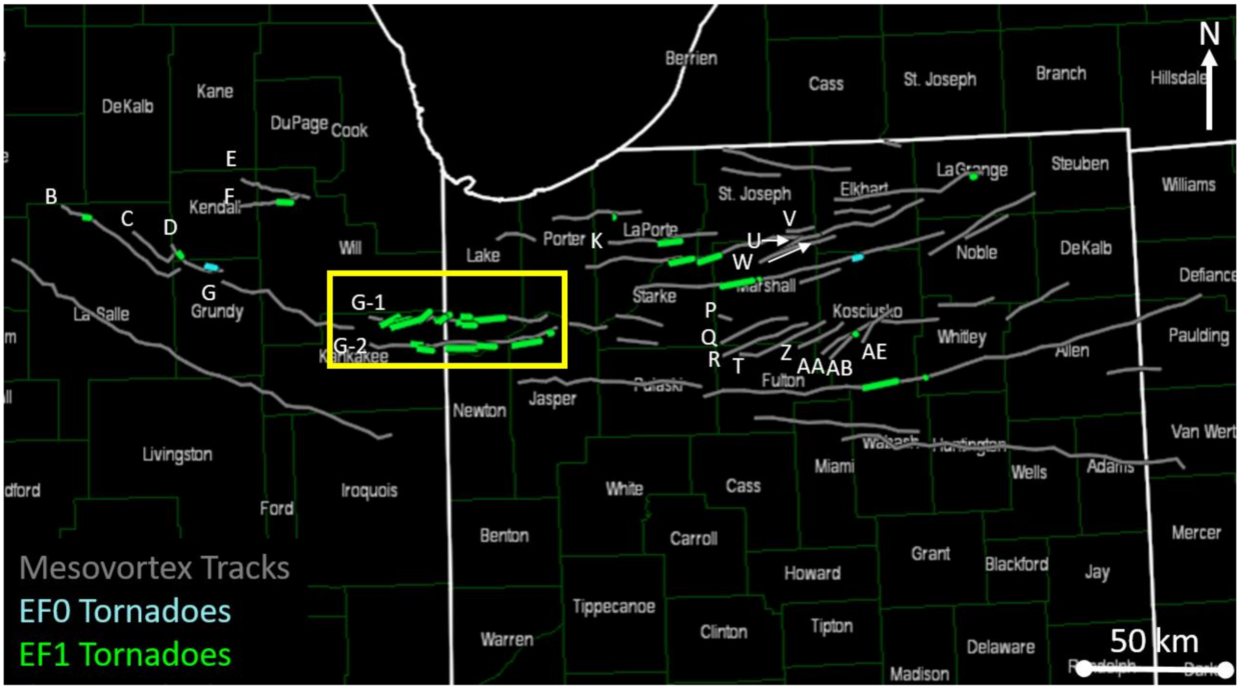

Figure 1: Overview of all mesovortices and official *Storm Data* tornado tracks associated with the second QLCS on 30 June–1 July 2014. The location of mesovortices G-1 and G-2 is highlighted by the yellow box. Adapted from Fig. 2 of Lyza et al. (2017). *Click image to enlarge.*

radar data, and the newly available satellite imagery. Continued sources of uncertainty also are addressed. Finally, it discusses how these findings may impact operational forecasting, warning, and surveying of QLCS tornado events.

2. Mesoscale overview

Lyza et al. (2017) describes the synoptic-scale and broader mesoscale setup for the two severe QLCS events, which impacted the Midwest on 30 June–1 July 2014 (Fig. 2). The initial QLCS developed from a cluster of high-precipitation supercells over Nebraska and Iowa before moving into Illinois and Wisconsin. As this slowly decayed across northern Indiana and southern Lower Michigan, a sharp west-to-east thermal boundary remained over the region (Fig. 3), delineating the cold pool air from the first QLCS to the north and the warm sector airmass to the south. Two to three hours later, several new bands of convection consolidated into a second QLCS across Iowa, organizing and intensifying further upon crossing into northern Illinois. At the same time, the remnant thermal boundary began moving northward as an effective warm front. The Kankakee Valley tornado cluster would arise from a pair of mesovortices along the leading edge of the second QLCS near its intersection with the thermal boundary. The boundary, in combination with the moderate convective instability and strong low-level wind shear described in Lyza et al. (2017), led to an environment conducive to tornadoes and damaging nontornadic wind gusts.

3. Motivation for reanalyzing the official *Storm Data* summary of the Kankakee Valley tornado cluster

a. Overview of original survey activities and the official Storm Data *summary*

The initial ground survey for the second QLCS was coordinated by the Chicago National Weather Service (NWS) office on 1 July 2014, the morning after the event. Although no tornadoes had been reported explicitly, radar signatures and damage reports during the event had prompted NWS Chicago to issue multiple tornado warnings. It therefore was necessary to determine whether any of the damage might have been tornadic.

The survey team for the Kankakee Valley, consisting of the lead and second authors of this study (Lyza and Castro), examined portions of the damage from G-1 and G-2 and quickly determined that at least some likely was tornadic. This was inferred from the convergent, cyclonic nature of tree falls and debris transport at the various damage locations.

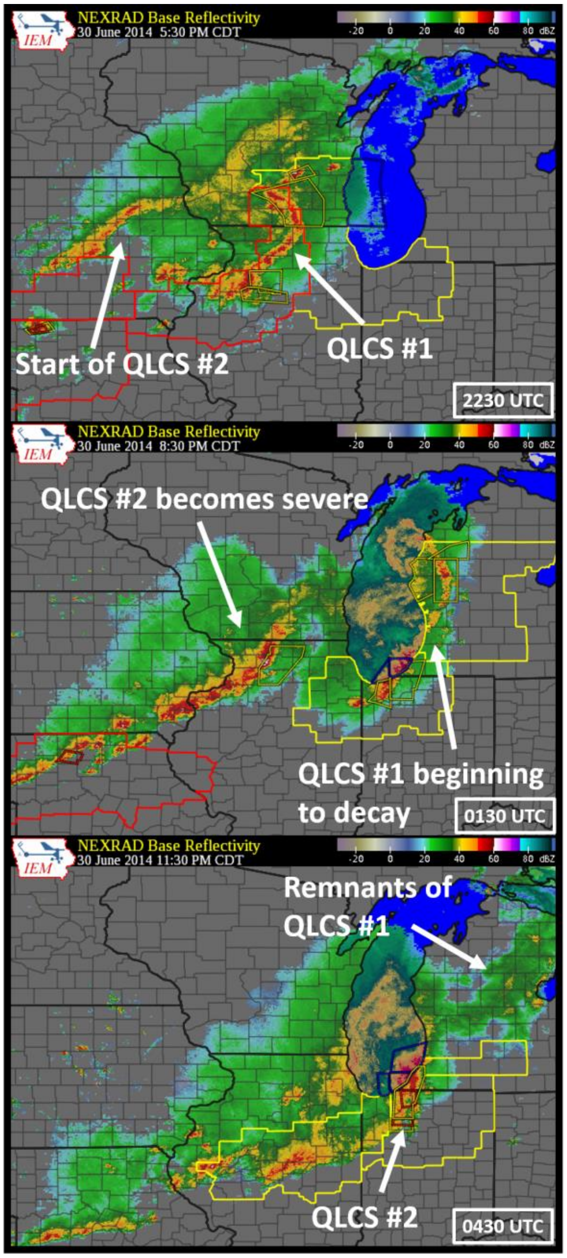

Figure 2: Figure 1 of Lyza et al. (2017), highlighting the evolution of the two QLCSs from 30 June–1 July 2014 across the Midwest. *Click image to enlarge.*

Additionally, given the spatial distribution of damage, including properties with considerable damage immediately adjacent to properties with none, the team concluded that multiple tornadoes likely were responsible. Several eyewitnesses who were present at suspected tornado locations also reported a short period of extreme winds and/or a palpable pressure change, including the popping of ears as damage was occurring.

An aerial survey was conducted by the third author (Lenning) on 8 July 2014 over portions of the Kankakee Valley, but this was limited to areas documented during the first ground survey. To gain a better understanding of the damage in areas not reached in the first two surveys, a second ground survey was conducted by the lead author (Lyza) on 23 July 2014. This uncovered additional areas of damage very similar to that seen during the initial survey, with narrow, convergent swaths. These results prompted a deliberative process to determine how to classify the aggregate total of damage areas.

Even after the second survey, it was not clear which areas of damage were linked together. The answer depended in large part on how the individual tornadoes were likely behaving within the broader parent mesovortices. Past QLCS tornado cluster cases provided conceptual models for how the tornadoes in G-1 and G-2 may have behaved. An event near Radom, IL, from 30 May 2004 seemed to offer a reasonable, though not perfect, model for the evolution of some of the tornadoes in the Kankakee Valley (NWS St. Louis 2018), particularly for the tornadoes associated with G-1. Tornadoes in that event evolved in a "cyclic" process, akin to the generation of tornado families (e.g., Agee et al. 1976) within a cyclic supercell thunderstorm (e.g., Lemon and Doswell 1979).

Application of the Radom conceptual model to the damage observed from G-1 led to the initial classification of eight tornadoes from this mesovortex. Analysis of damage associated with G-2 in slightly more populated and wooded areas closer to the Kankakee River revealed six more tornadoes. Together this brought the total for the Kankakee Valley to fourteen tornadoes in the June 2014 edition of *Storm Data*, completed at the end of August 2014. All were rated EF1, though evidence suggested some were at the threshold of EF2 rating. Additionally, the analysis identified a swath of widespread wind damage along the southern periphery of G-1 in northwest Indiana. This was attributed to the likely superpositioning of the southern edge of G-1 with a descending RIJ (Fig. 4).

b. Inconsistencies and inaccuracies in the original survey results

Despite the deliberative process of developing the official *Storm Data* entries for the Kankakee Valley damage, issues remained unresolved after submission of the initial results. At the time, each issue alone

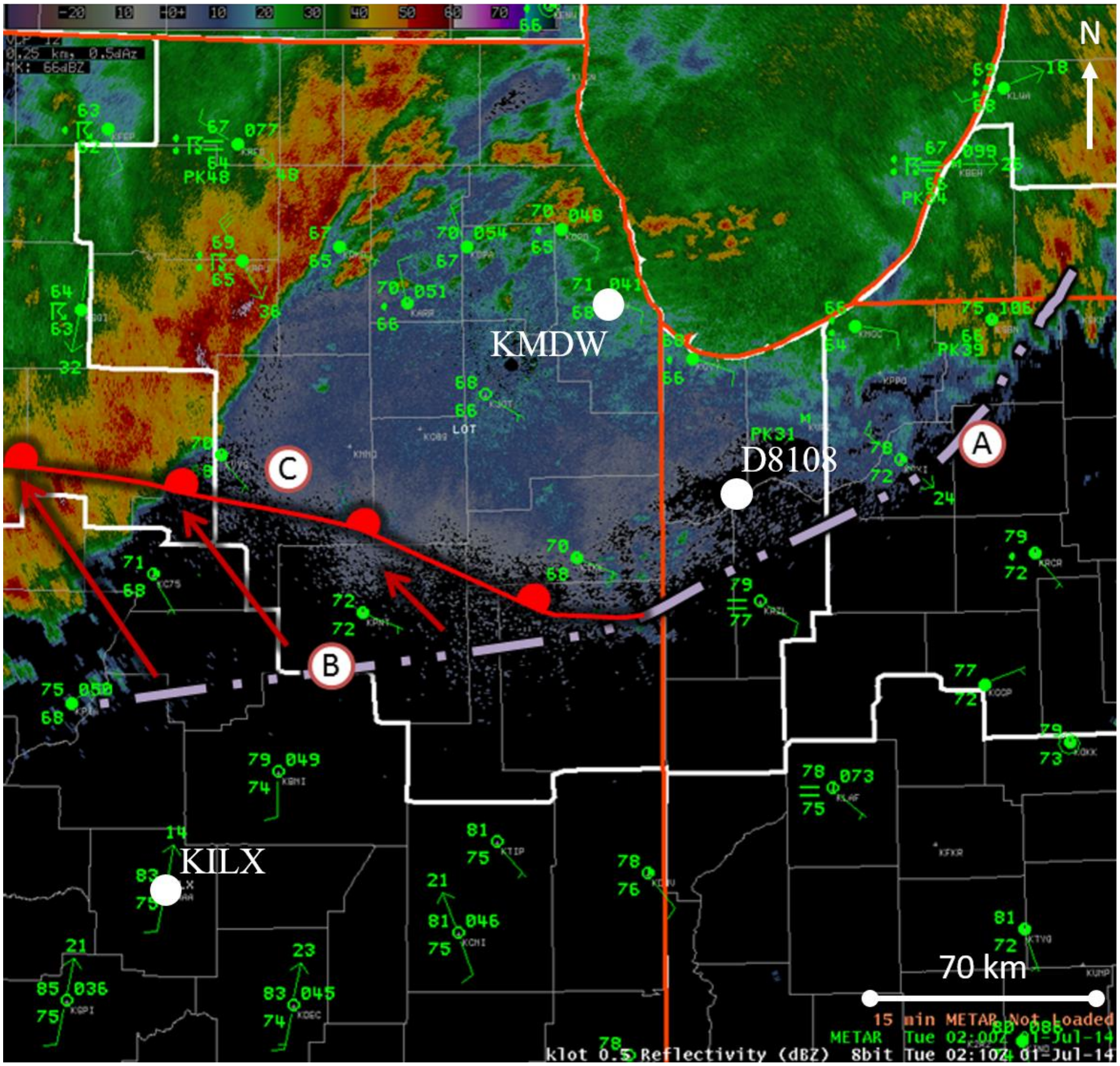

Figure 3: Overview of the progression of the thermal boundary associated with the first QLCS on 30 June 2014. The boundary settled as far south as the axis from point A to point B. The western end of the boundary began to return north first, reaching point C by 0200 UTC 1 July. The eastern end of the boundary would return northward to near D8108 by 0345 UTC. The locations of KMDW, KILX, and D8108 are shown. Figure adapted from Fig. 6 of Lyza et al. (2017). *Click image to enlarge.*

was not enough to warrant a different interpretation of the initial survey data. However, when considered as a whole, and especially when examined together with high- resolution satellite data, these unresolved issues eventually prompted a full reanalysis of the original survey results. It therefore is valuable to explore each of these issues in turn.

One of the first things noticed in the initial survey results was how the motion assigned to tornadoes associated with G-1 and G-2 differed substantially from the tornadoes upstream of this cluster. This was attributed to effects of G-1 and G-2 moving along the remnant thermal boundary discussed in Lyza et al. (2017). Individual tornadoes appeared to move eastward with these parent mesovortices while

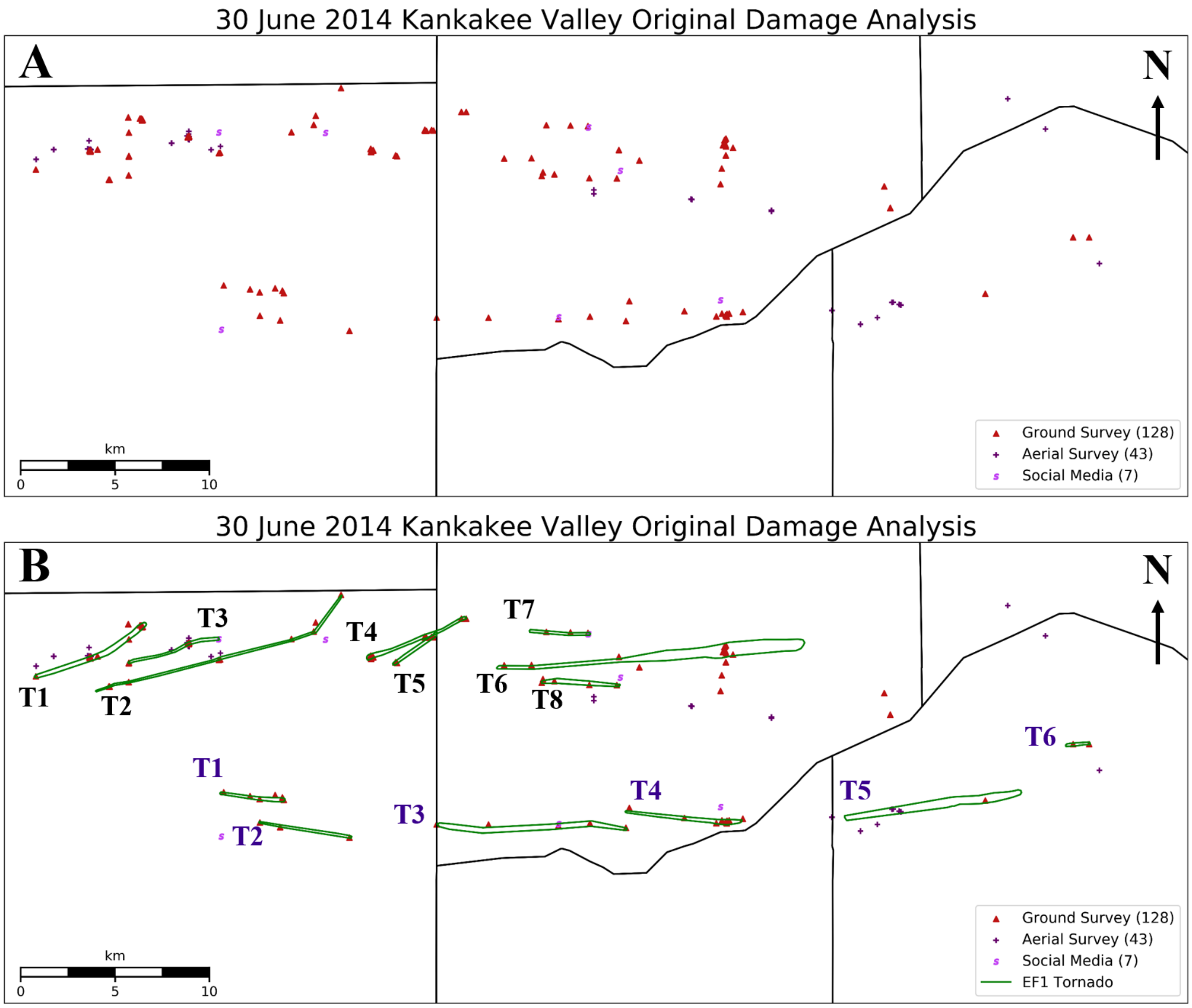

Figure 4: a) Overview map of the information points gathered from ground and aerial surveys, as well as from social media, in the wake of the 30 June 2014 Kankakee Valley tornado cluster. b) The official tornado tracks assessed for *Storm Data* in the Kankakee Valley overlaid the damage survey information points available at the time of *Storm Data* publication. The responsible mesovortex is denoted by color (black = G-1, navy = G-2), and the chronological order of occurrence is given by the number (T1 = tornado 1). *Click image to enlarge.*

cycling to the storm-relative left (north) within these mesovortices. In contrast to this east-northeast direction, the upstream tornadoes in northern Illinois moved toward the southeast or east-southeast. However, several downstream tracks in Indiana clearly exhibited motion toward the east or east-northeast. This supported the plausibility of the original track classifications but did not provide a definitive answer for path orientation in the Kankakee Valley.

Additional unresolved issues in the official results arose from multiple small-scale inconsistencies observed in the ground survey. These observations included:

- The first tornado attributed to G-1 damaging a farmstead northwest of Grant Park, IL, yet not damaging power lines or poles immediately east-northeast of the farmstead, "down-track" along the official path (Fig. 5);
- A snapped power pole northwest of the first G-1 tornado track that was left undocumented as tornadic damage, despite the nature of the damage suggesting a likely tornadic cause (Fig. 5);

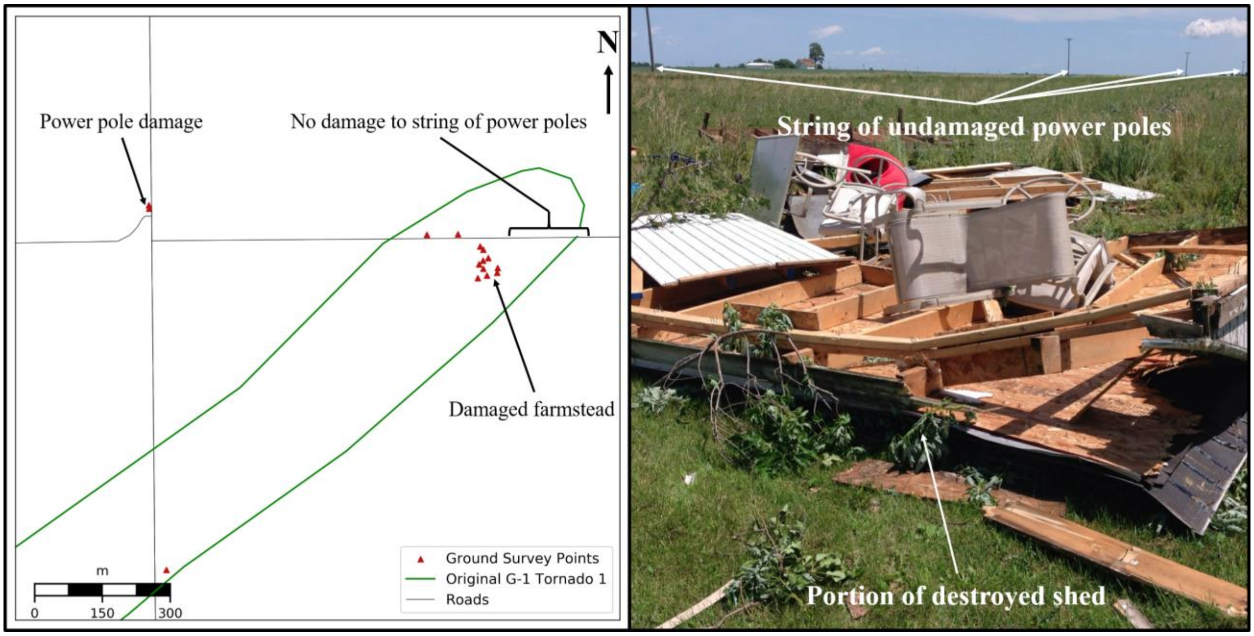

Figure 5: Left: Map illustrating inconsistencies in the first tornado associated with mesovortex G-1 from the original survey. This includes a lack of power line or pole damage immediately downstream of a farmstead that sustained EF1 damage and a snapped power pole northwest of the official track. Right: Picture looking northeast from farmstead, with portions of a destroyed shed in the foreground and undamaged power poles in the background. (Note: In the eventual reanalysis this damage is attributed to tornado 3 in Table 3.) *Click image to enlarge.*

- Intense tree damage at a farmstead along the third official track attributed to G-1 (including numerous snappings and uprootings as well as the destruction of a barn with most of the debris blown to the southeast). A barn directly across the street suffered no apparent damage despite being due east of the destroyed barn and within the official tornado track; and
- A 500-yd (457-m)-wide swath of damage farther east, near the end of the tornado swarm attributed to G-1, being attributed to a single tornado, with the aforementioned widespread wind damage identified as having begun immediately to its south. However, within the swath classified as tornado damage, a clear break in damage was noted, with no crop or other damage (Fig. 6).

Another potential issue with the official summary in *Storm Data* arose later during an examination by the sixth author of debris signatures in the second QLCS (Clayton et al. 2016). That study noted the eastward movement of a debris plume associated with one of the stronger damage tracks northwest of Grant Park, IL. Previous studies have examined the location and movement of debris signatures (Speheger and Smith 2006, Van Den Broeke 2015) or debris plumes (Skow and Cogil 2017) relative to damage points on the ground. While there is not always a clear relationship, especially at increasing distance from the radar, fallout often is favored to occur either in the storm-relative downwind direction of where debris originated (in the case of dispersion around the tornado vortex), or on the northwestern flank of the parent storm. Given the official tornado movement toward the east-northeast, the plume in this case would have been located southeast of the track (Fig. 7). This alone would not mean the original tornado path was incorrect, especially since other mechanisms also could be responsible for the behavior of the debris signature. However, it raised uncertainty about the accuracy of the original analysis.

A final and ultimately key piece of evidence suggesting that the initial analysis of the Kankakee Valley tornadoes was incorrect came from satellite imagery, time-stamped 30 May 2015 and made available in Google Earth. Although satellite imagery must be used with caution for damage-survey purposes, as explained in section 6, this imagery depicted a probable tornado track northeast of Grant Park, IL, oriented east-southeasterly (Fig. 8). After this feature was discovered, further examination revealed additional paths of possible tornado damage across the Kankakee Valley. Much of this damage also was logged during the ground

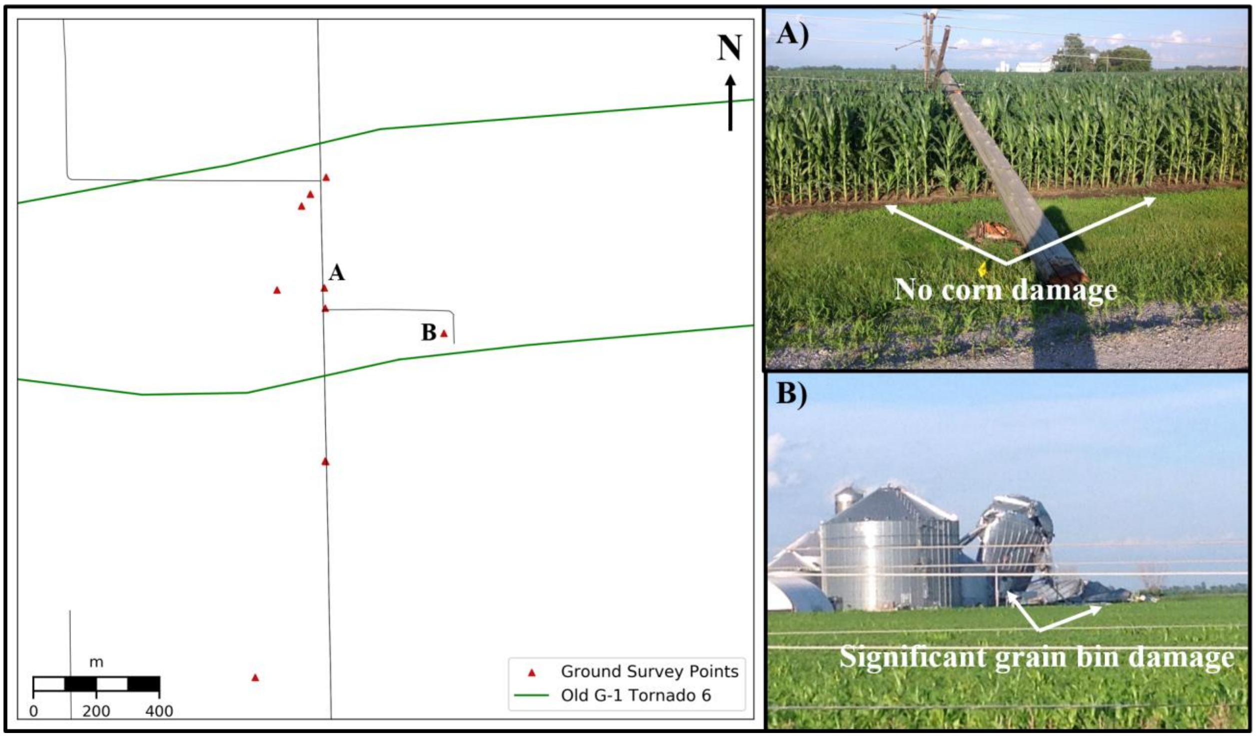

Figure 6: Map showing a portion of the original sixth tornado track associated with mesovortex G-1. The photos correspond to locations A and B on the map, with both looking east-southeast. Note the corn at location A is undisturbed, while the grain bins at location B are severely damaged. This disparity in damage suggests the power pole snapped at point A due to forces exerted on poles elsewhere along the highway. Additional damage occurred at the intersection north of location A (see Fig. A9). (Note: In the reanalysis, this damage is attributed to tornadoes 13 and 14 in Table 3.) *Click image to enlarge.*

surveys, though some was not visible from the available road network, some was missed by the survey teams, and some was logged but mischaracterized in the initial analysis.

Again, each of these issues alone was not enough to warrant a different interpretation of the initial survey data. Some of this information was not even available when the official *Storm Data* results were published. However, considered as a whole, the previously described inconsistencies, along with the newly available satellite evidence, motivated a full reanalysis. The remaining discussion describes the methodology and results of this new analysis.

4. Reanalysis data and methodology

This reanalysis incorporates radar data, the newly available satellite imagery, and the original ground and aerial surveys. The ground surveys were conducted on 1 July and 23 July and an aerial survey took place on 8 July. Data from all three surveys were placed into Google Earth to aid in compositing of information.

As previously mentioned, satellite imagery within Google Earth itself revealed additional damage not cataloged during the initial surveys. The latest pre-event imagery was dated 25 September 2013 and the earliest post-event imagery was dated 30 May 2015. Google Earth did not provide specific information on the image resolution, but consultation with a satellite expert indicated it to be at least 3 m, and potentially 1 m or better (J. Bell, personal comm.).

As with data from ground and aerial surveys, locations of apparent or potential damage seen on satellite imagery were annotated in the Google Earth program. Areas lacking damage within the paths of mesovortices G-1 and G-2 also were noted. Section 6 discusses the various uncertainties when using satellite imagery for damage analysis, including the potential that a different severe weather event might have produced the damage.

An overarching potential error in this analysis lies in the determination of tornadic and nontornadic damage at lower EF-scale values. This uncertainty is

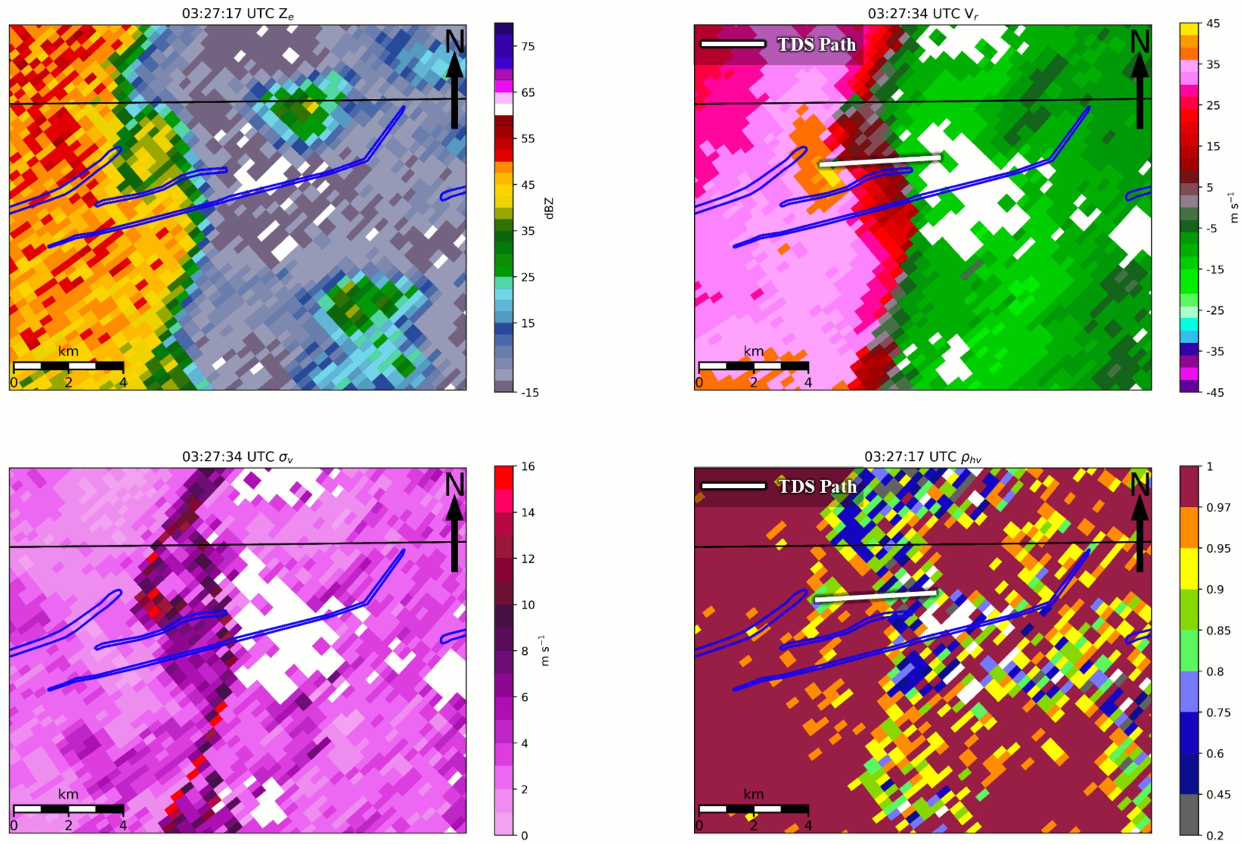

Figure 7: Four-panel 0.5° plan position indicators (PPIs) of equivalent reflectivity factor (Z_e; upper-left), base velocity (V_r; upper right), spectrum width (σ_v; lower left), and correlation coefficient (ρ_{hv}; lower right) from the Chicago/Romeoville (KLOT) WSR-88D at 0327 and 0330 UTC 1 July 2014, highlighting the disparity between the first official tornado track of G-1 (T1) and the evolution of the tornado debris signature (TDS). Blue polygons indicate tornado paths as entered into *Storm Data*, equivalent to those given in Fig. 4. *Click image to enlarge and animate.*

expressed at length in Forbes and Wakimoto (1983). Much of the uncertainty arises from the loss of clear signatures of circulation in weak tornadic vortices with fast translation. The high translational speed can offset the wind speed on the storm-relative left side of the vortex and add to the wind speed on the right side, ultimately causing all the damage to be oriented in roughly the same direction.

In determining whether location damage was tornadic, we assessed: 1) whether damage was cyclonic or convergent in nature; 2) sharpness of the damage gradient; and 3) whether the path exhibited a high length-to-width aspect ratio (Knupp 2000). Items (2) and (3) were not always simple to assess in either the damage surveys or in satellite imagery due to the presence of barren fields, soybean fields (which are more resistant to damage at weaker wind speeds than corn or trees), and, in the case of ground survey information, accessibility via road.

Analysis of data from the Chicago-Romeoville (KLOT) WSR-88D supported additional refinement of damage causality and track information. In areas where ground survey, aerial survey, and/or satellite analysis suggested damage likely was tornadic, a desire to avoid mislabeling it as such prompted examination of additional evidence. This included velocity couplets, spectrum width (σ_v) maxima, and polarimetric indications of debris.

Due to the complicated nature of the velocity signatures, identification of enhanced shear zones and velocity couplets initially was qualitative, focusing on azimuthally adjacent maxima and minima in Doppler velocity values (Fig. 9a). Later, a more formal quantitative approach was developed to analyze wind shear signatures embedded within mesovortices thought to be associated with tornadoes produced by G-1 and G-2. This approach includes the following steps:

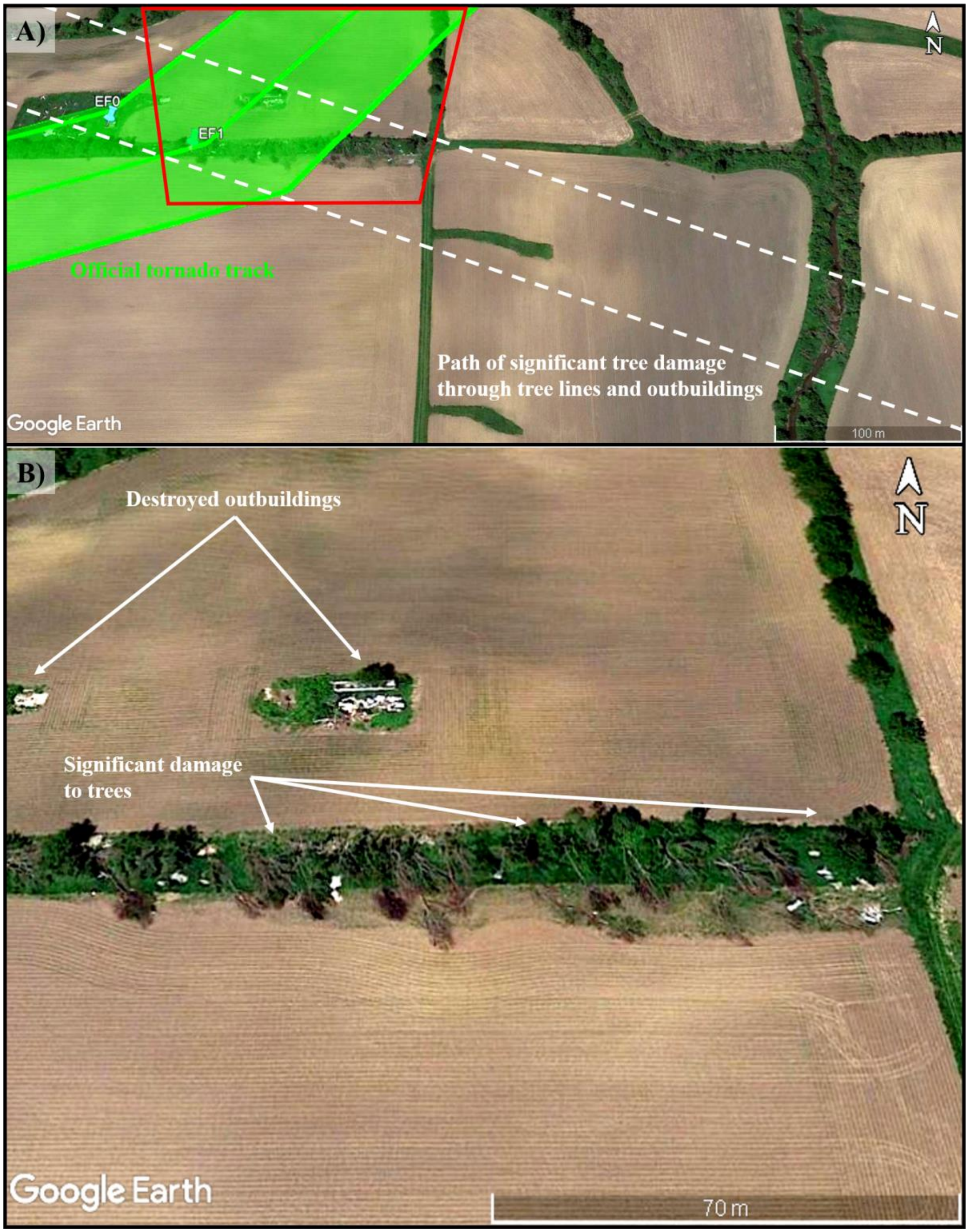

Figure 8: a) Map showing the official third tornado track of G-1 (green) overlaid on Google Earth satellite imagery that depicts a clear track of damage oriented in a different direction (white), and b) a zoomed view of Google Earth satellite imagery of tree and outbuilding damage within the area covered by the red box in (a). Note that the trapezoidal shape of the red box is due to a change in viewing angle between (a) and (b). *Click image to enlarge.*

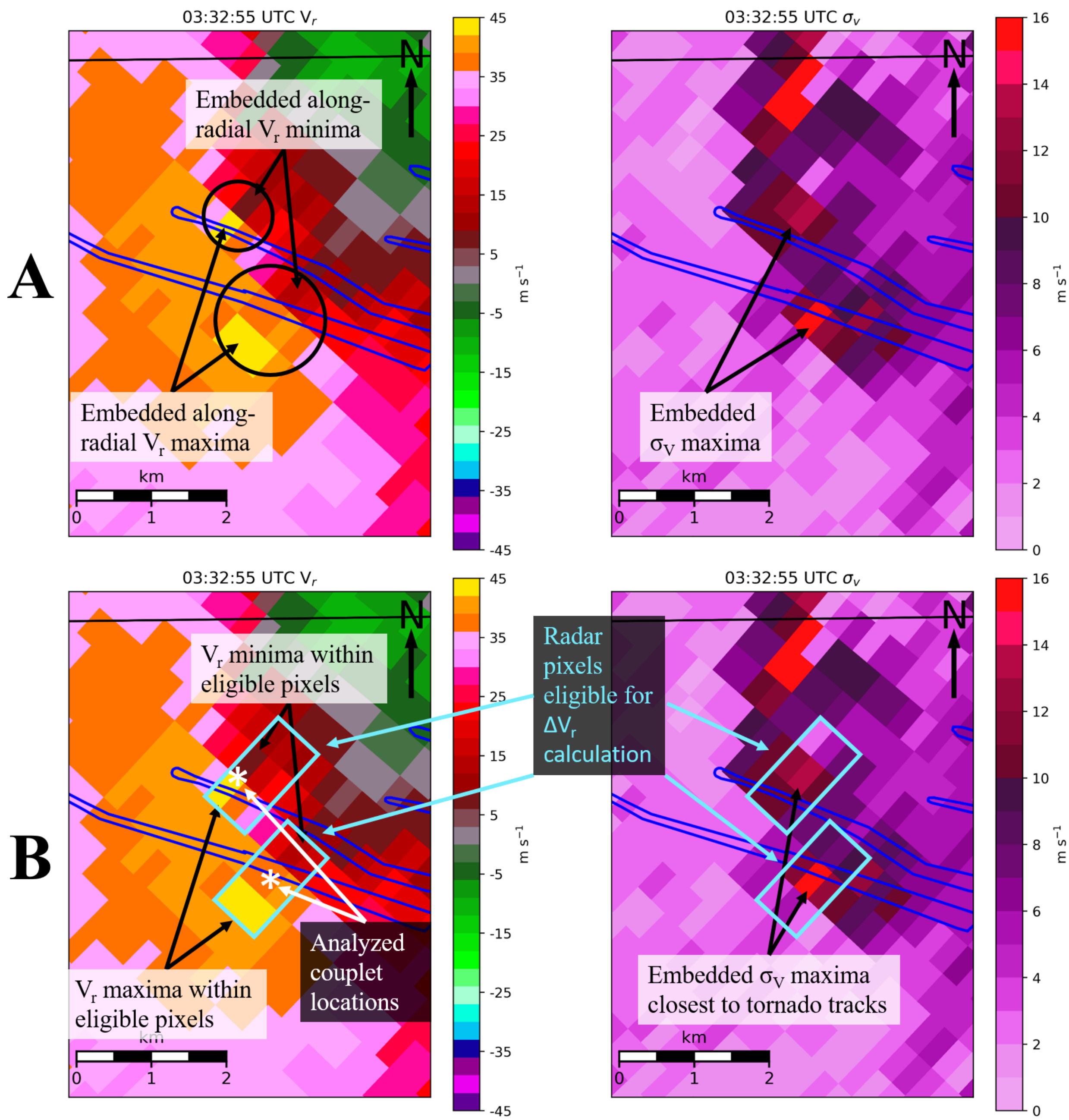

Figure 9: Two-panel 0.5° PPIs of V_r (left) and σ_v (right) at 0332 UTC 1 July 2014, exemplifying the identification of small-scale enhanced low-level rotation signatures within the broader mesovortex G-1, illustrating a) how areas of enhanced shear or velocity couplets were sought qualitatively, and b) the quantitative process for identifying enhanced shear zones and couplets likely associated with the tornadoes produced by mesovortices G-1 and G-2. The blue polygons indicate reanalyzed tornado tracks (detailed in section 5). These two rotational couplets are associated with tornadoes 5 (south) and 6 (north) from G-1 in Fig. 10. Note that a third enhanced-shear and σ_V region north of tornado 6 was likely associated with either tornado 7 or tornado 8, but it was not included in the analysis, because no suspected tornado damage was found in that area. *Click image to enlarge.*

1) Identify the likely tornado track;
2) Locate a maximum σ_V pixel closest to the tornado track within the broader mesovortex;
3) Find the maximum (maximum outbound) and minimum (maximum inbound) radial velocity (V_r) values within one pixel distance (adjacent or corner) of the σ_V maximum; and
4) Calculate the change in radial velocity (ΔV_r) between the two pixels (Fig. 9b).

The use of σ_V in this manner was motivated by the findings of Spoden et al. (2012) that values of 10.3 m s^{-1} (20 kt), collocated with a circulation in velocity, may highlight areas of increased tornado potential. While the Spoden et al. study does not cite a range dependence to its findings, increasing range from the scanning radar would have two effects: higher σ_V near concentrated circulations as velocities are averaged over larger bin volumes, and decreased confidence that a detected circulation corresponds to a tornado. While this analysis does not require a minimum threshold for σ_V maxima, these factors were considered when interpreting the radar data.

The quantitative analysis described above yielded 34 separate signatures associated with confirmed tornadoes between mesovortices G-1 and G-2. To assess the validity of the qualitative analysis, where the focus was on the identification of adjacent along-radial maxima and minima in Doppler velocity, the maximum and minimum V_r values were analyzed to determine whether or not they represented a local maximum or minimum V_r along their respective radials. Of the 34 observations, 22 contained both the local radial maximum and local radial minimum, while 10 others contained either the local minimum or local maximum. The results of the quantitative analysis are presented in section 5.

Finally, the presence or possible presence of debris as detected by correlation coefficient (ρ_{hv}) added confidence in declaring damage as tornadic. This was not, however, a requirement for associating a shear zone or couplet to a tornado. Most tornado tracks were not associated with clear debris signatures.

The absence of these velocity, σ_V, and debris signatures helped to support conclusions that many areas of damage were not tornadic. This was particularly the case with mesovortex G-1 in locations of likely microbursts within a broad swath of wind damage. These raised the question of whether additional tornadoes may have occurred, but Doppler velocity was relatively uniform and irrotational at the sampled radar beam height and σ_V was low, indicating uniformity of the flow and small values of turbulence. Figure 10 illustrates such an example, where radar imagery was used to boost confidence in declarations of tornadic and nontornadic damage.

Once damage survey data, satellite imagery, and radar information all were reviewed, sources of error in the observations were considered before the new survey results were finalized. These potential errors are discussed at length in section 6, but a key concern was whether damage seen in the satellite imagery was actually from this 30 June event or from another. To investigate, staff from NWS Chicago phoned residents at multiple locations where damage was observed on satellite. Every contacted resident confirmed property damage during this event.

In addition to the track reanalysis, the damage rating of each tornado was reevaluated on the Enhanced Fujita Scale using the expanded dataset of damage points. First, estimated wind speeds from the two points with the highest damage indicator (DI) and degree of damage (DOD) in each tornado path were averaged. Next, the speed was rounded up or down to the nearest 5-mph (2.2-m s^{-1}) increment to account for inherent uncertainty. Finally, an EF rating for each tornado was assigned based on this speed. The last author (Knupp) substantially contributed to the reanalysis of structural damage, while a tree damage expert (C. J. Peterson) was consulted in some of the tree damage reanalysis.

5. Reanalysis results for the Kankakee Valley tornado cluster

The reanalysis of the damage associated with mesovortices G-1 and G-2 across the Kankakee Valley led to the identification of eighteen tornadoes[2] and a large area of nontornadic wind damage (Fig. 11).

---

[2] As stated previously, damage was declared tornadic in nature if the preponderance of the survey evidence supported a concentrated vortex of ≥EF0 damage rating, including tree fall direction and debris dispersal, length-to-width aspect ratio, and eyewitness reports of pressure changes and/or very short damaging wind duration. Furthermore, evidence of concentrated, enhanced azimuthal shear from the KLOT radar in close proximity to the damage was used to further bolster identification of a damage swath as being tornadic. Significant debate does exist in the meteorological community regarding the taxonomy of QLCS-generated vortices, and we acknowledge that future definitions may exclude some of these as tornadoes.

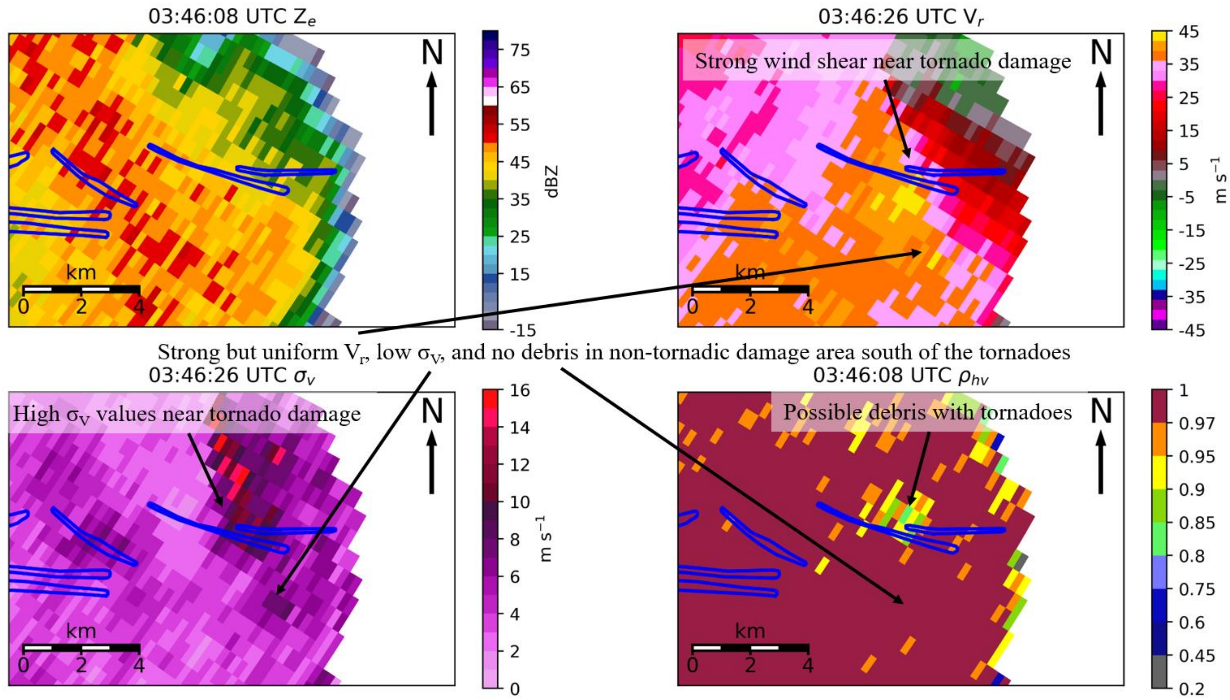

Figure 10: As in Fig. 4 at 0346 UTC, showing how radar signatures helped increase confidence in declaring areas of likely tornadic (strong wind shear, high σ_V, and possible debris) versus nontornadic (uniform velocity, low σ_V, no debris) wind damage. The reanalyzed tornado tracks are shown in blue. *Click image to enlarge.*

Three of the tornadoes were rated EF0, thirteen were rated EF1, and two were rated EF2. Remarkably, all occurred within the span of 36 min, from 0322 UTC to 0358 UTC (Fig. 12). On average, a new tornado formed once every 1.9 min. At least three tornadoes were ongoing simultaneously for a continuous 21-min period from 0324–0345 UTC, and as many as five tornadoes occurred simultaneously (Fig. 13). For all tornadoes from G-1 and G-2 combined, the minimum, mean, and maximum observed path lengths were 1.1, 8.0 and 25.5 km, respectively. The minimum, mean, and maximum estimated path widths were 40, 210 and 410 m, respectively.

The reanalyzed Kankakee Valley cluster yields 33 total tornadoes from the entirety of the second QLCS. All occurred in the Chicago/Romeoville (LOT) and Northern Indiana (IWX) NWS county warning areas (CWAs). Using the destruction potential index (DPI; Thompson and Vescio 1998) as a metric for event severity, this ranks as the seventh most potentially destructive tornado event for the LOT and IWX CWAs during the 10-y period from 2009–2018 (Table 1).

Table 1: DPI values for the top-10 tornado events for the LOT and IWX NWS county warning areas (CWAs) from 2009–2018. These tally the entirety of all tornadoes that impacted either CWA, including path segments in adjacent CWAs, but exclude tornadoes from these events that impacted neither CWA. The 30 June 2014 event is highlighted in red, and the DPI for the Kankakee Valley cluster exclusively is also provided.

All Events	DPI
17 November 2013	247.7
5 June 2010	76.3
22 June 2015	64.5
9 April 2015	60.7
28 February 2017	50.2
5 November 2017	39.9
30 June 2014	35.5
Kankakee Valley cluster	26.9
22 June 2016	21.0
24 August 2016	11.1
22 May 2011	7.3

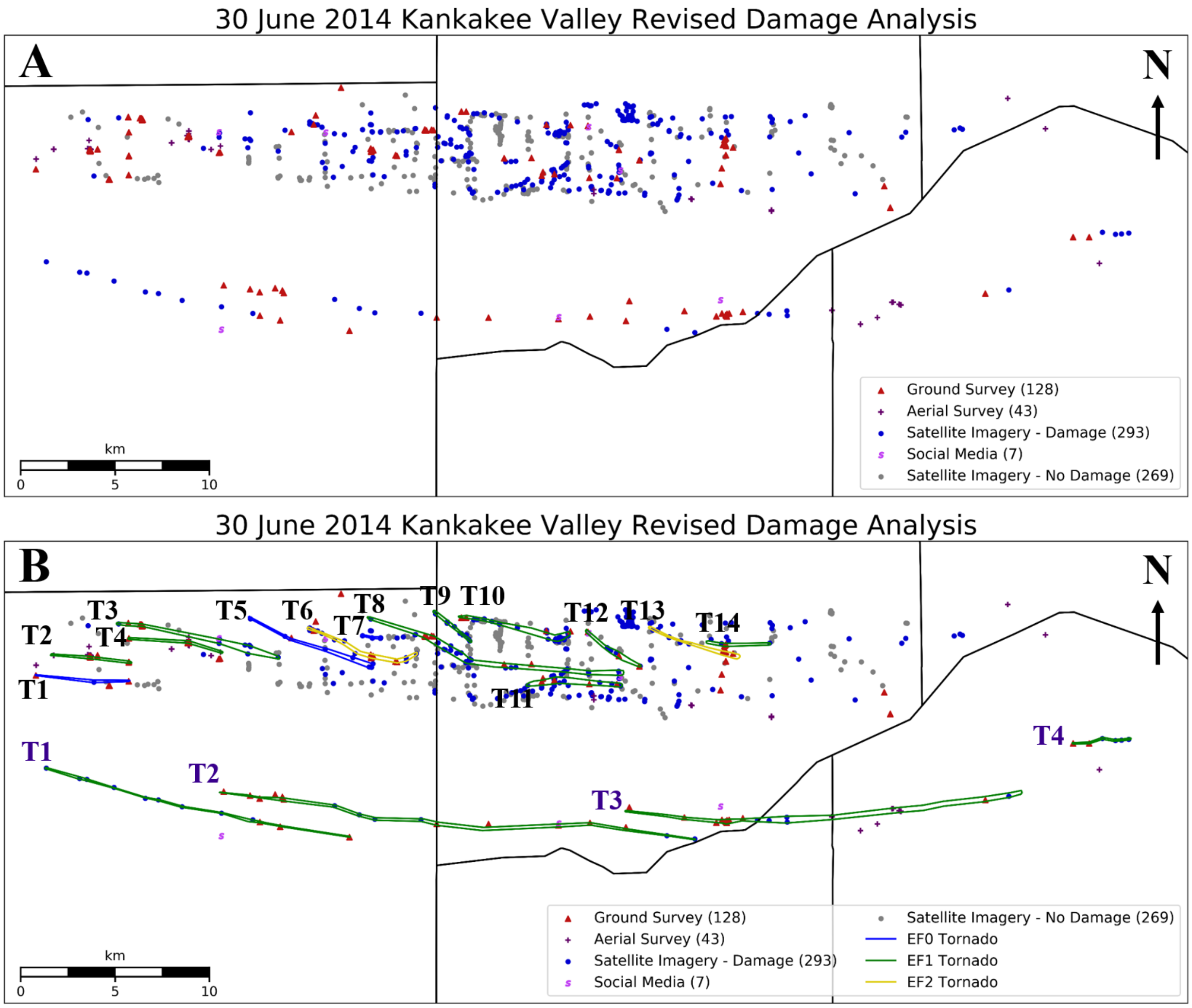

Figure 11: As in Fig. 4, with the addition of the information points gathered from Google Earth satellite imagery and the reanalyzed tornado tracks. *Click image to enlarge.*

Notably, this is one of only two events consisting exclusively of QLCS tornadoes to make the top-10 list of tornado events by DPI, across the combination of the LOT and IWX CWAs, during that time period. Its DPI (35.5) is approximately five times greater than the other strictly QLCS event (22 May 2011—7.3). The Kankakee Valley cluster alone accounts for 75.8% of the DPI for the second 30 June 2014 QLCS (26.9) and is approximately 3.7 times the DPI of the 22 May 2011 tornado event.

The quantitative radar analysis described in section 4 is summarized in Table 2. The minimum peak ΔV_r observed for the tornadoes was 18.5 m s^{-1} with tornado 11 of G-1, while the maximum peak ΔV_r observed was 40.5 m s^{-1} with G-1 tornado 4. Only tornadoes 1 and 9 from G-1 were not associated with absolute σ_v maxima exceeding 10.3 m s^{-1} during their lifecycles, with absolute σ_v maxima of 9.5 m s^{-1} and 10.0 m s^{-1}, respectively. Every tornado is associated with at least one identifiable embedded enhanced shear or velocity couplet signature using the previously described methodology.

A general tendency can be seen for ΔV_r to decrease, both from the first to last observation for tornadoes with multiple observations, and from earlier tornadoes to later tornadoes. While the former pattern does not have a readily identifiable cause, the latter pattern may be due to the mesovortices moving away from KLOT during the observation period, leading to larger bin volumes, more averaging of velocity values, and thus suppressed Doppler velocity. No pattern is evident in σ_v, despite the hypothesis that values may increase with increasing distance from KLOT, as discussed in section 4 (Fig. 14).

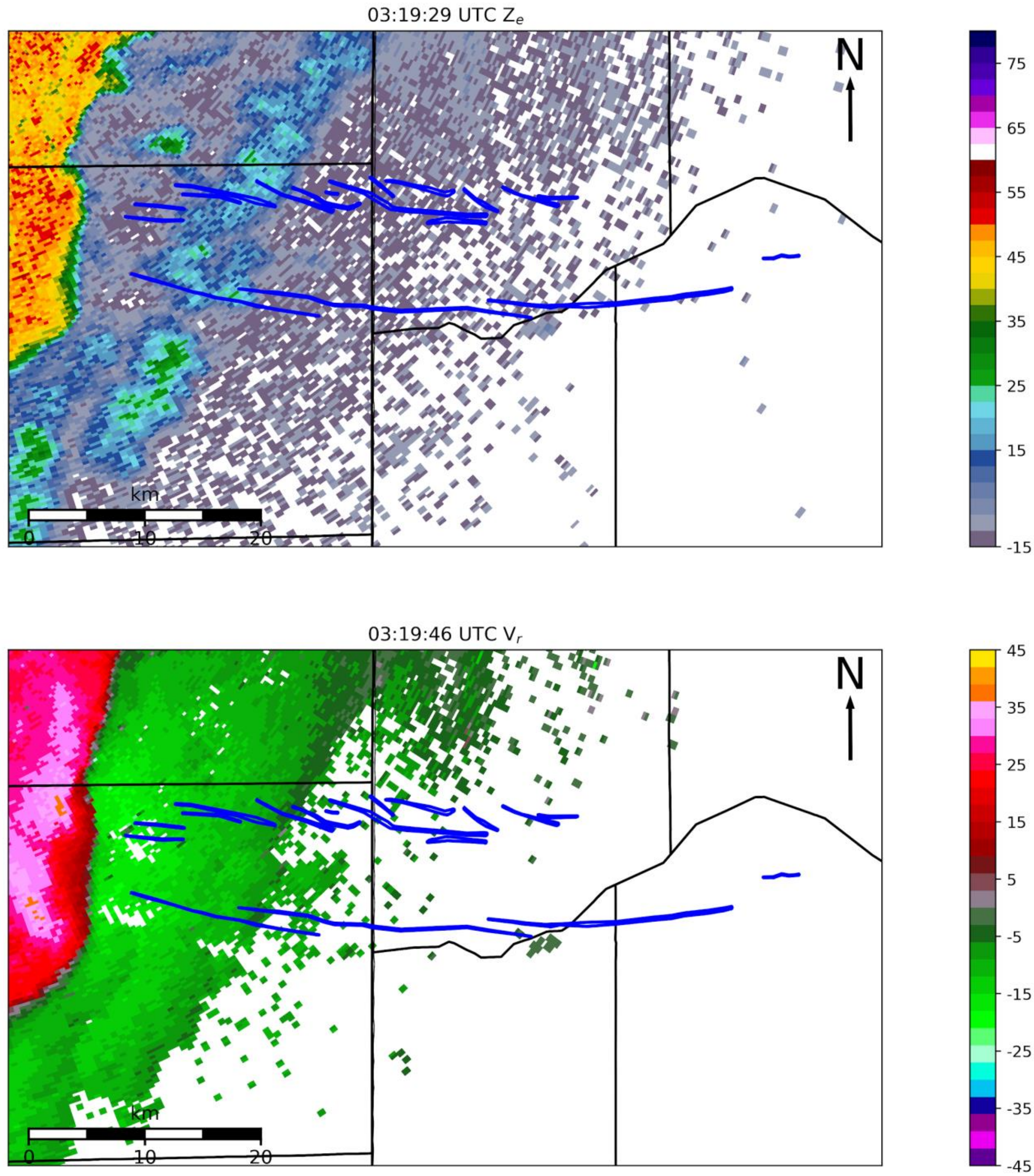

Figure 12: Overview loop of 0.5° Z_e and V_r from 0319−0402 UTC 1 July 2014, with the reanalyzed Kankakee Valley tornado tracks (blue) overlaid. The northern swath of tornadoes is associated with G-1, and the southern swath is associated with G-2. *Click image to enlarge and animate.*

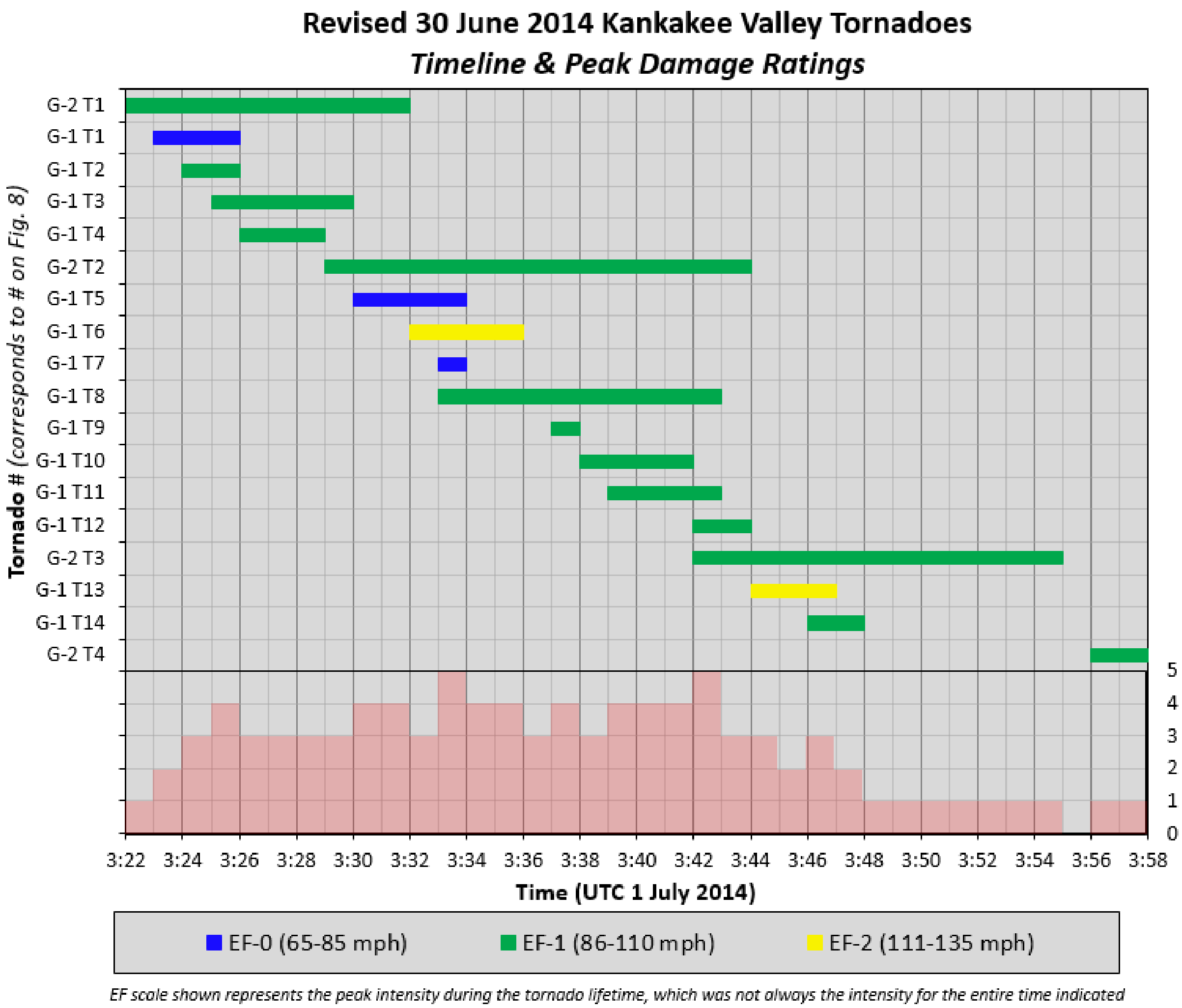

Figure 13: Timeline of occurrence for each reanalyzed tornado track associated with the Kankakee Valley tornado cluster (horizontal bars), and a histogram of tornado occurrence by each minute between 0322−0358 UTC (red vertical bars).

The following sections summarize the reanalysis results for mesovortices G-1 and G-2 individually. The reanalysis offers our best interpretation of the damage based on the available data detailed in section 3. This analysis may not match the true evolution of this event, as substantial uncertainty remains. This analysis merely offers a better interpretation of the damage than the official *Storm Data* record. As such, this analysis still may contain errors, some of which may be substantial. In general, confidence in this analysis decreases from west to east, particularly for mesovortex G-1 as it moved away from radar coverage and also into an area where potential damage indicators were increasingly sparse along its path. Specific sources of uncertainty are highlighted in section 6. Detailed descriptions of the damage associated with the tornadoes produced by G-1 and G-2 can be found in Appendices A and B, respectively.

a. Mesovortex G-1

Mesovortex G-1 was the northern and more prolific of the two mesovortices to impact the Kankakee Valley. As described in Lyza et al. (2017), this mesovortex propagated directly along a remnant thermal boundary from the first QLCS that passed through that evening. This has been shown to increase low-level convergence and vorticity stretching available to mesovortices (Wheatley and Trapp 2008) and may have led to G-1 being stronger, larger, and deeper than G-2, which was south of and farther removed from the boundary.

In the original analysis, G-1 and G-2 together produced fourteen tornadoes in the Kankakee Valley. In the reanalysis, G-1 alone is identified as having produced fourteen tornadoes, whereas *Storm Data* officially records just eight. In the original *Storm Data*, all tornado tracks were based only on information from the ground and aerial surveys. Three of the fourteen reassessed tracks consist purely of these survey points. Nine more are comprised of points declared tornadic in the original surveys plus additional points from satellite imagery. The other two only contain points that were newly classified as tornadic: tornado 7 with damage noted in passing during the first ground survey but not thoroughly investigated at the time (plus satellite-indicated damage points); and tornado 9 with damage discovered in satellite imagery along a clear, narrow track of high length-to-width aspect ratio.

Based on the examination of KLOT radar data as discussed in section 4, all of the declared tornadoes are accompanied by enhanced radial shear within the broader mesovortex and by enhanced σ_v near the center of the radial shear region. Tornadoes 3 and 13 were associated with TDSs or debris plumes. Areas of wind damage identified as nontornadic were accompanied by more uniform strong Doppler velocity values and lower values of σ_V (Fig. 10).

Google Earth satellite imagery played a pivotal role in reassessing the damage from G-1. As described in section 2b, satellite imagery of damage from G-1 (tornado 6) indicated inaccuracies in the original analysis (Fig. 8). The imagery aided in determining the tracks of all tornadoes within G-1, except for tornadoes 1, 2, and 4. Appendix A provides numerous additional examples of the role that Google Earth imagery played in the reanalysis. Ultimately, the mean tornado track orientation was changed from the original east-northeast direction in *Storm Data* to east-southeast. The reanalysis also addressed other documented inconsistencies in the original survey results, such as that highlighted in Fig. 6 (Fig. 15).

These fourteen tornadoes with G-1 occurred within the span of approximately 25 min, with numerous instances of multiple simultaneously ongoing tornadoes and rapid, successive tornado occurrence. Widespread nontornadic wind damage also occurred along the southern edge of the mesovortex. One area experienced winds equivalent to EF1 or low-end EF2 rating.

This analysis represents a wholesale change from the initial *Storm Data* entries. The official *Storm Data* statistics for G-1 include eight EF1 tornadoes and one large area of nontornadic wind damage. The changes to G-1 do not merely represent the addition of six tornadoes but the complete reorientation and reorganization of the tornado tracks. Given the rural nature of much of the area, the ground survey and aerial survey information was insufficient for developing a full understanding of how the tornadoes moved and behaved within G-1. The addition of satellite imagery, highlighting numerous additional damage areas, together with analyses of radar data, led to the discovery that many of the points connected to each other in the official *Storm Data* results actually were caused by separate tornadoes. Table 3 provides statistics for each tornado, while Appendix A describes each tornado track in detail.

Along with the reevaluation of tornado tracks from G-1, each rating estimate also was reassessed through a more detailed examination of the original ground survey data and consultation with outside experts. The damage reanalysis led to three tornadoes receiving EF0 ratings and two tornadoes receiving EF2 ratings, whereas the original survey analysis featured no EF0 or EF2 tornado tracks.

b. Mesovortex G-2

The damage associated with mesovortex G-2 was more limited than with G-1. While G-1 was responsible for an extensive array of tornadic and nontornadic wind damage, damage associated with G-2 was generally limited to four tornado tracks. Three of these were rather long, however, with path lengths >15 km. Modifications to G-2 survey results from the original *Storm Data* also were more limited than for G-1. All changes consisted of either the extension of a known track or connection of multiple known tracks. This led to a decrease in the number of tornadoes assessed with G-2, from six in *Storm Data* to four in this analysis. Table 4 summarizes each of the tornadoes associated with G-2, while detailed descriptions for each tornado can be found in Appendix B. The original assessment of G-2 was found to be approximately correct, regarding track orientation and general evolution of tornadoes within the mesovortex.

Table 2: Summary of the quantitative radar analysis for the Kankakee Valley tornadoes. MV is mesovortex identifier. "Outbound" is the maximum outbound V_r, "Inbound" is the minimum or "maximum inbound" V_r, "Lat" and "Lon" are the latitude and longitude points of the approximate center of the assessed couplet (the midpoint between the "Inbound" and "Outbound" pixels), "Out max?" indicates whether the "Outbound" value represents a local along-radial maximum in Doppler velocity, and "In max?" indicates whether the "Inbound" value represents a local along-radial minimum (or maximum inbound) in V_r.

Time (UTC)	MV	Tornado	Outbound (m s^{-1})	Inbound (m s^{-1})	ΔV_r (m s^{-1})	σ_V max (m s^{-1})	Lat (°)	Lon (°)	Out max?	In max?
3:25:06	G-1	1	39.0	19.5	19.5	9.5	41.2592	–87.7430	Yes	Yes
	G-1	2	35.5	16.0	19.5	11.0	41.2673	–87.7507	No	Yes
	G-2	1	25.0	–3.5	28.5	12.5	41.2047	–87.7370	No	Yes
3:27:34	G-1	3	36.5	8.0	28.5	16.5	41.2787	–87.6994	No	No
	G-1	4	49.5	9.0	40.5	15.0	41.2756	–87.6991	Yes	Yes
	G-2	1	38.5	1.0	37.5	14.0	41.1964	–87.6874	Yes	Yes
3:30:27	G-1	3	39.0	17.0	22.0	10.5	41.2699	–87.6524	Yes	Yes
	G-1	5	36.5	–2.5	39.0	11.0	41.2863	–87.6516	Yes	Yes
	G-2	1	35.5	12.5	23.0	10.0	41.1911	–87.6378	No	No
	G-2	2	41.5	6.5	35.0	15.0	41.1964	–87.6431	Yes	Yes
3:32:55	G-1	5	44.0	13.0	31.0	16.0	41.2628	–87.5945	Yes	Yes
	G-1	6	45.5	7.5	38.0	15.0	41.2755	–87.6009	Yes	Yes
	G-2	2	39.5	13.5	26.0	13.0	41.1894	–87.5941	Yes	Yes
3:35:46	G-1	6	45.5	17.0	28.5	15.5	41.2665	–87.5462	Yes	Yes
	G-1	7	44.0	16.0	28.0	13.0	41.2745	–87.5489	Yes	No
	G-1	8	39.5	15.5	24.0	12.0	41.2818	–87.5525	Yes	Yes
	G-2	2	37.5	14.5	23.0	12.5	41.1919	–87.5340	Yes	Yes
3:38:15	G-1	8	45.0	22.0	23.0	13.0	41.2697	–87.4996	Yes	No
	G-1	9	40.0	18.0	22.0	10.0	41.2775	–87.5057	No	Yes
	G-1	10	31.0	–0.5	31.5	16.5	41.2892	–87.5057	Yes	Yes
	G-2	2	38.0	15.0	23.0	11.5	41.1920	–87.4839	Yes	Yes
3:41:06	G-1	8	46.0	26.5	19.5	11.0	41.2604	–87.4519	Yes	Yes
	G-1	10	42.0	21.5	20.5	9.0	41.2743	–87.4551	Yes	No
	G-1	11	43.0	24.5	18.5	10.5	41.2557	–87.4434	Yes	Yes
	G-2	2	35.0	13.5	21.5	12.0	41.1875	–87.4335	Yes	Yes
3:43:34	G-1	12	43.0	23.0	20.0	13.0	41.2717	–87.4139	Yes	Yes
	G-2	3	32.0	7.0	25.0	13.0	41.1908	–87.3910	Yes	Yes
3:46:26	G-1	13	43.0	20.5	22.5	12.5	41.2677	–87.3518	Yes	No
	G-1	14	39.0	17.5	21.5	11.5	41.2762	–87.3571	No	Yes
	G-2	3	33.5	14.5	19.0	12.5	41.1880	–87.3275	Yes	Yes
3:48:54	G-2	3	32.0	5.5	26.5	13.0	41.1923	–87.2849	No	Yes
3:51:46	G-2	3	34.5	16.5	18.0	10.0	41.1914	–87.2213	Yes	Yes
3:54:14	G-2	3	32.5	24.0	8.5	9.5	41.2039	–87.1723	Yes	Yes
3:57:07	G-2	4	29.5	1.5	28.0	14.0	41.2321	–87.1137	Yes	No

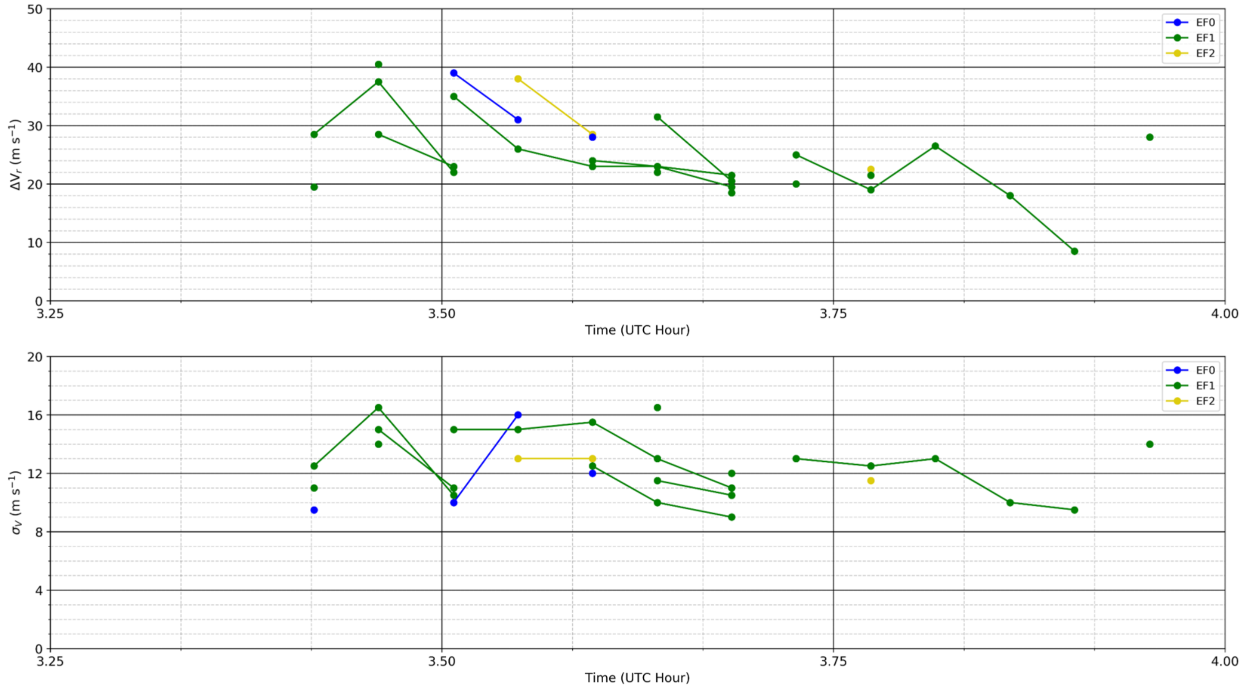

Figure 14: Time series of ΔV_r (top) and maximum σ_V (bottom) for all tornadoes from mesovortices G-1 and G-2. Damage ratings colored as in legend at top right of each panel.

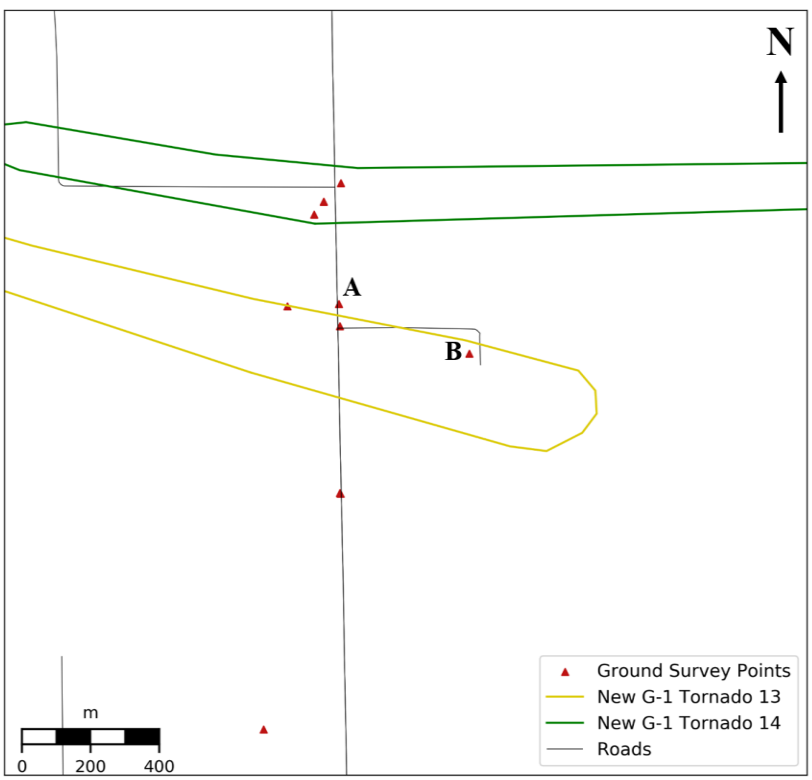

Figure 15: As in the map from Fig. 6, with the reanalyzed tornado tracks overlaying the damage points. Note that point A, the location of the snapped power pole that was located directly adjacent to an undamaged corn crop is no longer included in a tornado track. *Click image to enlarge and animate a before-and-after comparison with the original survey track.*

Table 3: Summary table for all reanalyzed tornado tracks associated with mesovortex G-1. Start and end times are estimated from radar. "Max DI/DOD" indicates the maximum EF-scale damage indicator/degree of damage combination used to rate the damage. Red entries in the Max DI/DOD indicate where the lower-bound estimated wind gust was applied for a given DI, while blue entries indicate where the expected value estimated wind gust was applied.

Reanalyzed Tornado Information for Mesovortex G-1							
Damage ID	Start Time	End Time	Path Length	Path Width	EF Rating	Max DI/DOD	Estimated Maximum Wind Speed (3-s Gust)
Tornado 1	0323 UTC	0325 UTC	5.0 km	40 m	EF0	DI 24/DOD 3	38.0 m s^{-1} (85 mph)
Tornado 2	0324 UTC	0325 UTC	4.3 km	100 m	EF1	DI 1/DOD 6 D1 27/DOD 3	42.5 m s^{-1} (95 mph)
Tornado 3	0325 UTC	0329 UTC	8.9 km	410 m	EF1	DI 1/DOD 8 DI 27/DOD 4	49.2 m s^{-1} (110 mph)
Tornado 4	0326 UTC	0328 UTC	5.1 km	100 m	EF1	DI 24/DOD 2 DI 27/DOD 4	46.9 m s^{-1} (105 mph)
Tornado 5	0330 UTC	0333 UTC	7.1 km	270 m	EF0	DI 27/DOD 3	33.5 m s^{-1} (75 mph)
Tornado 6	0332 UTC	0335 UTC	6.3 km	220 m	EF2	DI 1/DOD 8 DI 2/DOD 5	51.4 m s^{-1} (115 mph)
Tornado 7	0333 UTC	0333 UTC	1.1 km	110 m	EF0	DI 1/DOD 4 DI 2/DOD 2	38.0 m s^{-1} (85 mph)
Tornado 8	0333 UTC	0344 UTC	14.2 km	380 m	EF1	DI 27/DOD 4 DI 28/DOD 4	49.2 m s^{-1} (110 mph)
Tornado 9	0337 UTC	0337 UTC	2.6 km	160 m	EF1	DI 27/DOD 3 DI 28/DOD 3	40.2 m s^{-1} (90 mph)
Tornado 10	0338 UTC	0341 UTC	6.1 km	240 m	EF1	DI 27/DOD 2 DI 27/DOD 4	44.7 m s^{-1} (100 mph)
Tornado 11	0339 UTC	0342 UTC	5.1 km	340 m	EF1	DI 27/DOD 4 DI 28/DOD 4	46.9 m s^{-1} (105 mph)
Tornado 12	0342 UTC	0343 UTC	3.5 km	290 m	EF1	DI 27/DOD 2 DI 27/DOD 4	44.7 m s^{-1} (100 mph)
Tornado 13	0344 UTC	0346 UTC	5.1 km	270 m	EF2	DI 24/DOD 4 DI 27/DOD 4	51.4 m s^{-1} (115 mph)
Tornado 14	0346 UTC	0347 UTC	3.4 km	170 m	EF1	DI 24/DOD 2 DI 27/DOD 4	46.9 m s^{-1} (105 mph)

Table 4: As in Table 3, for mesovortex G-2.

Reanalyzed Damage Information for Mesovortex G-2							
Damage ID	Start Time	End Time	Path Length	Path Width	EF Rating	Max DI/DOD	Estimated Maximum Wind Speed (3-s Gust)
Tornado 1	0322 UTC	0331 UTC	16.6 km	140 m	EF1	DI 1/DOD 4 DI 27/DOD 3	40.2 m s^{-1} (90 mph)
Tornado 2	0329 UTC	0343 UTC	25.5 km	160 m	EF1	DI 24/DOD 3 DI 27/DOD 4	49.2 m s^{-1} (110 mph)
Tornado 3	0342 UTC	0354 UTC	21.2 km	360 m	EF1	DI 1/DOD 8 DI 27/DOD 4	49.2 m s^{-1} (110 mph)
Tornado 4	0356 UTC	0357 UTC	3.2 km	90 m	EF1	DI 1/DOD 6 DI 24/DOD 3	46.9 m s^{-1} (105 mph)

6. Sources of uncertainty during the survey reanalysis

As mentioned in section 4, there are several sources of uncertainty and possible error in this reanalysis. First is that the number of potential damage indicators generally decreases from west to east, particularly along the track of mesovortex G-1. This was somewhat mitigated for G-2 as it passed over the town of DeMotte, but became more of a problem as it moved across rural areas northeast of DeMotte.

Minimum radar beam height above ground level also increased from west to east along the tracks of G-1 and G-2. They moved away from the KLOT radar while still being distant from the Northern Indiana WSR-88D (KIWX). This led to a decreased ability to detect smaller-scale areas of rotation (larger bin size) and TDSs (higher beam elevation). The loss of potential damage indicators and degradation in low-level radar coverage reduces the overall confidence in the analysis of the damage across southeastern Lake, southwestern Porter, and northern Jasper Counties.

A potential source of error in interpreting satellite data is the time frame between the available imagery. Because no imagery is available between September 2013 and May 2015, knowledge of other severe weather events during that time is necessary to avoid assigning damage to the wrong event. *Storm Data* indicates that severe weather was reported near where G-1 and G-2 passed on 17 November 2013, 21 June 2014, and 20 September 2014. Reports also were logged elsewhere within the affected counties on 11 May 2014, 20 May 2014, 14 July 2014, and 19 August 2014, but away from where G-1 and G-2 passed.

The 17 November 2013 event was a prolific tornado outbreak with widespread convective damaging winds across Illinois and Indiana. While one EF1 tornado and two reports of winds >26 m s^{-1} (50 kt) were recorded in the vicinity of where G-1 and G-2 would pass later, the storm motion on 17 November 2013 was from the southwest at over 26 m s^{-1}, making it rather unlikely that damage from 17 November 2013 would be easily confused with damage on 30 June 2014. In the analysis of satellite imagery, the stark difference in storm motion led to the exclusion of one damage point in the analysis. This point consisted of multiple trees along the Illinois/Indiana state line downed in a north-northeasterly direction. In contrast, damage from 30 June 2014 was most commonly found to be oriented in directions ranging from southeast to east-northeast.

The 21 June 2014 event produced damage near areas impacted north of Grant Park on 30 June. However, this was one of the areas most thoroughly surveyed by ground teams in the wake of the 30 June event. Additionally, a phone call to residents of a property where damage was observed on satellite imagery confirmed that this damage (as part of tornado 5 with G-1) did indeed occur on 30 June.

The 20 September 2014 event likely poses the greatest challenges when ascertaining the cause of observed damage during the time period between satellite images. This event featured a QLCS moving eastward across northeastern Illinois and northern Indiana, roughly in the same direction as the 30 June 2014 event. Three of the *Storm Data* wind-damage entries from that event occurred near where G-1 and G-2 had passed nearly three months prior. One report, an estimated wind gust of 31 m s^{-1} (61 kt), occurred in the town of Lowell. *Storm Data* entries from that day do not include any specific remarks about wind damage within the areas later impacted by G-1 and G-2. Still, some of the damage points outside of the analyzed tornado tracks may have been from the 20 September event, despite the fact that the 30 June 2014 event was far more damaging. This uncertainty is partially why a clustering of damage points north of G-1 tornado 12 (Fig. 11b) was not assigned to any tornado track in this reanalysis, despite suggestions from KLOT radar data that one or more tornadoes may have occurred in this area.

In addition to other events occurring between the satellite imagery dates, an event on 4 June 2011 posed a substantial challenge to determining damage sources via satellite imagery across southeastern Lake and northern Jasper counties. This event was characterized by an intense high-precipitation supercell that produced a widespread macroburst and embedded microbursts within its rear-flank downdraft. Damage from this event was prolific, with a widespread area of estimated winds >40 m s^{-1} (>90 mph). Because this event occurred before the 2013 satellite imagery, the damage was already evident. The challenge posed by the 4 June 2011 event is that it produced extensive tree damage in areas directly impacted by G-1 and G-2, potentially masking damage produced by processes related to those mesovortices (Fig. 16). Unfortunately, the areas impacted most heavily by the 4 June event correspond to areas previously discussed as lacking damage indicators relative to areas impacted farther to the west on 30 June 2014. The end result is that many of the few damage indicators present in southeastern Lake County and northern Jasper

Figure 16: Google Earth satellite imagery loop showing damage progression to a grove of trees from 26 August 2010 to 30 May 2015, showing damage from rear-flank downdraft wind damage on 4 June 2011 and an EF1 tornado on 30 June 2014. *Click image to enlarge and animate.*

County already featured antecedent damage from 4 June 2011, further complicating the reanalysis efforts in these areas.

Preventative clearing to avoid future damage is another source of possible uncertainty, particularly in the satellite-aided analysis. This was partially the case with a resident contacted in the path of tornado 5 of mesovortex G-1. The residence, identified as potentially sustaining damage during the 30 June event, did in fact sustain damage. However, some of the "damage" apparent in the satellite imagery was actually removal of trees and large limbs to prevent damage in future severe wind events. Distinguishing damage from preventative clearing is extremely difficult.

Further uncertainty is added to the analysis by the infestation of ash trees across the Kankakee Valley by the emerald ash borer beetle. This beetle was already well-established in the region prior to 2014 and eventually kills infested ash trees (USDA 2018). Therefore, the obvious decay or removal of trees detected by satellite imagery may not be related to 30 June 2014 or any other storm event but by emerald ash borer infestation. Tree removal may be due either to infestation or death of a tree or by preemptive removal of an ash tree from a property. Determining tree species beyond distinguishing between deciduous and coniferous trees within the satellite imagery is a daunting task.

In order to increase confidence in identified areas of possible damage being linked to wind instead of preventative clearing or ash borer damage, the following conditions were sought:

- Loss of numerous trees on properties, with variation in tree size and shape;
- Loss of coniferous trees;
- Properties experiencing apparent tree loss organized in a linear (point-to-point-to-point) fashion, with a lack of damage to surrounding properties located off of the path;
- Confirmation from contacted residents regarding the nature of the damage;
- Strong evidence of damage having occurred to the trees (e.g., fallen trees still laying across the ground);
- Evidence of damage to structures or other features on the property; and
- Close proximity to damage found on the ground and aerial surveys.

The previously mentioned cluster of suspected damage points north of G-1 tornado 12 is the best example of suspected damage that was excluded from the final assessment due to insufficient coverage by the criteria above, as well as uncertainty lent by the previously discussed event on 20 September 2014. While many properties in Lowell did lose trees and some of the confirmed damage tracks did extrapolate back into the area of unknown damage, the number of properties impacted and the scope of possible impacts across the southern end of Lowell indicated that some of the tree removal may have been due to other causes, such as preventative removal to avoid future damage, emerald ash borer infestation, etc. Determining what damage was associated with 30 June 2014 was nearly impossible in town, outside of the areas that were either close to damage surveyed during the ground surveys or confirmed via contact with residents. Every resident contacted noted that at least some of the possible damage identified in satellite imagery was indeed associated with the second 30 June 2014 QLCS. Residents could not be contacted at some of the locations where suspected damage was found via satellite imagery. However, the positive response from other residents suggests that using satellite imagery to augment ground and aerial surveys is feasible to at least reasonable accuracy. This is particularly the case when considering the previous bulleted list.

7. Operational considerations

A potentially tornadic QLCS poses many challenges to the operational forecaster. These include appropriate pre-event messaging, effective warning strategies during the event, and accurate post-event damage assessment. Insights from this detailed reanalysis of the 30 June 2014 QLCS are applicable during all three of these phases.

The mesoanalysis performed during previous 30 June 2014 studies supported the idea that tornadoes were possible on the evening of the event. This detailed damage reanalysis concluded that tornadoes up to EF2 rating occurred. Recognition of this potential prior to future events in a similar environment and with similar convective mode would be an important component of pre-event messaging.

For an operational warning meteorologist, this study also reinforces the importance of recognizing specific and at times subtle radar signals along with their correlation to potential damage. In a QLCS, broad mesocyclones alone, especially in the immediate wake of a previous QLCS, may not and often should not prompt the issuance of tornado warnings. In this particular event, tornado warnings were issued, but only after tornadoes formed. Brotzge et al. (2013) found that this is not unusual for QLCS tornado warnings, which have significantly lower performance than warnings for supercell tornadoes. An earlier, clearer recognition of the true threat posed by a QLCS would support warnings with a greater probability of detection and lead time. This also would allow the potential impact to life and property to be communicated more accurately in the text of impact-based warnings (IBWs; Ripberger et al. 2015) issued by all NWS offices as of February 2017.

Recognizing the potential for a large mesovortex to produce a complicated pattern of tornadic and nontornadic wind damage also aids in the analysis of damage during the post-event phase. Widespread damage might initially be attributed to nontornadic winds after a cursory examination. However, a more extensive analysis based on the composite of multiple datasets may lend confidence to a conclusion that damage was instead due to multiple tornadoes, or a combination of tornadoes and severe thunderstorm winds.

8. Summary and conclusions

A particularly complex and destructive convective wind event occurred across the Kankakee Valley area of northeast Illinois and northwest Indiana on 30 June–1 July 2014. The most substantial damage was associated with a pair of large mesovortices on the leading edge of the second of two derecho-producing QLCSs that evening. An analysis performed shortly after the event revealed many tornadoes over a relatively small geographic region. However, given the complex evolution of this event, numerous inconsistencies remained in the official *Storm Data* results.

A reanalysis of this damage was motivated by these inconsistencies and by newly available Google Earth high-resolution satellite imagery. This reanalysis uncovered 18 separate tornadoes, four more than originally documented, along with notable nontornadic wind damage. Two of these tornadoes are rated EF2, and three are EF0, whereas all tornadoes originally listed in *Storm Data* were EF1. The Google Earth satellite imagery also demonstrated that most tornado tracks were oriented differently than in the initial assessment.

QLCS events can be prolific tornado producers on the weak half of the tornado rating spectrum and on occasion can generate numerous weak, short-tracked tornadoes in very close proximity both in space and time. This ability has been demonstrated in this case, in the Radom case, the case presented in Skow and Cogil (2017), and others such as Knupp et al. (2014). Nontornadic winds cannot be assumed just because damage occurred over a relatively broad area. Widespread convective wind damage can be produced by a concentrated cluster of tornadoes as well as by downbursts. These events can be very difficult to classify accurately depending on: 1) the breadth and intricacy of the damage pattern, 2) the available damage indicators and road networks in the impacted areas, 3) the proximity of the nearest available radar and its scanning strategy during the event, and 4) the availability of aerial survey and satellite imagery information.

The 30 June 2014 Kankakee Valley part of this event presents an excellent example of a complex, destructive QLCS. With an WSR-88D now able to scan its lowest elevation approximately every minute through the MESO-SAILS strategy (Chrisman 2014), together with increasing availability of aerial photography and high-resolution satellite imagery, QLCS tornado clusters are increasingly likely to be detected, either in real-time or in post-event analysis. For such complex events, the closer reanalysis presented in this study highlights the critical importance of integrating as many data sources as possible to derive a proper conclusion. The analysis and research of 30 June 2014 prior to this study, including documentation in *Storm Data* and in Lyza et al. (2017), were based on ground and aerial surveys along with a basic mesoanalysis. This deeper investigation included polarimetric radar analysis, high-resolution satellite imagery comparisons, phone calls to selected locations, and consultation with external experts. This led to survey results that were much more consistent with the observed damage.

Further in-depth studies of substantial QLCS events, particularly those with large, long-lived mesovortices, are encouraged. Such studies will increase our understanding of the physical processes responsible for tornadoes and damaging winds in a QLCS. These studies could include numerical simulations and observational field projects. Especially valuable would be development of a conceptual model explaining the evolution of tornado clusters occasionally observed in such events. At the same time, intensive survey efforts can continue to relate QLCS radar signatures to damage. The knowledge gained will readily inform the evolution of best practices for the warning of QLCS hazards in support of NWS Weather-Ready Nation initiatives.

ACKNOWLEDGEMENTS

The late Ron Przybylinski (NWS St. Louis) assisted in the initial identification of this event as a tornado cluster, Dr. Chris Peterson (Department of Plant Biology, University of Georgia) was consulted in the re-evaluation of tree damage from the event, Barrett Goudeau (UAH-SWIRLL) assisted with the creation of the radar animations shown in this paper, Jordan Bell (UAH Earth System Science Center) was consulted for satellite imagery interpretation and information, and Alyssa Woodward (University of Oklahoma) assisted with editing of this manuscript. Partial funding for this work was provided by the University of Alabama in Huntsville's Earth System Science Center (UAH ESSC), the UAH Research and Creative Experience for Undergraduates (RCEU) program, the NOAA Ernest F. Hollings Scholarship program, and NOAA via Award 191001.363513.048 from the Northern Gulf Institute.

The scientific results and conclusions, as well as any view or opinions expressed herein, are those of the author(s) and do not necessarily reflect the views of NWS, NOAA, or the Department of Commerce.

APPENDIX A

This appendix details the damage-producing events associated with mesovortex G-1. See Table 3 for tornado path statistics. Tornadoes are listed in chronological order and additional wind damage is described at the end of the appendix.

Tornado 1:

- Damage: Corn pressed down, one standard wooden power pole snapped.
- Sources of damage information: First ground survey.
- Evidence of tornadic nature of damage: Narrow swath, power pole fell to the west (against storm motion), Google Earth satellite imagery.
- Radar characteristics: Velocity couplet with maximum ΔV_r of 19.5 m s^{-1} embedded within G-1, σ_v maximum of 9.5 m s^{-1} (just below the 10.3 m s^{-1} threshold of Spoden et al. 2012).
- Changes from *Storm Data*: Incorporates damage from the original T1 and T2 tracks (see Fig. 4 to reference original tornado tracks), downgrade to EF0 rating.

Tornado 2:

- Damage: Hardwood trees snapped and uprooted, two of four exterior walls blown out of large machine shed.
- Sources of damage evidence: First ground survey.
- Evidence of tornadic nature of damage: Narrow, cyclonic/convergent path.
- Radar characteristics: Embedded velocity couplet with maximum ΔV_r of 19.5 m s^{-1} within G-1, σ_v maximum of 11.0 m s^{-1}.
- Changes from *Storm Data*: Incorporates damage from the original T1 and T3 tracks.

Tornado 3:

- Damage: Numerous softwood and hardwood trees snapped and uprooted; one softwood tree snapped and tossed approximately 27 m (30 yd); "flagging" (removal of most or all branches on the upstream-facing side) of trees in the most intense damage core; large shed completely blown away, with all six of the 6 × 6 in (15 × 15 cm) posts pulled out of the ground, as well as four of the six concrete anchors for the posts, with two of the anchors tossed and not found during the survey; minor buckling of a house foundation; snapped wooden power pole; damaged corn crop.
- Sources of damage evidence: First ground survey, Google Earth satellite imagery.
- Evidence of tornadic nature of damage: Strongly convergent debris field and damage orientation; possible evidence of multiple vortices in the corn crop and tree damage distribution and layout.
- Radar characteristics: Velocity couplet with maximum ΔV_r of 28.5 m s^{-1}; σ_v maximum of 11 m s^{-1} along the entire duration of the analyzed track, with an absolute maximum of 16.5 m s^{-1}; TDS (Fig. 7).
- Changes from *Storm Data*: Incorporates damage from the original T1, T2, and T3 tracks, addition of numerous Google Earth satellite imagery damage points to construct the second half of the tornado track.

Tornado 4:

- Damage: Numerous hardwood trees snapped and uprooted; barn destroyed, with the top half of the barn blown off and the rest shifted off the foundation; 4000-lb (1814-kg) trailer moved 40–50 ft (12−15 m); large branches and limbs snapped off of trees; snapped wooden power pole crossbar.
- Sources of damage evidence: First ground survey, aerial survey.
- Evidence of tornadic nature of damage: Convergent tree fall and debris dispersion pattern.
- Radar characteristics: Strong velocity couplet with maximum ΔV_r of 40.5 m s^{-1} embedded in the larger circulation, σ_v maximum of 15.0 m s^{-1}.
- Changes from *Storm Data*: Incorporates damage from the original T1 and T3 tracks, includes aerial survey information that was not included in the official *Storm Data* entries.

Tornado 5:

- Damage: Greenhouse damaged, large limbs snapped, roof damage to a house.
- Sources of damage evidence: Second ground survey, Google Earth satellite imagery.
- Evidence of tornadic nature of damage: Narrow, concentrated path of damage noted in both ground survey and satellite imagery.
- Radar characteristics: Velocity couplet with maximum ΔV_r of 37.5 m s^{-1} (Fig. 9), σ_v maximum of 11.0 m s^{-1}.
- Changes from *Storm Data*: Incorporates damage from the original T2 track, addition of Google Earth satellite imagery data points to construct a majority of the path, downgrade to EF0 rating.
- Notes: Phone call to owner of house with new roof and trees missing in the Google Earth imagery confirmed damage occurred on 30 June 2014 (Fig. A1).

Tornado 6:

- Damage: Home destroyed (torqued on its foundation beyond repair); projectile debris, including a large tree limb through the second-story wall of the home (Fig. A2); numerous barns and outbuildings destroyed, including complete destruction of a 90 × 60 ft (27 × 18 m), three-story barn; damage to a small Lutheran church, including the entirety of a large stained-glass window blown out (including frame) and torquing of the structure on its foundation; severe damage (snapping and uprooting) to hardwood trees, including nearly 100% tree fall along a couple tree lines in the core of the path.
- Sources of damage evidence: First and second ground surveys, Google Earth satellite imagery.
- Evidence of tornadic nature of damage: Convergent tree fall and debris dispersion patterns, eyewitnesses described pressure change and ears popping as damage occurred.

Figure A1: Before-and-after loop of Google Earth satellite imagery showing damage to a farmstead from tornado 5 associated with mesovortex G-1. *Click image to enlarge and animate.*

- Radar characteristics: Strong velocity couplet with maximum ΔV_r of 38.0 m s^{-1} embedded in the larger mesovortex (Fig. 9), σ_v maximum of 15.5 m s^{-1}; lowering in ρ_{hv} that may be representative of debris, akin to a debris "plume" (Skow and Cogil 2017).
- Changes from *Storm Data*: Incorporates damage from the original T2, T4, and T5 tracks, addition of Google Earth satellite imagery damage points, upgrade to EF2 rating.

Tornado 7:

- Damage: Roof damage to a house and barn, swimming pool damaged, tree damage.
- Sources of damage evidence: First ground survey, Google Earth satellite imagery (Fig. A3).
- Evidence of tornadic nature of damage: Concentrated, narrow swath of damage.
- Radar characteristics: Velocity couplet with maximum ΔV_r of 28.0 m s^{-1}; σ_v maximum of 13.0 m s^{-1}.
- Changes from *Storm Data*: None of this damage was included in the original *Storm Data* analysis; satellite imagery was used to find additional damage surrounding the barn, which was noted but not closely examined in the first ground survey.
- Notes: σ_v maximum and velocity couplet were detected immediately after the official end point of the tornado, indicative that the tornado may have lasted longer than revealed by damage indicators (much of the area immediately downstream from the last damage point consists of open fields).

Tornado 8:

- Damage: Home under construction (but sealed) suffered this damage: exterior wall of the garage blown out, part of a second-story exterior wall blown in, and portion of the roof structure removed; well-built barn with substantial roof damage; substantial tree damage, with numerous large hardwood and softwood trees snapped, uprooted, and partially stripped of branches (Fig. A4).
- Sources of damage evidence: First and second ground surveys, Google Earth satellite imagery.
- Evidence of tornadic nature of damage: Concentrated, narrow, convergent swath of damage.

- Radar characteristics: Velocity couplet with maximum ΔV_r of 24.0 m s^{-1}, σ_v maximum of >10 m s^{-1} noted during the lifespan of the tornado until around the time of its dissipation.
- Changes from *Storm Data*: Incorporates damage from the original T4, T5, and T6, addition of Google Earth satellite imagery damage points.

Figure A2: a) Before-and-after Google Earth satellite loop of the farmstead most heavily impacted by tornado 6 of mesovortex G-1. b) Picture of the destroyed three-story barn. c) A tree limb impaled into a second-story bedroom of the house on the farmstead. *Click image to enlarge and animate.*

Tornado 9:

- Damage: Large hardwood trees felled.
- Sources of damage evidence: Google Earth satellite imagery (Fig. A5).
- Evidence of tornadic nature of damage: Concentrated, narrow damage path.
- Radar characteristics: Velocity couplet with maximum ΔV_r of 22.0 m s^{-1}, σ_v maximum of 10.0 m s^{-1}.
- Changes from *Storm Data*: None of this damage was included in the original *Storm Data* analysis.

Tornado 10:

- Damage: Hardwood trees snapped and uprooted; large limbs snapped off of trees; roof damage to a barn.
- Sources of damage evidence: First and second ground surveys, Google Earth satellite imagery.
- Evidence of tornadic nature of damage: Concentrated, narrow damage path.
- Radar characteristics: Velocity couplet with maximum ΔV_r of 31.5 m s^{-1}, σ_v maximum of 16.5 m s^{-1}.

- Changes from *Storm Data*: Incorporates damage from the original T4 and T7, addition of Google Earth satellite imagery damage points.
- Notes: May be related to or part of tornado 12 (Fig. A6).

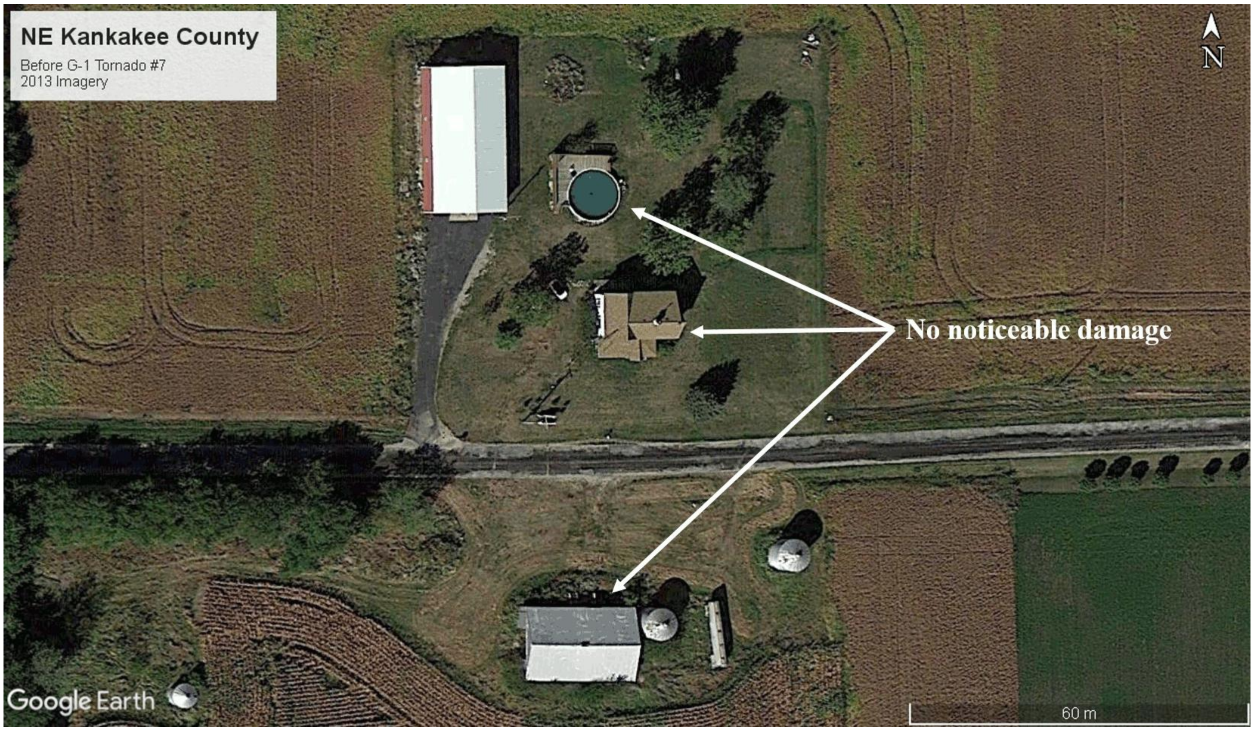

Figure A3: Before and after loop of Google Earth satellite imagery of damage sustained to a farmstead from tornado 7 of mesovortex G-1. *Click image to enlarge and animate.*

Tornado 11:

- Sources of damage evidence: Second ground survey, Google Earth satellite imagery.
- Evidence of tornadic nature of damage: Concentrated, narrow, strongly convergent damage path (Fig. A7).
- Radar characteristics: Velocity couplet with maximum ΔV_r of 18.5 m s^{-1}, σ_v maximum of 10.5 m s^{-1}.
- Changes from *Storm Data*: Minor extension to the beginning of original T8 using Google Earth satellite imagery, otherwise the same track as T8.

Tornado 12:

- Damage: Numerous trees snapped and uprooted.
- Sources of damage evidence: Second ground survey, Google Earth satellite imagery (Fig. A8).
- Evidence of tornadic nature of damage: Narrow, cyclonic-convergent tree fall pattern.
- Radar characteristics: Velocity couplet with maximum ΔV_r of 20.0 m s^{-1}, σ_v maximum of 13 m s^{-1}.
- Changes from *Storm Data*: Incorporates damage from the original T6 and T7, addition of Google Earth satellite imagery damage points.
- Notes: May be related to or part of tornado 10 (Fig. A6); connecting tornadoes 10 and 12 would require an assumption that a singular tornado either completed a tight loop or inflection near the center of mesovortex G-1, and asserting such a behavior would be strongly speculative, given the general lack of evidence.

Tornado 13:

- Damage: Outbuildings destroyed; numerous trees snapped and uprooted; two large grain bins destroyed, with one completely collapsed and one partially collapsed; numerous large high-tension wooden power poles snapped; crop damage.
- Sources of damage evidence: First ground survey (Fig. 6b), Google Earth satellite imagery.

- Evidence of tornadic nature of damage: Cyclonic-convergent damage path.
- Radar characteristics: Embedded couplet with maximum ΔV_r of 22.5 m s^{-1}, σ_v maximum of >10 m s^{-1} observed until dissipation, possible debris (Fig. 10).
- Changes from *Storm Data*: Incorporates damage from the original T6, addition of Google Earth satellite imagery damage points, upgrade to EF2 rating, split from damage now associated with tornado 14 due to inconsistencies highlighted in Fig. 6.
- Notes: Given the proximity of a large-scale nontornadic wind damage event immediately south of this track, the path length and particularly the path width of this tornado are even more uncertain than of many of the other tornadoes associated with G-1.

Figure A4: Examples of damage from tornado 8 of mesovortex G-1 at peak rating. *Click image to enlarge.*

Tornado 14:

- Damage: Large barn destroyed, with top half of barn ripped off and the bottom half severely damaged; numerous trees snapped and uprooted (Fig. A9).
- Sources of damage evidence: First ground survey, Google Earth satellite imagery.
- Evidence of tornadic nature of damage: Strongly cyclonic-convergent nature of the damage path.
- Radar characteristics: Velocity couplet with maximum ΔV_r of 21.5 m s^{-1}, σ_v maximum of 11.5 m s^{-1} observed until dissipation.
- Changes from *Storm Data*: Incorporates damage from the original T6, addition of Google Earth satellite imagery damage points, split from damage now associated with tornado 13 due to inconsistencies highlighted in Fig. 6.

Widespread, nontornadic damage was also observed south of the corridor of tornadic activity with G-1. This wind damage began south of tornadoes 1 and 2, where minor tree damage was observed. The nontornadic wind damage slowly became more intense and expansive as G-1 moved eastward. Across Lake County, IN, the wind damage along the southern periphery of G-1 was widespread and intense, estimated at up to EF1 rating. Evidence of microbursts in corn crop, tree, and power pole damage were observed. Observations from KLOT radar indicated very high but relatively uniform Doppler velocity and low σ_V over these areas, further supporting the damage being nontornadic in nature.

In addition to the widespread tornadic and nontornadic damage, satellite imagery indicated possible damage from the south side of Lowell eastward into southwestern Porter County. KLOT radar data does indicate at least one possible tight velocity couplet moving along this path. However, the lack of any damage surveys, either ground or aerial, and the location of the possible couplet within G-1 relative to the other tornadic couplets, simply lead to too much uncertainty to declare one or more tornado tracks in this region. The assessment within that area is further complicated by the close proximity to the starting points for tornadoes 13 and 14. In fact, some of the damage may actually be from tornadoes 13 and 14. While the location of this possible damage along the northern periphery of G-1 reduces the likelihood of the damage being nontornadic, the complexity and lack of concrete information in this region led the authors to not declare a definitive cause. Tornadoes 13 and 14 may have started earlier than indicated in this analysis, and one or more additional tornadoes not analyzed in this paper may have occurred.

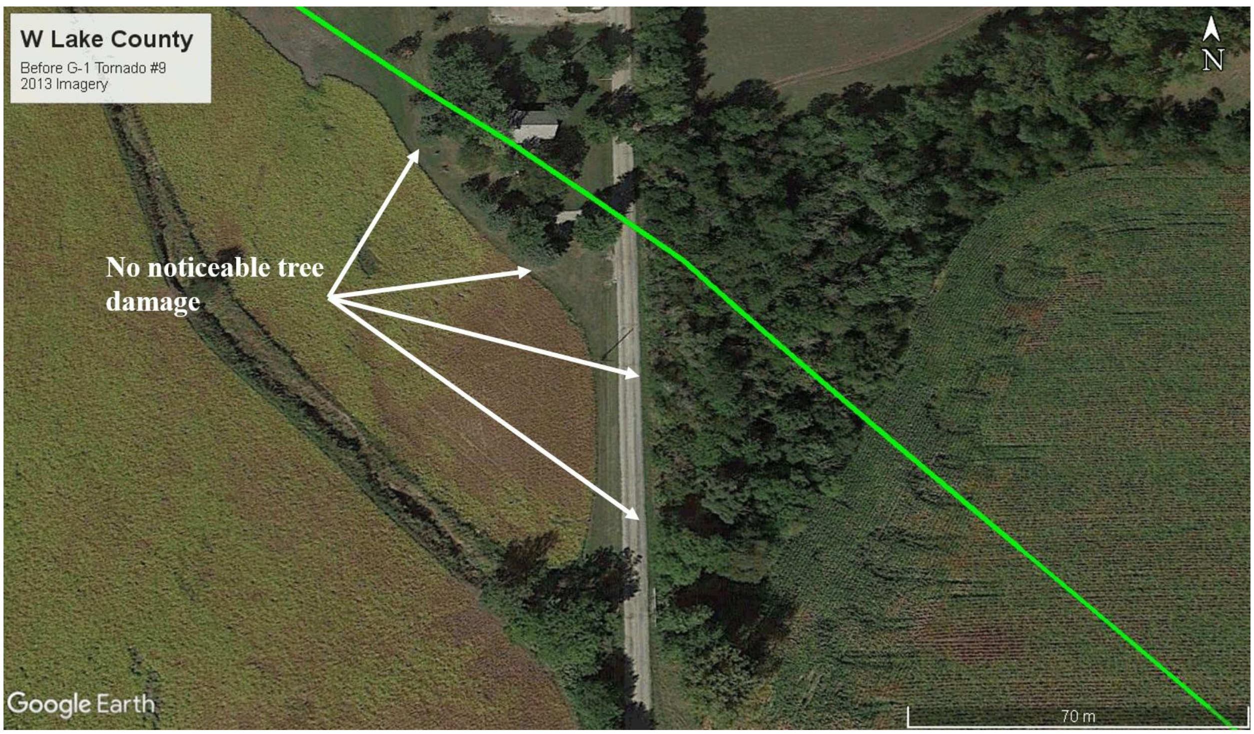

Figure A5: Before and after loop of Google Earth satellite imagery showing some of the damage associated with tornado 9 from mesovortex G-1. The green line indicates the estimated center line of the tornado path. *Click image to enlarge and animate.*

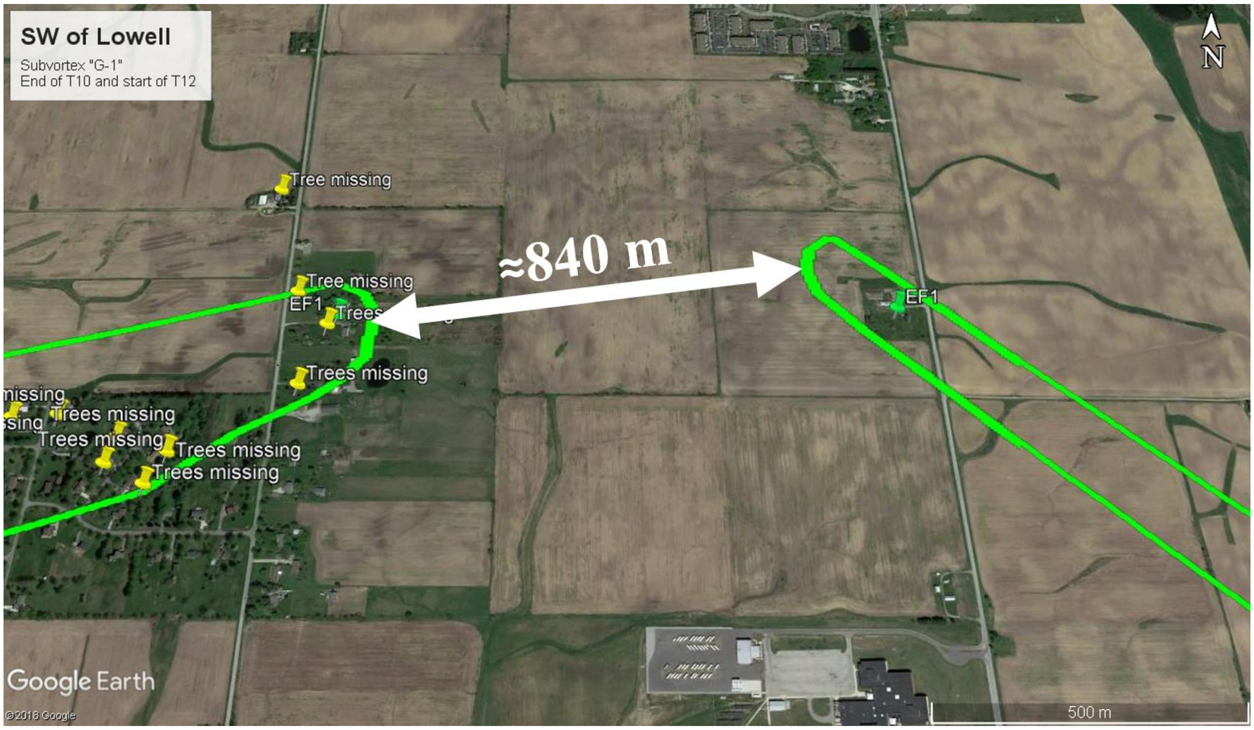

Figure A6: Overview of the end of tornado 10 and start of tornado 12 associated with mesovortex G-1 (green polygons), showing the close proximity of the terminus points and the sharp change of direction between the two tracks. *Click image to enlarge.*

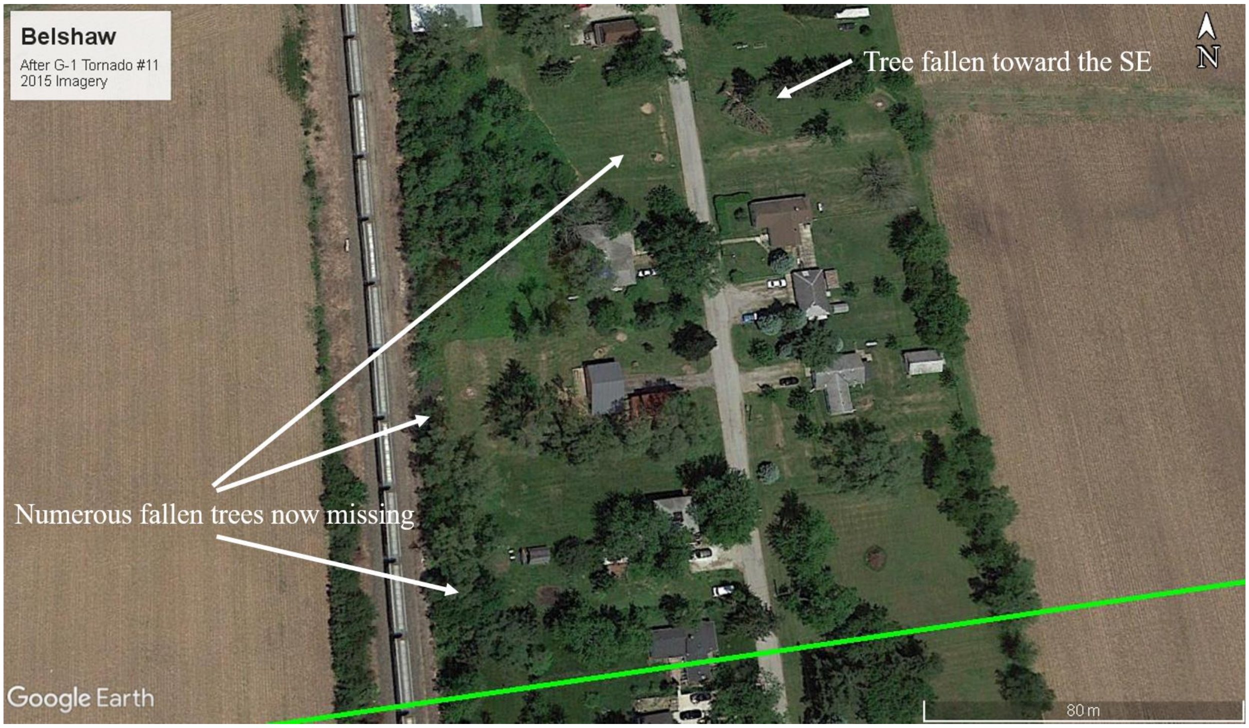

Figure A7: Google Earth satellite imagery of a damaged neighborhood in Belshaw, IN, impacted by tornado 11 of mesovortex G-1. The green line indicates the approximate center line of the tornado damage track. Note the tree fallen to the southeast, convergent toward the center line. *Click image to enlarge.*

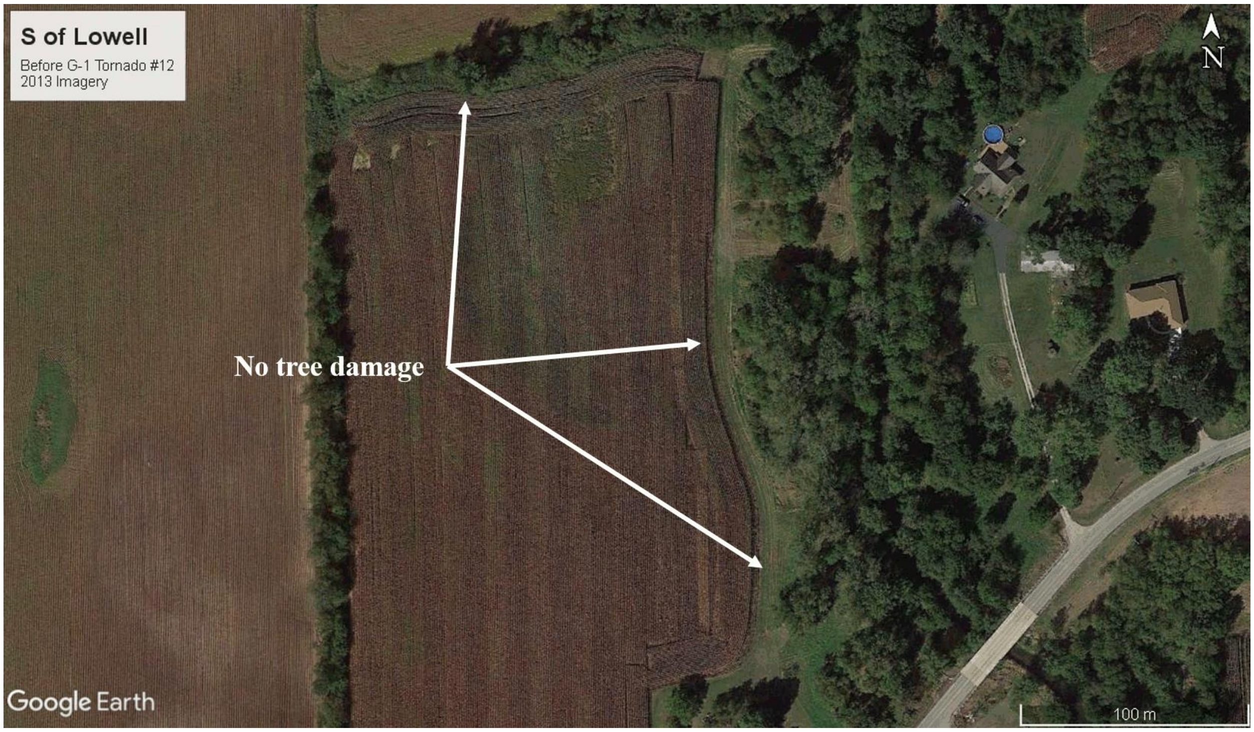

<u>Figure A8</u>: Before-and-after loop of Google Earth satellite imagery of substantial tree damage associated with tornado 12 from mesovortex G-1. *Click image to enlarge and animate.*

<u>Figure A9</u>: a) Before-and-after loop of Google Earth satellite imagery showing damage to a farmstead caused by tornado 14 of mesovortex G-1. b) Destroyed barn at the farmstead shown in (a), as found on the first ground survey. *Click image to enlarge and animate.*

APPENDIX B

This appendix details the damage-producing events associated with mesovortex G-2. See Table 4 for tornado path statistics. Tornadoes are listed below in chronological order.

Tornado 1:

- Damage: Numerous trees snapped and uprooted; roof damage to a barn.
- Sources of damage information: Second ground survey, Google Earth satellite imagery.
- Evidence of tornadic nature of damage: Narrow swath, convergent damage.
- Radar characteristics: Velocity couplet with maximum ΔV_r of 37.5 m s^{-1}, σ_V maximum of 14.0 m s^{-1}.
- Changes from *Storm Data*: Significant extension to the beginning of the original T2 track (see Fig. 4 to reference original tornado tracks).

Tornado 2:

- Damage: Numerous hardwood trees snapped and uprooted; roof damage to a barn.
- Sources of damage information: Second ground survey, Google Earth satellite imagery
- Evidence of tornadic nature of damage: Long, narrow swath of convergent damage.
- Radar characteristics: Velocity couplet with maximum ΔV_r of 35.0 m s^{-1}, σ_V maximum of >10 m s^{-1} during its lifespan.
- Changes from *Storm Data*: Combination of original T1 and T3 through the addition of Google Earth satellite imagery damage points.
- Notes: Longest tornado track of the Kankakee Valley cluster.

Tornado 3:

- Damage: Numerous hardwood trees snapped and uprooted, with at least one area of >50% tree fall; complete destruction of a large barn; damage to houses in Shelby and DeMotte from both wind and falling trees, including destruction of a house in Shelby from a large fallen tree.
- Sources of damage information: First ground survey, aerial survey, Google Earth satellite imagery (Fig. B1).
- Evidence of tornadic nature of damage: Long, narrow swath of cyclonic-convergent damage.
- Radar characteristics: Velocity couplet with maximum ΔV_r of 26.5 m s^{-1}, σ_V maximum of >10 m s^{-1} during its lifespan.

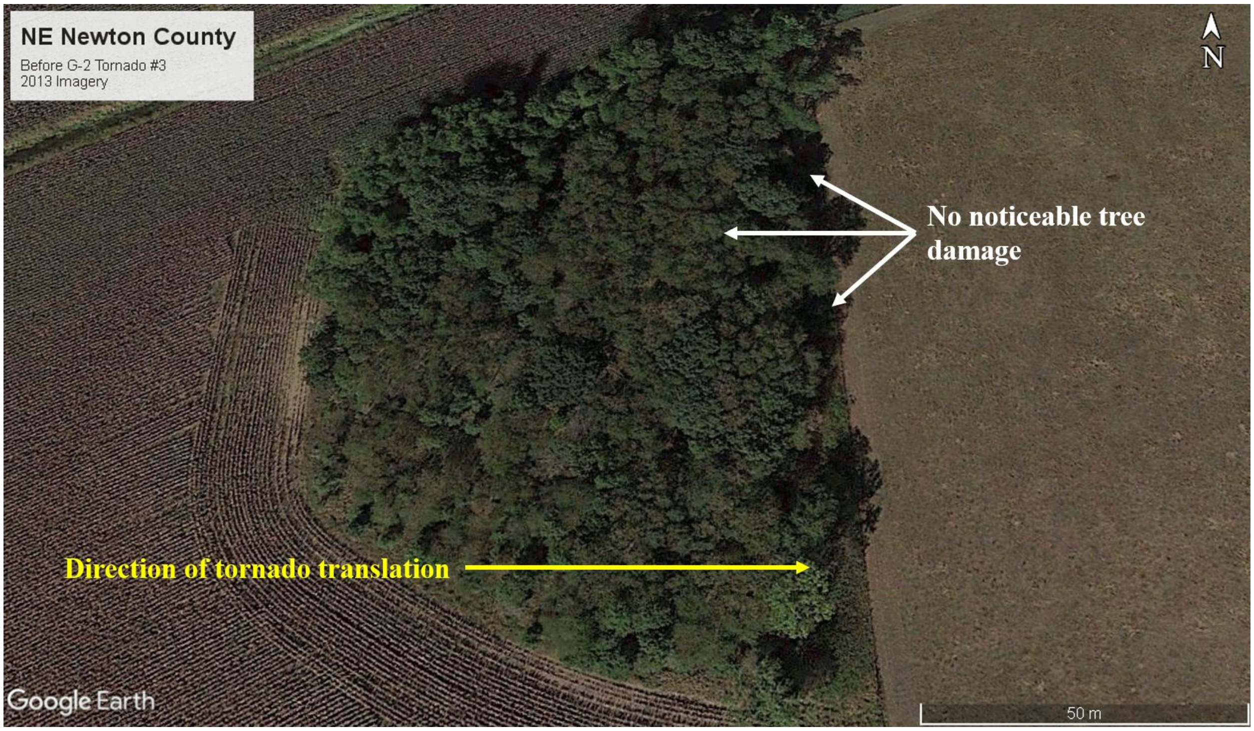

Figure B1: Before-and-after satellite imagery loop of damage found in northeastern Newton County, IN, to connect the Shelby and DeMotte tornado damage tracks. *Click image to enlarge and animate.*

- Changes from *Storm Data*: Combination of original T4 and T5 tracks and extension of the end of the original T5 track through the addition of Google Earth satellite imagery damage points.

Tornado 4:

- Damage: Large pole barn with roof blown off and multiple walls collapsed; numerous trees snapped and uprooted.
- Sources of damage information: First ground survey, Google Earth satellite imagery.
- Evidence of tornadic nature of damage: Long, narrow swath of cyclonic-convergent damage.
- Radar characteristics: Velocity couplet with maximum ΔV_r of 28.0 m s^{-1}, σ_V maximum of 14.0 m s^{-1}.
- Changes from *Storm Data*: Extension at the end of the original T6 track through the addition of Google Earth satellite imagery damage points.

Evidence of isolated nontornadic wind damage at the southern periphery of the mesovortex was also found during the aerial survey.

REFERENCES

Agee, E. M., J. T. Snow, and P. R. Clare, 1976: Multiple vortex features in the tornado cyclone and the occurrence of tornado families. *Mon. Wea. Rev.*, **104**, 552–563.

Atkins, N. T., and M. St. Laurent, 2009a: Bow echo mesovortices, part I: Processes that influence their damaging potential. *Mon. Wea. Rev.*, **137**, 1497–1513.

——, and ——, 2009b: Bow echo mesovortices, part II: Their genesis. *Mon. Wea. Rev.*, **137**, 1514–1532.

——, J. M. Arnott, R. W. Przybylinski, R. A. Wolf, and B. D. Ketcham, 2004: Vortex structure and evolution within bow echoes. Part I: Single-Doppler and damage analysis of the 29 June 1998 derecho. *Mon. Wea. Rev.*, **132**, 2224–2242.

——, and C. S. Bouchard, R. W. Przybylinski, R. J. Trapp, and G. Schmocker, 2005: Damaging Surface Winds within the 10 June 2003 Saint Louis Bow Echo during BAMEX. Mon. Wea. Rev., **133**, 2275–2296.

Brotzge, J. A., S. E. Nelson, R. L. Thompson, and B. T. Smith, 2013: Tornado probability of detection and lead time as a function of convective mode and environmental parameters. *Wea. Forecasting*, **28**, 1261–1275.

Brown, R. A., L. R. Lemon, and D. W. Burgess, 1978: Tornado detection by pulsed Doppler radar. *Mon. Wea. Rev.*, **106**, 29–38.

Brown, T. M., D. Liang, and J. A. Womble, 2012: Predicting ground-based damage states from windstorms using remote-sensing imagery. *Wind Struct.*, **15**, 369–383.

Burow, D., B. Rundquist, and C. Atkinson, 2017: NDVI change analysis and damage mapping of the Vilonia, Arkansas tornado, 27 April 2014. *Pap. Appl. Geog.*, **3** (1), 85–100.

Chrisman, J., 2014: Multiple Elevation Scan Option for SAILS (MESO-SAILS). NWS/Radar Operations Center, 27 pp. [Available online at https://www.roc.noaa.gov/WSR88D/PublicDocs/NewTechnology/MESO-SAILS_Description_Briefing_Jan_2014.pdf.]

Clayton, A. W., A. W. Lyza, R. Wade, and K. R. Knupp, 2016: An analysis of tornado debris signatures in the 30 June—1 July 2014 quasi-linear convective system tornado outbreak. Preprints, *28th Conf. on Severe Local Storms*, Portland, OR, Amer. Meteor. Soc., P1.12.

Coniglio, M. C., and D. J. Stensrud, 2004: Interpreting the climatology of derechos. *Wea. Forecasting*, **19**, 595–605.

Corfidi, S. F., M. C. Coniglio, A. E. Cohen, and C. M. Mead, 2016: A proposed revision to the definition of “derecho.” *Bull. Amer. Meteor. Soc.*, **97**, 935–949.

Eilts, M. D., J. T. Johnson, E. D. Mitchell, R. J. Lynn, P. Spencer, S. Cobb, and T. M. Smith, 1996: Damaging downburst prediction and detection algorithm for the WSR-88D. Preprints, *18th Conf. On Severe Local Storms*, San Francisco, Amer. Meteor. Soc., 541–545.

Forbes, G. S., and R. M. Wakimoto, 1983: A concentrated outbreak of tornadoes, downbursts and microbursts, and implications regarding vortex classification. *Mon. Wea. Rev.*, **111**, 220–235.

Guastini, C. T., and L. F. Bosart: 2016: Analysis of a progressive derecho climatology and associated formation environments. *Mon. Wea. Rev.*, **144**, 1363–1382.

Jedlovec, G. J., U. Nair, and S. L. Haines, 2006: Detection of storm damage tracks with EOS data. *Wea. Forecasting*, **21**, 249–267

Johns, R. H., and W. D. Hirt, 1987: Derechos: Widespread convectively induced windstorms. *Wea. Forecasting*, **2**, 32–49.

Kingfield, D. M., and K. M de Beurs, 2017: Landsat identification of tornado damage by land cover and an evaluation of damage recovery in forests. *J. Appl. Meteor. Climatol.*, **56**, 965–987.

Knupp, K. R., 2000: Narrow streaks of "straight-line" wind damage. Do tornadoes or microbursts produce them? Preprints, *20th Conf. on Severe Local Storms*, Orlando, FL, Amer. Meteor. Soc., 644–645.

____, and Coauthors, 2014: Meteorological overview of the devastating 27 April 2011 tornado outbreak. *Bull. Amer. Meteor. Soc.*, **95**, 1041–1062.

Lemon, L. R., and C. A. Doswell III, 1979: Severe thunderstorm evolution and mesocyclone structure as related to tornadogenesis. *Mon. Wea. Rev.*, **107,** 1184–1197.

Lyza, A. W., and Coauthors, 2016: Utilization of multiple platforms in a high-resolution tornado damage survey: The 31 March 2016 Hartselle-Priceville, Alabama EF2 tornado during VORTEX-SE. Preprints, *28th Conf. on Severe Local Storms*, Portland, OR, Amer. Meteor. Soc., P2.80.

——, A. W. Clayton, K. R. Knupp, E. Lenning, M. T. Friedlein, R. Castro, and E. S. Bentley, 2017: Analysis of mesovortex characteristics, behavior, and interactions during the second 30 June–1 July 2014 Midwestern derecho event. *Electronic J. Severe Storms Meteor.*, **12** (2), 1–33.

Molthan, A. L., J. R. Bell, T. A. Cole, and J. E. Burks, 2014: Satellite-based identification of tornado damage tracks from the 27 April 2011 severe weather outbreak. *J. Oper. Meteor.*, **2** (16), 191–208.

NCEI, cited 2018: *Storm Data*. [Available online at https://www.ncdc.noaa.gov/IPS/sd/sd.html]

NWS St. Louis, cited 2018: Severe weather outbreak: May 30th, 2004. [Available online at https://www.weather.gov/media/lsx/Events/05_30_2004.pdf]

Przybylinski, R. W., 1995: The bow echo: Observations, numerical simulations, and severe weather detection methods. *Wea. Forecasting*, **10**, 203–218.

Ripberger, J. T., C. L. Silva, H. C. Jenkins-Smith, and M. James, 2015: The influence of consequence-based messages on public responses to tornado warnings. *Bull. Amer. Meteor. Soc.*, **96**, 577–590.

Ryzhkov, A. V., T. J. Schuur, D. W. Burgess, D. S. Zrnic, 2005: Polarimetric tornado detection. *J. Appl. Meteor.*, **44**, 557–570.

Schultz, C. J., and Coauthors, 2012: Dual-polarization tornadic debris signatures. Part I: Examples and utility in an operational setting. *Electronic J. Oper. Meteor.*, **13** (9), 120−137.

——, and Coauthors, 2012: Dual-polarization tornadic debris signatures Part II: Comparisons and caveats. *Electronic J. Operational Meteor.*, **13** (10), 138−150.

Skow, K. D., and C. Cogil, 2017: A high-resolution aerial survey and radar analysis of quasi-linear convective system surface vortex damage paths from 31 August 2014. *Wea. Forecasting*, **32**, 441–467.

Smith, B. T., R. L. Thompson, J. S. Grams, and C. Broyles, 2012: Convective modes for significant severe thunderstorms in the contiguous United States. Part I: Storm classification and climatology. *Wea. Forecasting*, **27**, 1114–1135.

——, T. E. Castellanos, A. C. Winters, C. M. Mead, A. R. Dean, and R. L. Thompson, 2013: Measured severe convective wind climatology and associated convective modes of thunderstorms in the contiguous United States, 2003–09. *Wea. Forecasting*, **28**, 229–236.

Smull, B. F., and R. A. Houze, 1987: Rear inflow in squall lines with trailing stratiform precipitation. *Mon. Wea. Rev.*, **115**, 2869–2889.

Speheger, D. A., and R. D. Smith, 2006: On the imprecision of radar signature locations and storm path forecasts. *Natl. Wea. Dig.*, **30**, 3–10.

Spoden, P. J., R. A. Wolf, and L. R. Lemon, 2012: Operational uses of spectrum width. *Electronic J. Severe Storms Meteor.*, **7** (2), 1–28.

Thompson, R. L., and M. D. Vescio, 1998: The destruction potential index: A method for comparing tornado days. Preprints, *19th Conf. on Severe Local Storms*, Minneapolis, MN, Amer. Meteor. Soc., 280–282.

——, C. M. Mead, and R. Edwards, 2007: Effective storm-relative helicity and bulk shear in supercell thunderstorm environments. *Wea. Forecasting*, **22**, 102–115.

Trapp, R. J., and M. L. Weisman, 2003: Low-level mesovortices within squall lines and bow echoes. Part II: their genesis and implications. *Mon. Wea. Rev.*, **131**, 2804–2823.

——, S. A. Tessendorf, E. S. Godfrey, and H. E. Brooks, 2005: Tornadoes from squall lines and bow echoes. Part I: Climatological distribution. *Wea. Forecasting*, **20**, 23–34.

USDA, cited 2018: Cooperative emerald ash borer project: EAB county detections. [Available online at https://www.aphis.usda.gov/plant_health/plant_pest_info/emerald_ash_b/downloads/NewCountyDetectionMap2013.pdf]

Van Den Broeke, M. S., 2015: Polarimetric tornadic debris signature variability and debris fallout signatures. *J. Applied Meteor. Climatol.*, **54**, 2389–2405.

Wakimoto, R. M., H. V. Murphey, A. Nester, D. P. Jorgensen, and N. T. Atkins, 2006a: High winds generated by bow echoes. Part I: Overview of the Omaha bow echo 5 July 2003 storm during BAMEX. *Mon. Wea. Rev.*, **134**, 2793–2812.

——, ——, C. A. Davis, and N. T. Atkins, 2006b: High winds generated by bow echoes. Part II: The relationship between the mesovortices and damaging straight-line winds. *Mon. Wea. Rev.*, **134**, 2813–2829.

Weisman, M. L., 1992: Convectively generated rear-inflow jets in the evolution of long-lived mesoconvective systems. *J. Atmos. Sci.*, **49**, 1826–1847.

——, 1993: The genesis of severe, long-lived bow echoes. *J. Atmos. Sci.*, **50**, 645–670.

——, and R. J. Trapp, 2003: Low-level mesovortices within squall lines and bow echoes. Part I: Overview and dependence on environmental shear. *Mon. Wea. Rev.*, **131**, 2779–2803.

Wheatley, D. M., and R. J. Trapp, 2008: The effect of mesoscale heterogeneity on the genesis and structure of mesovortices within quasi-linear convective systems. *Mon. Wea. Rev.*, **136**, 4220–4241.

——, ——, and N. T. Atkins, 2006: Radar and damage analysis of severe bow echoes observed during BAMEX. *Mon. Wea. Rev.*, **134**, 791–806.

WSEC, 2006: A recommendation for an enhanced Fujita scale (EF-scale). Wind Science and Engineering Center Rep., Texas Tech University, 108 pp. [Available online at http://www.depts.ttu.edu/nwi/Pubs/FScale/EFScale.pdf.]

Yuan, M., M. Dickens-Micozzi, and M. A. Magsig, 2002: Analysis of tornado damage tracks from the 3 May tornado outbreak using multispectral satellite imagery. *Wea. Forecasting*, **17**, 382–398.

REVIEWER COMMENTS

[Authors' responses in *blue italics*.]

REVIEWER A (Robert J. Trapp):

Initial Review:

Recommendation: Accept with minor revisions.

Synopsis: Using existing damage survey information, radar data, and images from Google Earth, the authors revised the tornado tracks and swaths of damaging winds generated by the QLCS on 30 June 2014 in northern Illinois-northern Indiana. They also found evidence of 4 tornadoes that were not included in the original damage assessment. The revised/additional tornado tracks were then used to create a conceptual model of QLCS tornado development with some resemblance to the development of subsidiary vortices in a multi-vortex tornado.

General/Major Comments: This paper contributes to the understanding of tornado and damaging winds within QLCSs, and seems worthy of eventual publication in EJSSM. It demonstrates how radar data can be helpful in post-event assessments, and also how satellite imagery available through Google Earth can additionally constrain these assessments.

We thank the reviewer for taking the time to perform this review, and we hope that our responses adequately address his concerns.

There are a number of limitations with the Google Earth imagery, as mostly recognized by the authors. Perhaps the primary limitation is the infrequency with which the images are updated; a further limitation is the uncertainty in the date stamp itself, which is assumed to apply to the entire image, but this would seem unlikely (see specific comments below). As possible, this potential issue should be investigated and documented, as should the general characteristics of the satellite data itself. For example, what is "high resolution" here? This request is made in part because this paper will likely motivate other similar studies of "event reanalysis".

We have investigated whether or not we can get this information. Google supplies the following information about its data sources for Google Earth:

https://support.google.com/earth/answer/6327779?hl=en

The key sentence on this page is as follows: "Google is not able to provide any more information about imagery it owns beyond what is displayed in Google Earth and Maps." For the 2013 and 2015 imagery, no information is provided beyond the standard copyright by Google on the imagery, as noted in the numerous figures where the imagery is utilized. We have consulted a satellite expert and his consultation indicated that the imagery is at least 3-m resolution, if not smaller. We have added this detail to the first paragraph of Section 4.

I do want to note here that the authors are not the first to use satellite data to aid in tornado damage assessment. Here's one:

Yuan, M., M. Dickens-Micozzi, and M. A. Magsig, 2002: Analysis of tornado damage tracks from the 3 May tornado outbreak using multispectral satellite imagery. *Wea. Forecasting*, **17**, 382–398.

I also recall a study ~10 (?) years ago (perhaps an SLS Conference preprint article?) on the use of Landsat-type imagery to reclassify a tornado in the Washington, DC area. There are several others in the literature. It is appropriate for the authors to mention these other efforts.

We have added the Yuan et al. citation as well as Jedlovec et al. (2006), Brown et al. (2012), Burow et al. (2017), and Kingfield and de Beurs (2017) to give a better idea of the scope of past work on satellite identification of tornado damage.

My only other substantial comment regards the conceptual model proposed by the authors. Although it is common to draw analogies between different scales of motion based on similarities in data, it is important to ensure that the dynamics are also similar (or least supportive of the phenomena) before placing too much emphasis on the analogy. I would argue that in this case, the endwall-vortex dynamics supporting subsidiary vortex formation in a multivortex tornado are absent in a QLCS mesovortex (see, for example, my paper:

Trapp, R.J., 2000: A clarification of vortex breakdown and tornadogenesis. *Mon. Wea. Rev.*, **128**, 888–895.)

The authors do provide qualifiers such as "a corresponding similarity in the underlying physical processes cannot be demonstrated from the data available for this study", and then also state that this model/analogy is meant to "motivate further investigation of mesovortex structure and evolution". However, because they do not provide any possible reasoning why the model/analogy may be invalid, I do worry about its premature acceptance and proliferation.

We have opted to remove the direct analogy to a multiple-vortex tornado structure. Given the damage patterns observed and the radar evolution, we stand by the general conceptual model for how the tornadoes were evolving within these two mesovortices. However, given that we do not have high-resolution mobile radar observations or dual-Doppler capabilities for analyzing the mesovortices, we agree that it is premature to directly compare the evolution of the tornadoes within the mesovortices to a multiple-vortex tornado structure. We have replaced this previous discussion with a comparison to the conceptual model presented in Schenkman et al. (2012, JAS) that another reviewer aptly pointed out may hold relevance to this case.

[Minor comments omitted...]

Second Review:

Reviewer recommendation: Accept with minor revisions.

Substantive/Major Comments: [In] section, the value of Section 7 is dubious. The authors offer a conceptual model for tornadogenenesis within the two MVs, but then go on to say that it some tornadoes fit the model, while others don't. In particular, the model seems to apply less to the stronger and more prolific MV. Moreover, the authors mention “other damaging wind mechanisms”, but don’t elaborate on what is meant by this. This conceptual model tells us nothing explicit about nontornadic winds.

I can appreciate that a conceptual model is simply a generalization, and I agree that the evolution is interesting, but I don't think that this model is quite ready to be included in the refereed literature. It's also outside of the reanalysis-scope of the paper in general. I recommend that section 7 be eliminated and used to motivate future work (e.g., the authors should try to find this behavior in other cases, and then develop robust physical reasoning to explain it).

We agree with the reviewer that such a model is premature. Therefore, we have removed Section 7 from the paper. Furthermore, we have amended former Section 8 (now Section 7) to remove references to the conceptual model and to focus on the importance of using this case as an example of how a single larger mesovortex can lead to multiple tornadoes forming within close proximity and how that may influence future damage survey efforts.

[Minor comments omitted...]

REVIEWER B (Bryan T. Smith):

Initial Review:

Reviewer recommendation: Decline.

General Comments: The authors have provided a well-written presentation of combining post-event damage survey information with non-conventional sources to describe the extent of damage from a QLCS tornado event. The notion of a new conceptual model to explain tornadogenesis within a QLCS mesovortex and adjusting earlier *Storm Data* tornado-survey information are the cornerstones provided by the authors for submitting this work for publication. I think the initial and subsequent damage survey analysis is an attempt to document a seemingly difficult damage field from a squall line with embedded mesovortex circulations. The paper provides documentation with varying degrees of supporting evidence to adjust *Storm Data* prepared originally by some of the authors. The EF ratings in the reanalysis are debatable and I have concerns about reproducibility of methods and results for revising some of the EF ratings for several tornadoes. The reanalysis did not appear to appropriately consider some of the nearby structures in close proximity to estimate the wind speed/EF rating, or the reanalysis seemingly relied too much on point data for determining EF rating rather than in context to surrounding damage indicators.

The merits for publication are largely dependent on the conceptual-model arguments proposed. However, I am unconvinced of the assertions provided by the authors and the current version of the manuscript lacks justifying evidence [i.e., observational evidence based on damage, observed sensing platform (mobile radar), numerical modeling] to support the claims of their proposed conceptual model. Furthermore, the manuscript appears deficient in using the EF-scale in order to appropriately reassign EF ratings for several tornadoes. I do not think further revisions of EF ratings and some of the tornado path refinements are enough to warrant justifying formal refereed publication with the conceptual model section removed. The authors gave no evidence-based support for operational utility despite the specific mention of these findings possibly impacting operations. Despite my recommendation to reject this paper for publication, I've tried to articulate my thoughts in order to provide information to perhaps be used to improve the paper if other reviewers and the editors do not agree with my recommendation.

While we disagree with the overall assessment of this manuscript, we hope that the dialogue that follows will clarify many of the points we attempted to make and shed light on the necessity of and motivation for this study.

Major Comments: In the Introduction re: how the findings may impact operations: Please remove this as it is currently mentioned, since this does not impact operations, an operational warning scenario, or operational workflow. I have found a concerning number of published studies that misuse and take undue association with the traditional use of the word operations when there is very little indirect association or connection to operations at all. However, if you are specifically referring to documentation of QLCS tornadoes from a damage survey standpoint, this can be connected indirectly to operations. I suggest the authors simply communicate how these findings would perhaps serve as one example in "post-event documentation" or a damage survey. There [also] was an operations mention in the Abstract. Please remove this mention.

We agree the paper would benefit from additional detail regarding the operational impacts of this case. Therefore, we have added a new section (Section 8 in this submission) to detail how lessons from this case could be applied to other cases both before, during, and after the event has occurred.

The Radom, IL event documented a "tornado family"damage pattern and the 30 June 2014 case only partially shows this pattern. It just shows a west-east progression of damage swaths with no preferred tornadogenesis-based damage swath on the right-side of the dissipating tornado damage swath. T1 to T2 from G-1 and T1 to T2 from G-2 show this, but otherwise there appears to be a contradictory damage pattern not supporting the Radom, IL damage pattern.

We have clarified this discussion to indicate that the analogy to the Radom event was more applied to G-1, which is a point that should have been made at the outset. The damage point distribution from G-1 after the initial surveys led to Radom being an apt comparison at the time. The Radom event was not considered in the analysis in G-2. G-2 benefited both by being somewhat less complex in its evolution and in moving over slightly more populated and wooded areas closer to the Kankakee River. This made determining which damage points were linked together along the path of G-2 an easier task than with G-1 (although G-2 still required significant revision in this project).

Based on the description of survey results in section 2b, the authors describe the difficulty of discerning weak damage caused by a tornado and straight-line wind. I'd like the authors to at least cite references to acknowledge the difficulty and the inherent uncertainty of differentiating between the two by using formal references. Burgess and Doswell (1988?) and some of the formal EF-scale publications would be a good start.

Doswell and Burgess (1988) make no statements about differentiating between tornadic and non-tornadic wind damage. We already emphasize these points with the end of the 3rd paragraph of the introduction section. "The damage associated with both tornadoes and non-tornadic winds, therefore, can be of similar magnitude and in close proximity to each other (e.g., Forbes and Wakimoto 1983). Furthermore, while derecho-producing MCSs lead to widespread non-tornadic wind damage, QLCSs also can produce widespread damage associated with numerous tornadoes (e.g. Knupp et al. 2014, Skow and Cogil 2017). The occurrence of "widespread damage," therefore, does not necessarily serve as exculpatory evidence against some or even all of the damage being tornadic." To further emphasize this point, we have added the parenthetical phrase "which can complicate damage assessment efforts" to the end of the first sentence in the previous block quotation.

Referring to the debris fallout—I think the authors are overextending here. These tornadoes are short-track. The motion of the tornado does not necessarily have to parallel a debris plume at 1800 ft (549 m) ARL. Smith and Spegeher (2006) found WSR-88D signatures at times differed from where damage was located by several miles, and in rare cases, 5–8 mi (8–13 km)! I noticed one scan (0327 UTC from KLOT) with a reduction in cross-correlation coefficient data to indicate debris when examining this specific tornado case. Please remove. I am not sure a version of this paragraph adds value to the paper given the limitations I mentioned above.

We will not be removing this paragraph unless requested by the editor. We reference Skow and Cogil (2017) for more on "debris plumes", or signatures associated with debris not meeting traditional TDS criteria. For this case, the freezing height was at ≈4.3 km AGL (Clayton et al. 2016) and no hail was reported in the vicinity of the Kankakee Valley mesovortices. In reviewing Spegeher and Smith (2006), the mean error in radar circulation center versus tornado location for a tornado 20–50 mi(32–80 km) from a radar site is 0.6 mi (1 km). In this case, the evolution documented in this paragraph was 25–30 mi (40–48 km). from KLOT, at the lower end of this range. Also, given the results from Van Den Broeke (2015) and the low-level wind shear profile from 30 June 2014, such errors in the debris location would be far more likely to be north of the tornado location, given a shear vector toward the north-northeast or northeast (see hodograph on the composite sounding in new Fig. 4), not south of the tornado location. The point of this paragraph is to illustrate that the TDS displacement is to the east/southeast of where the original track termination was analyzed, given the clear TDS at 0327 UTC and the continued "debris plume" remnant at 0330 UTC.

This [corn/soybean] figure is sloppy and without a doubt incorrect. I am quite shocked and disappointed this mistake made it to this stage of the review process! [Former] Fig. 5b is not corn but soybeans. There are a few corn stalks standing in the field because of leftover seed from the prior year. I find this very concerning given the level of detail the authors, some of which were involved in the survey process, are making a case for publishing a reanalysis of damage survey information. A sign on the left side of Fig. 5b remains undisturbed. If corn can't be damaged, then the winds were arguably not very intense at least along this north-south road. It seems like the net effect of a small number of failed power poles caused a greater number of them to fail. I noticed 107–110-mph (48–49 m s^{-1}) estimated speeds were assigned to the power pole damage both at the "damaged corn" point and the undamaged corn. I saw the aftermath of the 13 July 2004 derecho event near the start of the event's path along I-74 in eastern Illinois. There were pockets of blown-down corn with a couple of overturned semis. The winds were likely much lower than 110 mph (49 m s^{-1}), perhaps 75–85 mph (34–38 m s^{-1}). In Fig. 5a, the corn is not visibly damaged. It seemed like the most noteworthy damage along this road was the damage to the grain bin 200 yd (183 m) east of Fig. 5b's location (may or may not have been empty). Other damage to the north of these points were attributed to 100+ mph (<45 m s^{-1}) estimated winds. These damage indicators were a dilapidated barn and a hardwood tree in the backyard of a home. I will revisit this point about arguably excessive estimated wind speeds based on damage (EF ratings) later in the review.

Figure 5b (now Fig. 8b) consists of severely damaged to flattened corn with some weedy, short growth in the foreground closer to the highway. The first and second authors conducted the ground damage survey and specifically recall and noted the severity of the corn crop damage in the field shown in the figure and in surrounding fields. The transition from the weedy growth to corn is roughly delineating by the red line shown below:

The entire point of the figure is that this area was misevaluated in the original survey. The purpose of section 2 (now section 3) was to summarize the original survey results, how they came about, and what is wrong with them (there are numerous problems with the original results, which serves as one of the primary motivations for this paper). Additionally, under both the old and new analysis, some of this damage is identified as tornadic in nature along the northern side of the damage swath where convergence was more prevalent and a tornado debris signature was evident, and a non-tornadic damage swath being identified where damage became non-convergent in nature. For further evidence, please take the following picture, taken south of the photo in 5b (now Fig. 8b), looking northeast, into account:

We acknowledge and regret that the picture above is not the best resolution (this picture is directly off the DAT, which uses IPad cameras, but please note the abundance of pressed-down stalks in the foreground. This was significant corn damage, and the authors have correctly identified it as such. What the reviewer noted as "leftover seed from the prior year" is actually the few stalks that were not pressed down toward the ground. It should also be noted that the area where the authors took this picture shown immediately above was labeled as non-tornadic wind damage both in the original survey and in the reanalysis. The tornado classification along the north side of the damage swath was determined in part by the TDS from KLOT, a relative maximum in the severity of the corn damage, and from the grain bin damage shown above, where the bins were felled in a north-south direction, with the corn to the south being pressed down from west to east.

Also, the location north of the figure received much more damage than the reviewer implies. At this site, the barn was destroyed and numerous trees were snapped and felled in a strongly cyclonic-convergent direction, with tree falls on the north side of the damage area toward the south and tree falls on the south side of the damage area to the east. We describe this in Appendix A under the description of tornado 14, the new tornado track in which this damage occurred.

This isn't necessarily a constructive criticism on the number of tornadoes' paths documented and the accompanying uncertainties with some of the damage, but I find this paper needs to explicitly enumerate the relative impact from this event because of the sizable number of tornadoes listed. Specifically, I strongly prefer this paper include information like the Destruction Potential Index (Vescio and Thompson 1998) or some other analogous metric, in order to compare this event to a few others and better articulate the overall impact.

I'm sure the authors are well aware of the recent investigations in central Iowa with a squall line where post-event analysis with latent high-resolution satellite imagery showed dozens of small paths where vegetation was damaged. This doesn't need a reply but I'm touching on the broader philosophical notion of tornado/nontornado. Should the NWS classify all of these small (sometimes tiny) convergent paths as tornadoes? It gets into the question of what is a tornado when all scales of vortices can be classified as tornado from deep/moist convection. I'd argue a relatively large percentage of QLCS tornadoes are in fact boundary-layer vortices that develop along the gust front/density gradient but are not connected to a deep updraft but rather more of partially forced sharp slab ascent with convective speeds (rather than synoptic speeds) associated with the rising air. In summary, please relate this event in context to other single tornadoes or several tornadoes from a single event since some emphasis has been on the tornado number. For example, the 17 November 2013 tornado outbreak affected Illinois and Indiana. This outbreak featured 25 and 30 tornadoes from Illinois and Indiana, respectively. The two supercell tornadoes that caused the EF4 [damage] in central and south-central Illinois were the remarkable events, not the dozens of weaker QLCS tornadoes farther east in parts of Indiana and adjacent states. Using DPI as a metric to proxy potential impact, the tornadoes from the 17 November 2013 tornadoes in Indiana exhibited a *much greater* impact compared to Indiana, in terms of the tornado hazard.

We feel this is not germane to the focus of this (already dense) paper. While we do mention the number of tornadoes several times, our focus is on the documentation of this event and the integration of surveys and remote platforms in forming a full picture of what transpired during the event. We make no allusion to the significance of this number other than it is a primary statistic of the event. We feel that attempting to place this in historical context would only serve to lengthen an already long manuscript.

Furthermore, this paper only investigates a relatively short portion of the entire evolution of the second derecho. As described in the first paper (Lyza et al. 2017), it is highly likely that the tornado count for this event is under-recorded, even taking the results from this paper into account. We report numerous instances of clear, distinct TDSs in Lyza et al. (2017) that went without formal surveys and/or tornado classifications. Additionally, we have already been able to uncover other likely tornado tracks from this event outside of the Kankakee Valley by pairing damage reports, satellite imagery, and radar data from other mesovortices. A cursory review of damage reports, satellite imagery, and radar data leads us to believe that the likely number of tornadoes that occurred with this event is conservatively within the range of 45–50, while the revisions in this paper would bring the "official" total to 33 if no other re-evaluations outside of the Kankakee Valley are taken into account.

The historical shortcomings of the official tornado record are not lost on the authors. However, we feel it irresponsible to make a focus of putting this event into any sort of historical context when we know with a high degree of confidence that even this paper does not alleviate other major errors in the recordkeeping of this event. Therefore, the purpose of this paper is left to focus on this one particular aspect of the second derecho, the cluster of tornado tracks and significant wind damage in the Kankakee Valley.

As for what does or does not constitute a tornado, we really do not wish to open this conversation with this paper. Our classification of "tornado" for these events is based on the fact that they are a) not gustnadoes, as the gust front of the QLCS is clearly not surging ahead of the convection, and b) not dust devils or other similar boundary-layer vortices. These circulations are clearly associated with the deep convective updrafts at the leading edge of the QLCS, they are deep enough to distort the Doppler velocity field, and a few of them are strong enough to loft debris to radar beam height, despite these vortices not being immediately adjacent to KLOT. Therefore, we classify these as tornadoes and leave the question of what types of vortices do or do not constitute tornadoes to be the subject of later work.

Re: mesovortex G-1: Since the *Storm Data* (8 tornadoes) vs. the reanalysis version (at least 14 tornadoes) is not conclusive at this point to the reading audience, I strongly urge the authors to differentiate the addition of the damage swaths as being introduced in the paper as "tornado-like damage swaths" or something similarly worded. It is optimal to articulate the uncertainty of classifying the damage swaths as finding additional damage that was either tornado-equivalent damage from straight-line winds or a weak tornado. Since the authors state these additional damage swaths were from tornadoes, just add a sentence stating the reason why the swaths were reclassified (i.e., convergent paths).

All but two of the new tracks consist at least partially of analyzed damage from the original Storm Data. In each case, the declaration of a tornado was based primarily off of the discovery of cyclonic-convergent *damage along a track with a high length-width aspect ratio. The satellite imagery was used primarily to fill in gaps along the actual tornado tracks and connect the proper damage points together. The only two tornadoes tracks introduced with no ground survey information are the new T5 and T9 described in Fig. 13 and in Appendix A. To communicate this, we have added the following sentences to that portion of the text: "Only two of the 14 reanalyzed tornado consisted of entirely satellite-derived damage information. All 12 other tracks had damage points that were declared tornadic in the original Storm Data, but were erroneously grouped with damage from other tornadoes to form the original track assessments."*

Section 4a Mesovortex G-1, 3rd paragraph: This appears to be favoring the classification of mesovortex plus damage equals the justification for tornado. I certainly concede this to be the case when a reduction in cross correlation coefficient is readily apparent. However, it is certainly possible that damage from a mesovortex may result in straight-line winds and not a tornado. This reanalysis appears to disproportionately seek tornado damage based on base-moment radar data. Can these same methods be applied at farther distance from a radar (higher ARL) and with broadening beam width? My initial thought is this methodology for tornado classification would be very difficult, if not impossible, to reproduce!

As previously stated, all but two of the 18 tornadoes identified in this paper were at least partially surveyed from the ground (T5 and T9 from G-1 being the exceptions). In every single case, damage was relatively narrow and cyclonic or convergent in nature at the ground-surveyed damage locations. Furthermore, the points of tornado damage stood in stark contrast to immediately adjacent areas that had no signs of wind damage whatsoever, as stated in the text. The discussion about the use of radar to aid in the analysis of the tornadoes is really focused on three points:

1) *The weaker-end spectrum of events where convergent and cyclonic wind may be more difficult to identify in the damage (discussed at length later on in these responses),*
2) *To aid in pairing the correct damage points together when most of the damage locations are small, discrete, and spaced apart relative to one another, and*
3) *To glean some basic information about how these tornadoes may have been evolving in the context of the broader parent mesovortex.*

Also, in the places where radar was weighed a bit more heavily in actually determining the cause of damage, it was most often used to rule out a tornado in areas where we were uncertain of the cause of damage, but could not completely rule out an embedded tornado during the damage survey. Most of the non-tornadic wind damage areas were determined by reviewing radar data and noting that there were no enhanced wind shear or circulation signatures in velocity and that spectrum width was low and relatively uniform, consistent with non-tornadic downburst winds. This analysis was necessary because there was evidence of microbursts, especially within the broad region of significant non-tornadic wind damage from G-1, and the orientation of these microbursts and the more significant wind damage areas led to uncertainty as to whether or not we had missed additional tornadoes, given the evidence of numerous tornado tracks nearby. In this case, radar gave us the confidence to leave areas south of T13 and T14 from G-1 as non-tornadic damage and in fact expand the area of non-tornadic damage based off satellite imagery of areas not originally surveyed. We have added this point within the main manuscript text.

Radar beam height has nothing to do with the damage at the ground and the *damage survey* (supplemented at times with reduction in cross-correlation coefficient) has everything to do with the documentation of tornado damage observed at the ground. There is either tornado damage or there is not. The degradation of low-level radar coverage has nothing to do with tornado damage. Radar data can be used to assist in scouting damage survey areas, but intertwining confidence in whether damage is caused by a tornado based on radar beam height is indirect and a slippery slope. Please edit if the currently worded statement is not what was intended—otherwise remove it from the paper.

The height of the radar beam above ground level and the size of a radar bin affect both the radial velocity interpretation AND the potential for debris detection through cross-correlation coefficient reduction. The complication of the damage pattern of a weak tornado caused by the effect of fast translation can make determining tornadic vs. non-tornadic damage very challenging (more discussion about this is provided in *later responses). While a TDS is certainly the most definitive evidence of a tornado on radar, the lack of a TDS does not preclude the cause of damage being tornadic in nature, and the presence of a tight rotational couplet can aid in damage classification if the initial damage survey is inconclusive. The role of the distance between radar and damage, therefore, is completely germane as currently discussed in this paper. The increase in distance between a radar and damage can adversely impact the declaration of damage as being tornadic or non-tornadic in nature, particularly in cases where fast translation can blur the distinction between tornadic and non-tornadic wind damage patterns. We have added some clarifying language to this effect, but stand steadfastly by the overall message intended in these statements.*

Mesovortex G-1 [text] and [then] Figs. 11–12: I think the authors overestimated the wind speeds and resulting EF scale associated with tornado #3 from mesovortex G-1. I find the damage survey analysis to likely be non-reproducible and varying, when considering a larger sample of qualified persons to conduct a reasonably accurate damage survey. The currently articulated justification given for an EF2 rating is an exposed area of heavily damaged softwood trees (based on trees evident in Fig. 12) and a small shed destroyed. What about the damage to the house? What appears to perhaps be a white pine tree in the damage photo is a species notorious for exhibiting damage compared to one-leader trunk oak trees. Considering the minor damage from the house located tens of feet away, it must be stressed that including the “whole picture” of the damage scene must be incorporated into the EF rating at this site. I fail to see compelling evidence of EF2 damage. It appears to be lower-end EF1. I independently had one of the world’s foremost experts on rating tornadoes and this person specifically mentioned upper EF0 and lower EF1 estimated wind speeds.

For EF2 ratings, we required that the average of the two maximal DIs at each location would still yield a maximum wind in the EF2 range. Why the house damage was minimal for the site where we label damage EF2 in tornado 3 is explained clearly with Fig. 17. While it is important to consider the context of an entire damage scene, that fact that a tornado’s wind speed can vary greatly over an extremely small distance should not be lost in the survey process. Just because a tornado impacts a property does not mean that the tornado expands such that the property sits completely within the radius of maximum wind.

One good example of this is a video of a tornado from Leighton, Alabama, on 8 May 2008. This video can be found here: https://www.youtube.com/watch?v=Tk4Q7eUoaUY. This tornado was rated EF2. Note the extremely small size of the vortex. It is strong enough to lift and move large cars and pickup trucks, but an immediately adjacent power pole is left untouched. The lack of damage to the house does not necessarily indicate a lack of intensity of the tornado, particularly in the context of the tree damage around and in front of the house being significantly weaker than the tree damage behind the house. Context is indeed useful and necessary, and in this case, the context of the surrounding damage indicates the house was not inside the radius of maximum wind.

Conceptual model: No supporting physical evidence is provided in the paper. The authors try to relate vortices within one of the largest documented tornadoes (3 May 1999 Mulhall, OK) and sampled by DOW data to WSR-88D imagery from KLOT. The DOW radar yielded a very high-resolution picture of the Mulhall tornado and incipient vortices, which provided great detail at a very close range and height ARL. Conversely, KLOT imagery for the Kankakee Valley tornado cluster is much lower resolution due to the physical radar itself (S-band) and the distance/height ARL issues. Furthermore, the resolution and scales of the vortices (i.e., Mulhall vs. Kankakee Valley tornadoes) are at least 1-2 orders of magnitude different! The WSR-88D can’t truly resolve a tornado even when there is a large vortex at close range. It can only show the larger parent circulation. Mobile radar is specifically equipped to complete this task and that is why smaller-scale vortices were resolved with the Mulhall event. The authors offer no mobile radar data supporting the notion of the conceptual model.

Furthermore, no numerical model simulation is provided. What should the audience take the conceptual model on, faith? The burden of proof is undoubtedly on the authors to supply a convincing argument for a new theory/conceptual model. Looping through KLOT WSR-88D imagery, I found no consistent signal that could be identified and thus applied to integrate radar signatures with the conceptual model that the authors propose. If the idea of tornadogenesis within the mesovortex towards the back of the larger vortex is supposedly truth, the tornado paths would subsequently form (due to the cyclonically rotating motion of the tornadic vortices around the parent mesovortex as the mesovortex moves east) on the right-flank of the parent mesovortex. The subsequent tornado paths would be located to the "right" of the dissipating tornado's path—similar to the Radom, IL tornado paths. This would be akin to the well documented "handoff" process that commonly occurs with supercell mesocyclones. The map of the tornado damage paths from the 30 June 2014 event actually shows subsequent tornado paths deviating to the "left" in most cases. This development of tornadoes to the left would be contradictory to the proposed conceptual model and would lead to questions concerning whether those paths are in fact microburst swaths rather than tornado paths.

The allusion to multiple-vortex tornadoes was used due to the similarity of the radar appearance as shown in former Fig. 18, as well as the similarity to the likely generation location of the 30 June 2014 tornadoes being located in the back of the parent vortex. Given the lack of mobile radar observations, dual-Doppler coverage, and simulation experiments, we have removed the analogy to multiple-vortex tornadoes. However, we stand by the original conceptual model figure, which was developed primarily off of the damage surveys and satellite imagery and through comparing the track results with KLOT radar data.

Additionally, the reviewer's idea of the conceptual model directly contradicts itself. "If the idea of tornadogenesis within the mesovortex towards the back of the larger vortex is supposedly truth, the tornado paths would subsequently form (due to the cyclonically rotating motion of the tornadic vortices around the parent mesovortex as the mesovortex moves east) on the right-flank of the parent mesovortex." These two statements are outwardly contradictory. The tornado paths begin at tornadogenesis. We do not propose tornadogenesis occurring or tornado paths beginning on the right side of the mesovortex. We propose them forming in the back of the mesovortices and revolving counterclockwise until dissipation on the right side. This would place the paths in the right-rear portion of each mesovortex, with a deflection of each track toward the left at the end of each tornado lifecycle and new tornado tracks beginning to the left, not the right, of old tornado tracks. Fig. 21 illustrates how tornadogenesis in the back of each mesovortex would lead to new tornadoes forming to the left of the previous tornadoes, as is seen in each case for G-2 and in most cases for G-1 and which the reviewer seems to think is contradictory to what should happen. It is not contradictory. The reviewer's idea of paths starting the right side of the mesovortex is not in concert with what we describe in the text or in the conceptual model presented in Fig. 21, nor is it consistent with what would actually happen for tornadogenesis occurring in the back ends of each mesovortex and dissipating on the right flanks.

The conceptual model should not be taken simply on faith. It was not developed simply on faith. It was developed by closely linking the damage survey results to the radar evolution. We are quite cognizant of the fact that the radar data are insufficient to fully resolve individual tornadoes and all the intricacies of their evolutions. The regions of enhanced shear and spectrum width within G-1 and G-2 are maximized in the rears of each mesovortex, and the tornado track behaviors are generally consistent with a rearward location of tornadogenesis and right-flank location of dissipation within each mesovortex, as explained in Section 6. The proposed conceptual model is simply that: a proposal requiring further examination. Modeling studies certainly would shed light on the veracity of this proposal and therefore are encouraged, but are beyond the scope of this paper. We have datasets of a couple of these larger mesovortex cases that moved into high-resolution dual-Doppler coverage during VORTEX-SE (e.g. Knupp et al. presentation from the 2018 Severe Local Storms conference) that we hope will shed more light on the dynamics of these features.

The sentence mentioning, "Non-tornadic winds cannot be assumed just because damage occurred over a relatively broad area," is an incredible statement and I find it potentially disturbing and perhaps indicative of systematic bias in the manner in which damage was assigned the binary tornado or no tornado designation. I think it is a fair assumption when a broad swath of wind damage is observed from damaging gusts, it is not caused by a tornado or series of tornadoes. Conversely, tornadic winds cannot be assumed just because there was damage at the surface associated with a relatively crude depiction of a mesovortex circulation sampled at 2000–3000 ft above radar level! Please remove this statement.

We in no way imply or intend to imply that the mere presence of a mesovortex is sufficient to confirm a tornado. It would have been clearer for us to have stated something to the effect of "the mere presence of *numerous, concentrated damage reports over a broad area is not sufficient to presume non-tornadic wind damage in and of itself", and this is what we have done in this revision. We did not and do not intend to convey that a broad area of uniform or near-uniform wind damage is tornadic in nature or that the null hypothesis of causality of damage should always be tornadic in nature.*

I mentioned this elsewhere in the review comments but I figure I would mention it here as part of a constructive criticism of this paragraph in reference to 3) the proximity of the nearest available radar and the scanning strategy during the event. Other than dual-pol tornadic debris signature, radar should have *no* influence on the classification of a tornado. This can only be done *directly* via a post-event damage survey.

We strongly disagree with this assertion, and this is one of the major operational (or post-operational) points of this paper. In cases of fast-moving, weak tornadoes, radar can and should serve as a valuable influence in helping determine the cause of damage. A weak, fast-moving tornado can easily cause damage that appears nearly "straight-line" in nature, difficult to distinguish tornadic vs. non-tornadic wind damage. Consider the following example of an idealized Burgers-Rott vortex translating at 26 m s^{-1} *(50 kt).*

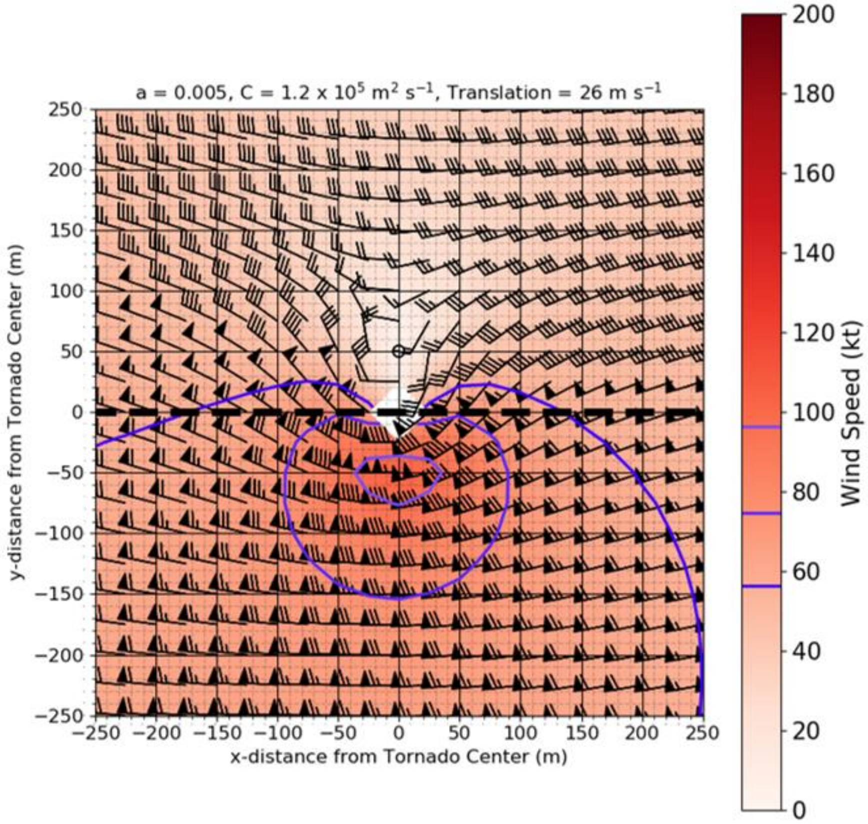

As shown by the blue EF-scale contours, if it is assumed that all of the translation velocity of the vortex can be added to the wind field of the vortex, then all but a small fraction of EF0+ winds would occur on the right side of the tornado relative to its translation. In the case of this idealized vortex, all EF1−EF2 damage would occur on the right-hand side. Furthermore, with a translation speed this fast, it is conceivable that trees, power poles, or other structures may reach their failure points at the front half of the tornado, and that features not damaged at the front end of the tornado may not be damaged in the back half. Certainly this is an idealized case that assumes a uniform wind field around the tornado center, but if most of the damage is caused at the leading edge of the tornado, the damage could conceivably appear cyclonic-divergent in nature. While radar alone absolutely cannot be used to definitively determine the presence of a tornado without a TDS being present, it is important to be able to incorporate it in cases where the cause of the damage is nebulous after a survey.

Appendix A, tornado documentation and EF rating: Tornado 1: A narrow corn flattening swath and 1 power pole broken (it could have fallen and been oriented in a westerly direction due to a multitude of factors) alone does not alone offer compelling evidence of a tornado!

In reviewing this tornado track, we discovered a homestead in satellite imagery very near the original track that lost a substantial number of trees (≥5) between the 2013 and 2015 satellite images. Given that the trees appeared healthy in the 2013 imagery and that the homestead was < ⅛ mi (0.2 km) from the original track, we have slightly modified G-1 tornado 1 to include this site. This analysis also prompted us to conduct a careful review of the rest of the satellite imagery along G-1. We found a couple additional likely damage points, consisting of tree falls that were still not cleared prior to the 2015 imagery, not found prior to original submission. We also examined several dozen additional locations near and within the path of G-1 to ensure that no noticeable damage was left out of the analysis, with these locations being noted as having no damage. When combined with the ground and aerial survey information as well as radar data, we decided to terminate G-1 tornado 3 earlier than in the prior submission and extend G-1 tornado #5 farther to the east-southeast past its original damage point.

These track changes do not indicate a substantive change in how we believe tornado evolution was occurring within the mesovortex but merely serves to better represent the information available through satellite imagery, the survey information, and radar data. Finally, we ceased discretizing the G-1 wind damage areas in order to acknowledge the likelihood that there were other areas on non-tornadic wind damage along the southern periphery of G-1 that are still not and will likely never be documented.

Tornado 3: Does not appear consistent with EF2. See the earlier comment on damage rating in the context of other structures.

This rating will be left as EF2. A full description of the context of the damage to this property, including reasoning as to why the house sustained minimal damage, is given in Section 5. This damage was not rated in a vacuum by the authors but also featured significant consultation with an arborist who is a foremost expert on tree damage from tornadoes. The expert was sent a representative photograph of the tree damage without any commentary about what we thought the damage rating should be so that he could form an independent opinion. That expert's suggestion was high-EF2 to low-EF3 damage. Using our methodology of blending maximal DODs independently yielded a low-EF2 rating, which we feel comfortable maintaining in light of the expert's opinion.

Tornado 6: An old/dilapidated barn EF2 rating while the nearby house had minimal damage. Does not appear to be rated in context to the other structures at the farmstead location.

This "nearby house" did not receive "minimal" damage. It was torqued enough on its foundation that it required demolition, as described in the text. Furthermore, additional structural damage to outbuildings near the beginning of the track further supports a low-EF2 rating.

Tornado 8: Damage does not appear consistent with EF2 but rather high-end EF0 or EF1.

We would like additional details on how the reviewer came to this conclusion. As described in the paper, EF2 ratings were assigned based on a blending of maximal DODs at a given damage location in order to account for the context of the damage scene in a more formal, at least somewhat-objective manner. Without an argument for this judgement, we are strongly inclined to maintain our original assessment, based off the DIs and DODs described in Table 2.

[Minor comments omitted...]

Second Review:

Reviewer recommendation: Decline.

General Comments: I am disappointed the authors failed to adequately address my very strong concerns about several issues I mentioned to be deficient in my original review. First, the authors did not provide enough observational evidence (i.e., radar) or a numerical simulation to support a proposed conceptual model of tornadogenesis within a mesovortex. Inappropriately relating radar data from a WSR-88D from ≈30 nmi (56 km) distance to features not resolvable to the resolution of a WSR-88D is one of my primary concerns.

Secondly, the classification of tornado damage versus straight-line wind damage is uncertain, especially when the damage is weak. The authors have expressed a reluctance, and in some cases, an uncompromising refusal to include mentions of uncertainty and compare this event using a metric (i.e., DPI) to other tornadic events. I highlighted portions of the paper where the assigned damage intensity is arguably not being considered in context to nearby structures/vegetation, and some of the estimated damage intensities (i.e., EF-scale, specific DIs' damage-assigned mph) appear inflated. In summary, I can't foresee the authors satisfying my primary concerns and it is with regret I recommend this paper be rejected for publication in EJSSM.

In the case the authors are willing to entirely remove the conceptual model section, reevaluate the damage intensities by an outside group of 3rd-party experts (I can offer names of willing experts), and include other suggestions (e.g., event comparison to DPI)—a path towards publication is possible. The paper would largely become a case study documenting the complexity of a tornadic QLCS. I realize the authors may be frustrated with my review and my current recommended decision. I wish the authors the best in whatever course of action they pursue.

The latest version of the text has been extensively edited in an attempt to address many points of miscommunication that were apparent after the second review, as well as address the reviewer's concerns.

Major Comments: The authors discuss in the first paragraph of section 8 (Operational considerations) how a potentially tornadic QLCS poses challenges, including the mention of pre-event messaging and effective warning strategies. There can be a link to pre-event messaging based on forecasts of the environment and updated technical information such as surface observations to describe outflow boundary placement and nuanced information from a sounding profile. There is an unsubstantiated link to warning strategies. Please discuss provide how warning strategies would be altered from existing strategies. Unless this is provided, it is this reviewer's opinion (operational forecasting background) that this study provides little applicability to "operations" except for describing a nuanced way of performing a storm survey and pre-event messaging. There is a mention of how this study may impact operations in section 1 [one sentence]. The operational impact should be readily apparent to the reader. Please provide additional information.

The discussion regarding applicability to warning strategies could indeed be strengthened. Section 8 now explains the relevance of this study to recognizing the tornadic potential of a QLCS, issuing appropriate warnings, achieving greater probability of detection and lead times for QLCS tornado warnings, and accurately communicating within impact-based warnings the hazards posed by a tornadic QLCS.

I've inserted a sounding from the SPC mesoanalysis archive for a point in southern Lake County, IN at 41.28N, 87.35W. I modified the surface for 76ºF (24ºC) temperature, 74 ºF (23ºC) dewpoint, and a surface wind 130º at 7 kt (3.5 m s^{-1}) based on Fig. 4. I likewise set the storm motion on the hodograph to 48 kt (24 m s^{-1}) around 275º. I did not go to the effort of trying to examine Wolcott, IN profiler data but I think the RAP-based mesoanalysis data (include wind-profile information) but I think the sounding profile is a reasonable proxy. The authors are welcome to use the sounding if they see fit.

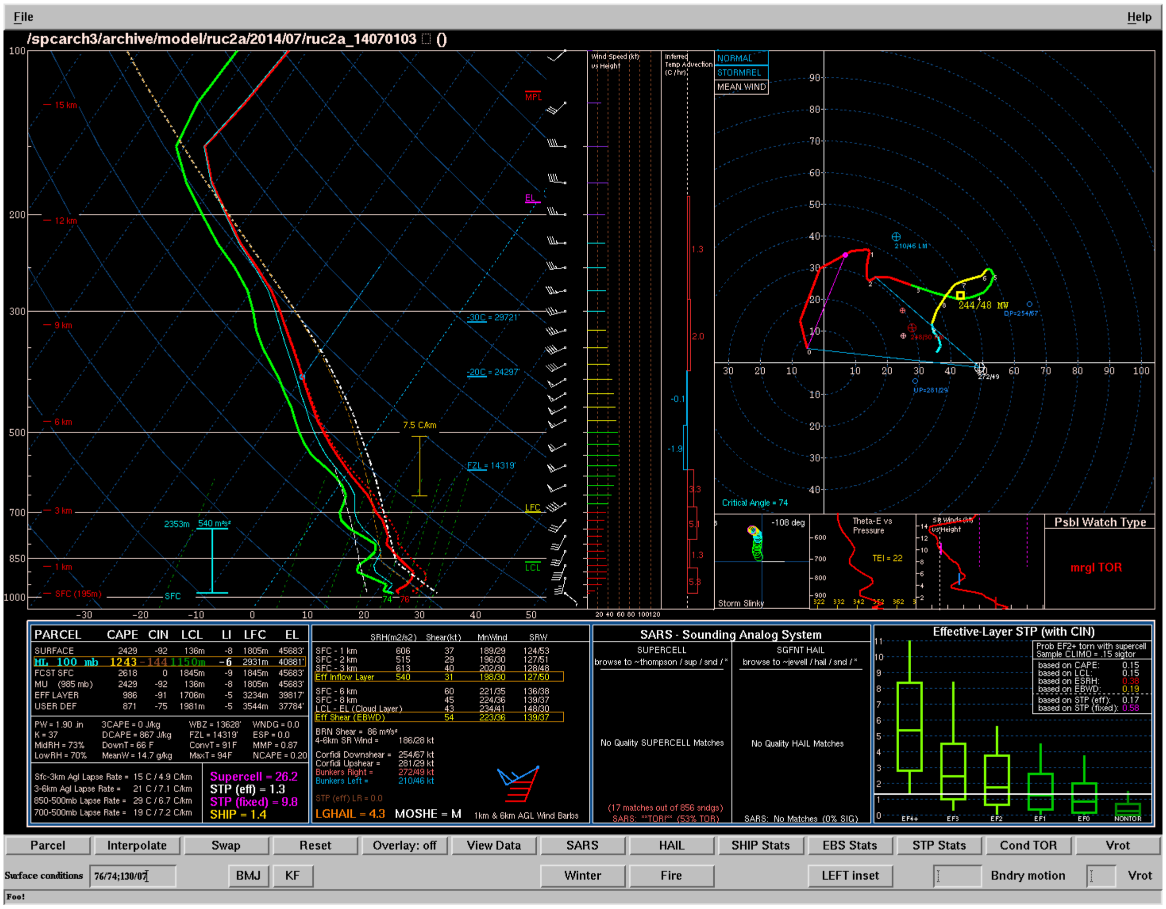

We opt not to use this sounding. The primary reason is that the moisture profile appears too dry in the storm-inflow layer immediately above the surface layer. While a similar moisture profile was observed by the AMDAR soundings at KMDW in the wake of the first QLCS, the 0000 UTC sounding from ILX indicated rich boundary-layer moisture extending up to ≈875 mb and likely is more representative of the storm-inflow layer above the surface inversion. Furthermore, the hydrolapse in the PBL on the RAP sounding is substantially more dramatic than that observed on the raw MDW sounding behind the first QLCS. The hydrolapse on the above RAP sounding appears to reach a minimum T_d of 13–14°C at ≈875 hPa. The MDW observed AMDAR sounding in the wake the first QLCS has a minimum PBL T_d of 17°C from 950–921 hPa in the remnant cold pool of the first QLCS. While we acknowledge that the composite sounding provided may contain errors, we believe that the likely errors in the RAP PBL profile preclude it from adding much useful information to the manuscript. 0000 UTC ILX sounding:

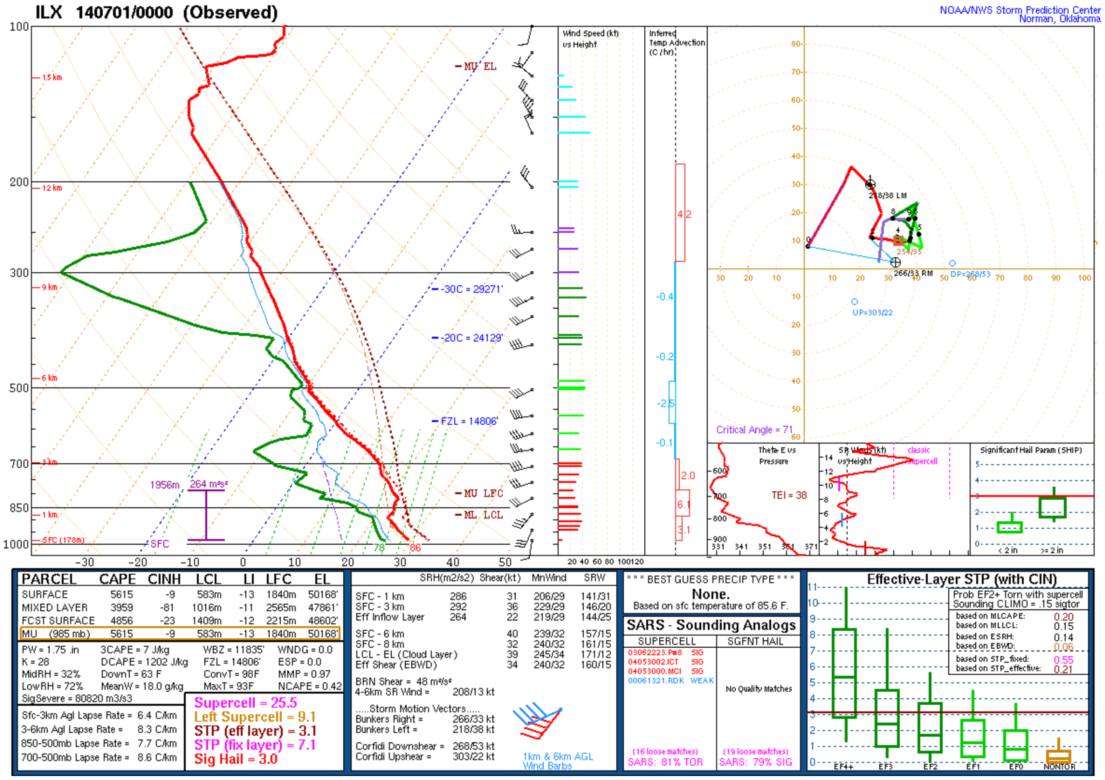

0237 UTC AMDAR sounding (Fig. 5 from Lyza et al. 2017):

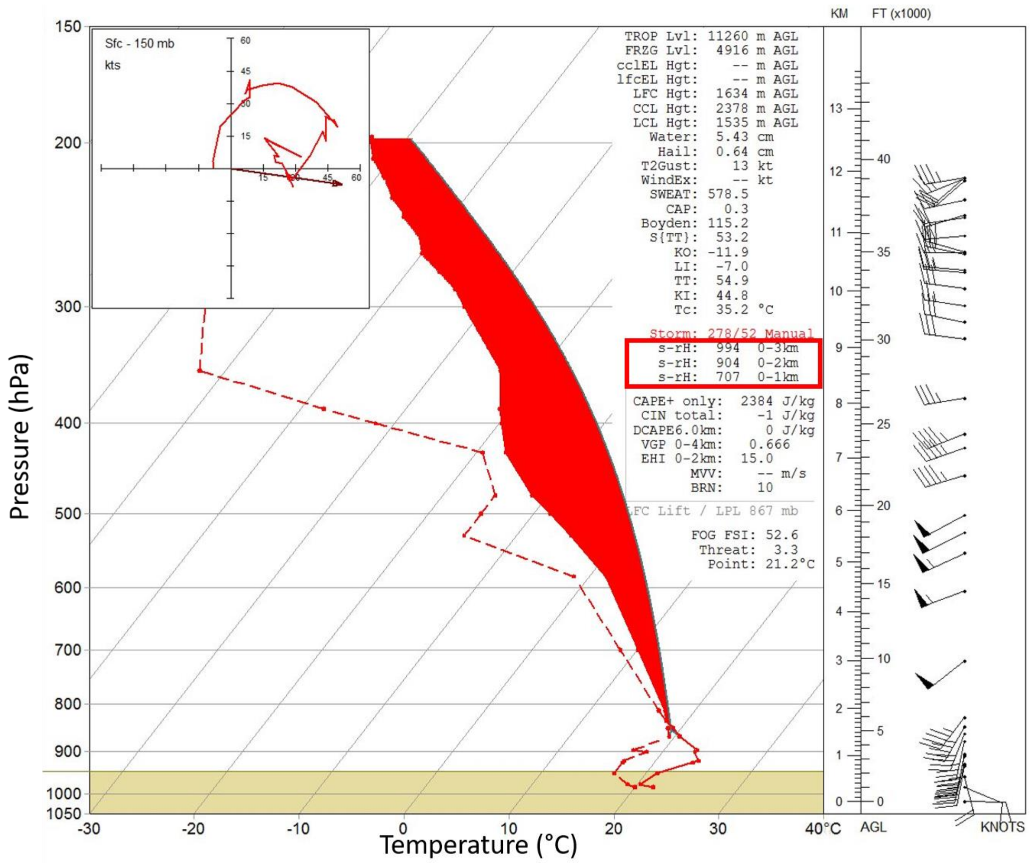

There is no radar-based evidence for making a strong association in the evolution (other than being mesovortex in character) between the Radom, IL and the Kankakee Valley events. I have examined both cases in great detail. What the authors are left with is an argumentative attempt in the tornadogenesis/tornado evolution process in terms of a series of tornadoes (from the Radom, IL event) to being similar for a few tornadoes and contradictory for others based on their damage pattern.

We understand this. The point of this section of the paper is to highlight exactly why the conclusions from our original survey efforts led to an incorrect assessment of the event. We have added clarifying language in the paper to discuss exactly the role that comparison of the 30 June event to Radom played in the initial results.

I guess I need to be more explicit in my request [re: discerning nontornadic vs. weak tornadic damage]. Please describe the relatively high uncertainty weak EF-scale damage poses to the classification of whether damage is tornadic or nontornadic. This has not been adequately addressed via acknowledgement in text and in references.

We have added a discussion about the uncertainty of damage cause designation at the end of section 4. Instead of Doswell and Burgess (1988), we cited Forbes and Wakimoto (1983), which explicitly discusses this uncertainty in the context of a complex QLCS tornado event.

I request the Editor examine this TDS signature since there is an impasse. The convective line motion is around ≈275° at ≈48 kt (24 m s^{-1}) based on archived KLOT imagery from around the time of the TDS signature. Why could the debris (possibly leaves) not be advected in a manner corresponding to the larger convective system motion once the "debris" was centrifuged from the vortex? I don't doubt other heavier or less aerodynamic debris was transported along the tornado path beneath radar beam height. The authors seem to be trying to explain a simple scenario with a more complex explanation. The point of including the Speheger and Smith 2006 reference is to convey to the audience where a signature is explicitly georeferenced on a radar display does not exactly correspond to where a related feature is located at the ground.

[Editor's Note: This doubtless is a debris signature, the question being its physical source. Was it tornadic, or lofted into the updraft in strong inflow? What is the evidence (and uncertainty) either way, at that distance, given beam-sampling considerations? If the authors choose to keep this discussion, the uncertainties involved in both debris source and tornado vs. debris location should be much more clearly addressed and articulated. This may be an acceptable compromise to the "impasse", depending on the discussion that results in the text.]

We have added additional discussion of the uncertainty of what caused the behavior of the TDS to the paper. The point of this discussion was not to firmly commit to a cause for the TDS behavior or provide it as absolute proof that the original surveys were wrong, but rather to describe it as part of a pattern of potential inconsistencies that we had observed prior to finding more definitive proof that the survey results were incorrect. We more clearly explain this in the paper now as well.

[Re: corn vs. soybean contention in former Fig. 5] I stand by my claim the authors have misinterpreted crop type in Fig. 8b and the damage survey includes vastly overestimated wind speeds associated with the damage along the road where the power poles have been snapped. The overestimation of wind speeds is still pervasive in this paper and I am using this specifically as one example. Figure 8a (looking east) is located roughly 30 m to the north of the west-east gravel driveway in the image below. Figure 8B was taken at the southeast part of the driveway-road intersection looking southeast. There is no corn damage located at Fig. 8A (located in the center portion of the tornado path) whereas shorter vegetation is shown in Fig. 8B. These are soybeans with sporadic stalks of corn interspersed from a previous year. The image I provided below shows a satellite image from late in the 2014 growing season (notice the damage to the grain silos). There are two different colors associated with the field located north and south of the west-east driveway and the crops are different to the north and south of the driveway. I rest my case, it was mostly a shorter crop in the field with most of it soybeans. Because the power poles were damaged but little if any corn damage was noticed at Fig. 8A, I completely refute the idea of 110-mph (49 m s^{-1}) estimated wind speeds snapped the power poles but left the corn undamaged! The authors need to correct the labeling in Fig. 8B or simply remove the figure from the paper.

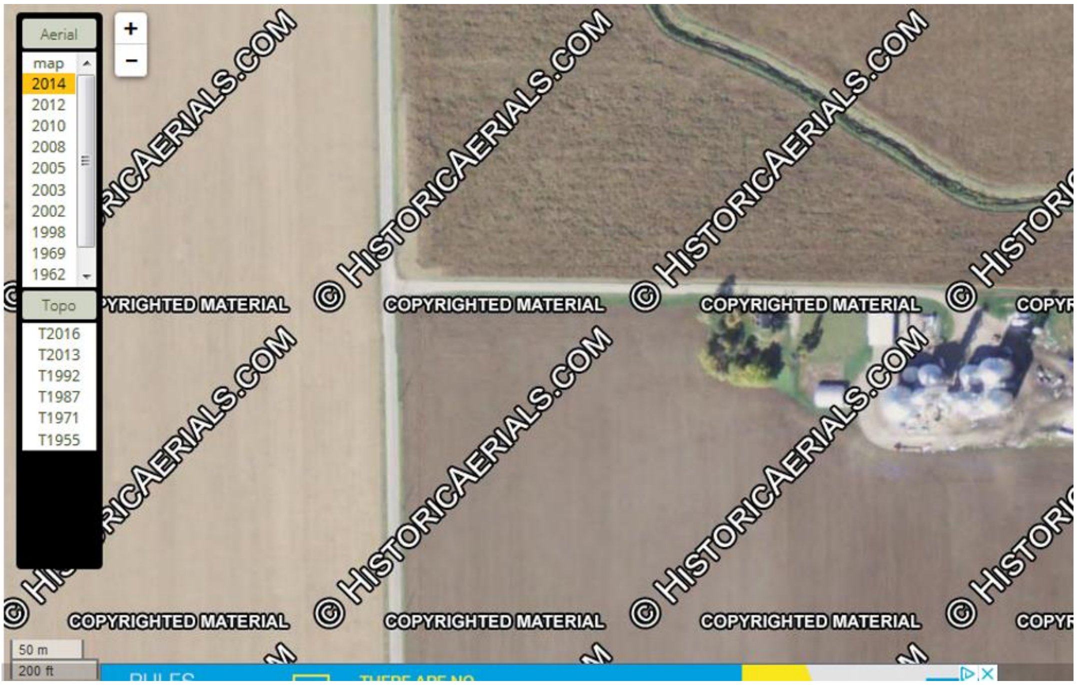

We are extremely confident in our assessment of crop type at this location. The imagery offered by the reviewer is not disproving of the authors' assessment. In fact, the reviewer has erroneously identified empty fields (the southeastern and the western fields) as fields definitively containing different crops from the northeastern field. The simplest explanation for the differences in field color, particularly given that this image is from late in the growing season, is that the bottom and left fields were already harvested. These barren fields could simply be different colors due to different soil moisture, possibly linked to the timing of the harvest and tilling for each field. We have a contemporaneous note in the DAT from the initial ground survey that states the third field, the one on the west side of the street, was also a corn field that sustained crop damage from the event.

As an aside, one of the co-authors consulted a brother who is a farmer in east-central Iowa. It has been common practice in recent years to treat soybean fields with an inexpensive (<$1.50 per acre) herbicide to eliminate rogue corn. This is well worth the cost since the rogue corn will reduce soybean yields. Thus, the presence of corn within soybean fields, especially of the density shown in the preceding images, is highly unlikely.

Furthermore, this argument about the type of crop that was present in these fields plays zero bearing in the final results presented in this paper. The discussion in Section 2 of the paper is about why the reanalysis was performed. The reviewer points out that, "Because the power poles were damaged but little if any corn damage was noticed at Figure 8A, I completely refute the idea of 110-mph (49 m s^{-1}) estimated wind speeds snapped the power poles but left the corn undamaged!" That is exactly the point of this part of the paper. The initial assessment included the point in 8A within an assessed tornado track. This is clearly wrong. We believe that the power pole damage at point A was due to a combination of tornadic and nontornadic winds to the south of point A and forces exerted along the power lines that led to the failure of the other poles to the north.

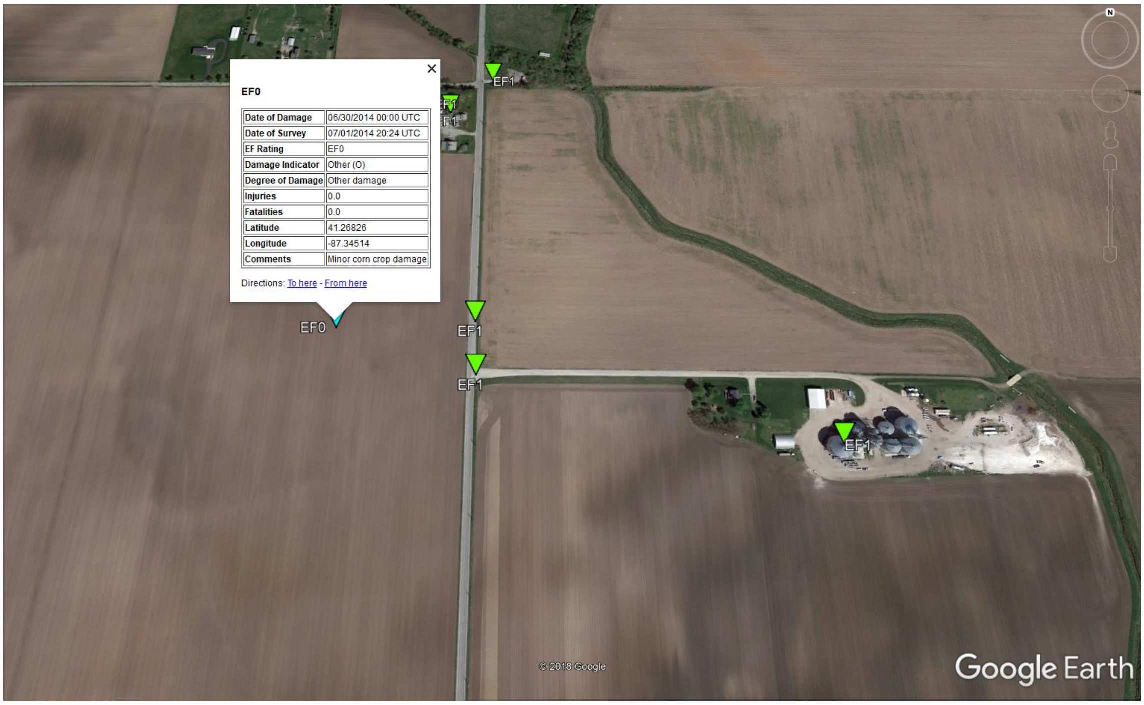

Even if the reviewer and reader were to believe that the crop damage at point B was nonexistent and that short crops were in place in that field, we know definitively that damaging wind occurred at this location due to the destruction of the large grain bins just east of the highway. We assess this damage to be tornadic nature based on:

1) The north-south failure of the grain bins, indicative of convergence toward the core of the damage;

2) The presence of satellite-discovered damage upstream of the location that lends itself to a continuous, long, narrow path; and

3) The presence of enhanced embedded shear, high spectrum width, and a possible TDS very near this location.

Some of this damage was confirmed through contacting property owners via telephone. Damage to the south of point B was attributed to non-tornadic winds due to its broad, divergent nature (albeit with pockets of enhanced damage, possibly due to microbursts), the lack of any enhanced spectrum width or shear signatures, and eyewitness interviews that noted a long period of damaging wind at those locations. Point A is not included in any tornado track, and we do not consider it to be a point where damaging wind occurred at all.

With all this having been said, because we cannot supply better-quality photographs of the crop damage nor contact the owners of the property, we have amended Fig. 8b and the map point to focus on the indisputable damage to the grain bins at that location. These bins, as stated above, serve to support the exact same argument originally made using the differences in the crop damage. Furthermore, we have added Fig. 18 to clearly illustrate how the reanalysis has changed our interpretation of the damage.

This paper needs a frame of reference in terms of overall damage potential from this event. I earlier suggested the Destruction Potential Index (Vescio and Thompson 1998) and this suggestion must have been lost within a general reply to my comment about what constitutes a tornado from a squall line and the gray area or spectrum that some vortices fall in between. I think it should be mentioned for a sentence or two. This is not an undue burden for the authors to provide to the reading audience.

[Editor's Note: A DPI calculation and comparison would be relatively straightforward to do, and would take a single paragraph if done concisely in context of a few previous events. It would enrich the paper without a burdensome or bloating amount of text.]

We have added a DPI calculation in the second paragraph of section 5. We chose to place it in context of DPI for other events that impacted the Chicago and Northern Indiana CWAs, which were the two CWAs impacted by the second 30 June 2014 QLCS (see new Table 2).

Section 5a Mesovortex G-1, 2nd paragraph, 3rd sentence. "Careful radar analysis…" should not be used as a factor to determine a tornado. The sampling of base moment radar data from KLOT does NOT support this tornado classification procedure when interpreting velocity bins/gates with a beam width of 0.3 nm (0.5 km) and ≈2800 ft (853 m) ARL. A concern about the reproducibility of identifying tornadoes has yet to be adequately articulated by the authors in their response. "[Also], in the places where radar was weighed a bit more heavily in actually determining the cause of damage, it was most often used to rule out a tornado in areas where we were uncertain of the cause of damage but could not completely rule out an embedded tornado during the damage survey." I want the authors to explicitly address in the paper how their methodology of discerning tornado damage from non-tornado damage may bias their results. More specifically, the authors acknowledge they did not use cross correlation coefficient data but rather used a subjective weighing of base moment data for determining tornado on a few of these cases. How would known radar limitations (i.e., range, beam width, height ARL) potentially affect the results? I contest the base moment data should not be used as a weighing factor due in part to some of these radar range issues. Storm surveys/post-event analysis should be used for this tornado/no-tornado classification.

We understand that Doppler radar cannot directly detect a tornado at any significant range away from the RDA. What we have been trying to communicate here is the detection of these enhanced regions of shear embedded within the broader mesovortices (i.e. at the TVS or "tornado cyclone" scales, not at the tornado scale). We regret that up to this point, our use of radar and the role it played in making a tornado/non-tornado call may not have been explained well. The updated text seeks to provide much more clarity but we also will offer specific details here.

Every tornado track except for G-1 tornadoes 7 and 9 had at least one damage location that was surveyed in one of the two original ground surveys and deemed to be tornadic, based strictly on the evidence at those damage locations (note: we listed tornado 5 in the response to the initial review erroneously as it did have a ground survey point that was originally deemed tornadic). Damage from tornado 7 was seen on the first ground survey while the team was being escorted to a different damage site (the house damaged in tornado 8), but a comprehensive survey of that damage was not performed. For all 12 tornadoes with ground survey points, those points gave us the confidence to declare those tracks tornadic prior to consideration of any radar data based on a preponderance/balance of the damage evidence. For G-1 tornado 9, the track is very clear in the Google Earth satellite imagery (see Appendix A), and thus also was deemed tornadic prior to the consideration of radar data. The primary role of the radar data was twofold: 1) to add further confidence to the tornado/non-tornado declarations, and 2) to boost our confidence in how we connected damage points. This was necessary since inaccessible open fields essentially produced gaps in our knowledge of track evolution, both by eliminating our ability to perform ground surveys in those areas and by producing gaps in the satellite-detected damage paths. This methodology was particularly useful for G-2, which featured several longer-lived tornadoes that spanned multiple 0.5º scans from KLOT.

The only location where we used radar data as a "tipping point" in the analysis for declaring damage tornadic was for the second half of G-1 tornado 13. That portion of Lake County, IN, is extremely open, with even very few tree lines. The few tree lines that do exist in that area were largely decimated by the 4 June 2011 RFD blowdown event that is referenced in Section 6. Without tracing the enhanced shear and spectrum width region within G-1 as it moved from the surveyed damage west of I-65 to the surveyed damage in the far southeastern corner of the county, we would not have been able to connect the damage points to each other. To the west of I-65, the satellite imagery shows a distinct path from the surveyed damage along IN S.R. 55 back into the southeastern corner of the town of Lowell, with a path of damage across several properties. To alleviate the concerns of the reviewer, we have opted to terminate the track of G-1 tornado 13 between IN S.R. 55 and I-65, consistent with the damage we can confidently declare as *tornadic based off of the damage survey and satellite imagery data alone, without assistance from the KLOT radar data.*

To further address the issue of reproducibility, we conducted a more thorough investigation of radar signatures associated with where we found tornado damage relative to the larger mesovortices. That analysis is presented in a later response and within Sections 4 and 5 of the manuscript.

To reiterate one of my points I am trying to convey above—radar information has nothing to do with whether damage is considered straight-line wind or tornadic. In absence of WSR-88D radar information, it doesn't matter. The damage is tornadic or not. A circulation evident in WSR-88D velocity data coupled with a reduction in cross-correlation coefficient is the only radar-based tornado signature that has gained acceptance in the meteorology community. The presence of a radar and radar distance therefore have no causality in the determination of tornado except for the exception articulated above. The authors mention this task of differentiating the cause of the damage is difficult. This is why I want explicit mention in the paper of the uncertainty of classifying weak damage as tornado or nontornado with references.

We have added a thorough discussion about the challenges of determining tornadic vs. nontornadic wind damage to the end of section 4, based on the Forbes and Wakimoto (1983) manuscript, which explicitly details the sources of such challenges.

I ask the Editor to review this impasse, since the authors chose to use a shed and highly exposed tree damage as basis for EF2 and minimally weight damage to structures (i.e., home) tens of feet away. The damage at this property location and other damage locations I have highlighted appears to be overestimated when considering the most likely scenario/reasonably reproducible for assigning peak estimated wind speeds to damage.

[Editor's note: Experienced surveyors of damage do incorporate contextual insights from adjoining DIs and not just rate individual DIs on an island, nor presume multiple or extremely small subvortices without additional/corroborating evidence for them (i.e., photos/video) that's typically not available anyway, and doesn't appear to be here. As such, and at a minimum, the uncertainty of the singular, most-intense DI(s) should be noted in context of weaker adjacent damage. In short, state the case for the rating but clearly articulate the uncertainty thereof.]

As we stated in the previous iteration of this paper, our assessment of the tornado damage ratings was not performed with the DI yielding the highest rating being placed in a vacuum. We explicitly required that the average of the two highest DI/DOD wind estimate values needed to be in the EF2 range for the tornado to be rated EF2. For each DI, we applied the expected value for the wind speed of the damage unless a clear reason to trend to the lower or upper bound was evident (i.e., a tree trunk or power pole was rotted, construction practices were clearly subpar, an outbuilding was structurally dilapidated, etc.).

In the case specifically mentioned above, we did not insinuate that multiple vortices existed in the tornado within this paper, but our underlying hypothesis as to what happened over the property can be summarized as either:

1) *The corner region of the tornado structure itself missed the house and the house was likely in the outer portion of the tornado boundary layer; or*
2) *The house was in the corner region of the tornado, but because the storm-relative left side of the vortex impacted the house, the effects of the tangential component of the wind were largely "cancelled" by the rapid translation of the tornado.*

This assumption was not merely based off the lack of damage to the house but the overall lesser degree of tree damage surrounding it, despite the trees largely being of a similar species to the portion of the tree line behind the house that experienced 100% snapping and flagging of west-facing branches and limbs. Furthermore, the tree falls near and north of the house were almost uniformly north-to-south, as was the corn crop damage immediately across the street from the house. These tree and corn falls were approximately 60° to the right of the estimated motion of the tornado and 90° to the right of the QLCS *motion vector, indicating that the dominant component of damaging wind was the toward the path of the center vortex. This observation from the damage survey is not inconsistent with the idealized translating Burgers-Rott vortex that we showed in the previous review, reposted here with a green box representing the approximate area where the strongest winds that impacted the house would be if our hypothesis were correct. Note again that in this diagram, the center of the tornado would be moving along the thick dashed line.*

Compare the Burgers-Rott vortex model above [in the first review response] to former Fig. 17 below, with the observed debris transport and tree fall directions on and around the property noted with the lavender arrows.

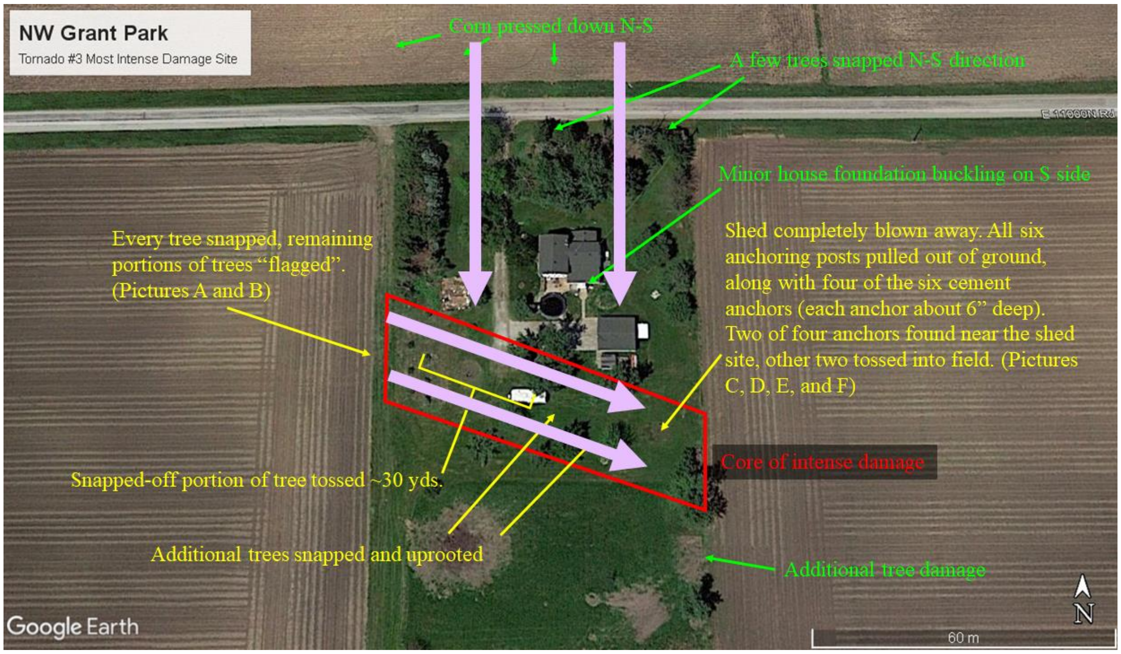

The survey team absolutely took context of the damage at this site (and other surveyed sites) into account when the formulating its conclusions regarding the strength of the damage and how and why damage occurred to some structures and perhaps not to others.

An additional note regarding this location: we did not include discussion of this in the paper, but there was evidence in the corn crop damage across the street and west of the impacted farmstead to indicate that some form of a complex translational or structural evolution actually did occur in this area. Consider the following image taken by the first ground survey team, where a fairly sharp bifurcation in corn fall along a sharply divergent axis was noted, with corn fall on the northwest side of the swath of damage being toward the north and northeast and corn fall on the east side of the swath of corn damage being toward the south. This southward falling corn damage continued eastward along the road to across the street from the farmstead, where a clear cyclonic-convergent damage signature was observed on the property as described above.

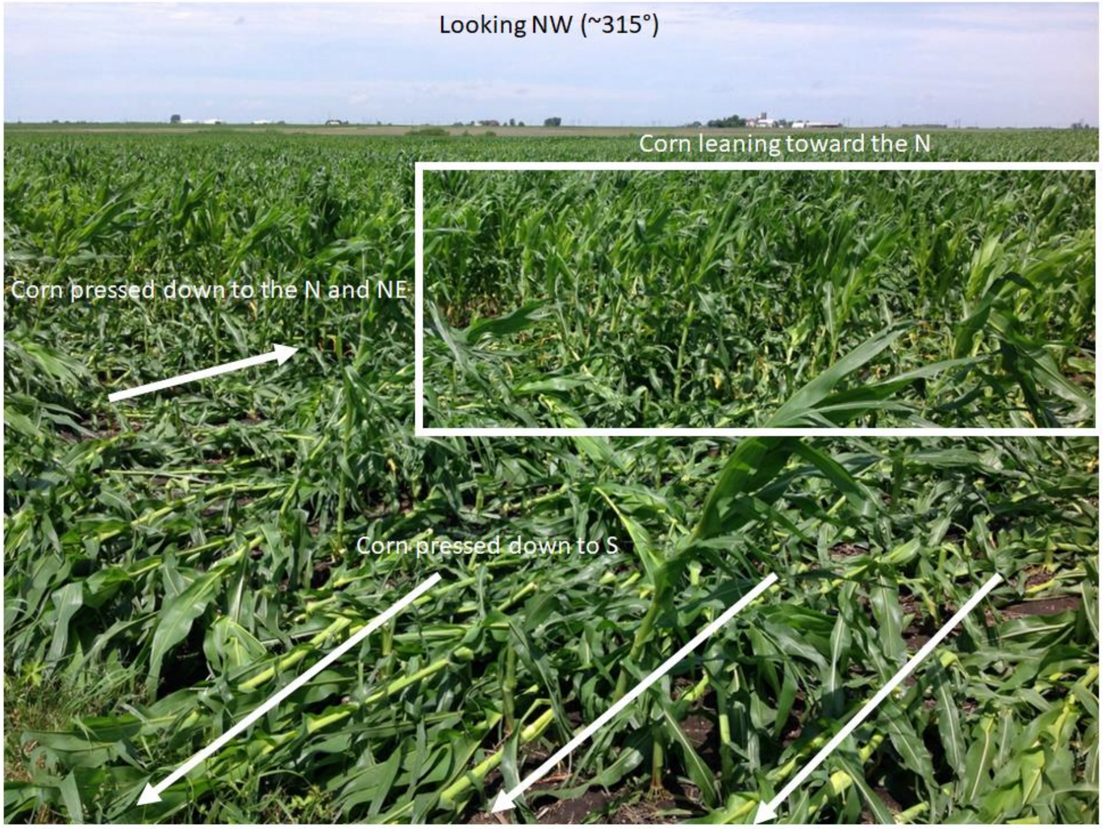

The above image from taken from the point highlighted by the thick red circle on the map from Fig. 9 below:

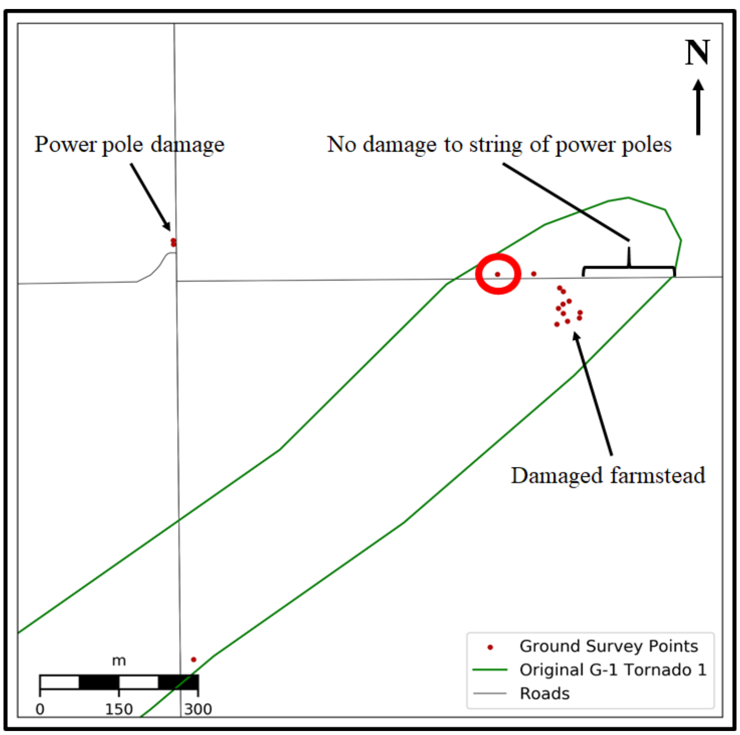

Corn fall did continue west of that point to about the western edge of the red circle. In that vicinity, the corn fall was nearly uniform toward the north until the very western edge of the corn damage, where falls were observed to be toward the northeast, as shown in the picture below.

We did not include analysis of this complex pattern of corn damage along the path of G-1 tornado 3 because we frankly cannot make any conclusive statements about its cause. However, in light of the comment made by the editor, we feel it is important to highlight that we do have evidence and reason to believe that a complex vortex evolution potentially occurred in this area.

With all of the above having been said, we understand the concern of the reviewer that some of the ratings may be, in his opinion, aggressive. It is our opinion, as coauthors, that it is the EF scale itself that largely ties our hands in how the ratings are applied. We know we are not alone in this belief. Grazulis has publicly expressed his concern that the transition to the EF scale has made EF2 ratings climatologically useless (e.g. https://twitter.com/sigtor2019/status/978280158841966592). We believe that many of the tornadoes we assessed as EF2 in this manuscript would not be given F2 ratings in the past, but we also feel bound to the EF scale as it is currently implemented in practice.

However, in our attempt to alleviate at least some of the reviewer's concerns about the ratings, we did decide to employ one further refining step to our final assignment of EF ratings in this revised version of the manuscript. In this, we round the maximum estimated 3-s gust to the nearest 5-mph (2.6-m s^{-1}) increment. This both serves to alleviate some of our trepidation about including our estimate of the maximum gust in the paper but also allows us a concrete, objective, reproducible reason to "downgrade" the two most marginal EF2-rated tornadoes (G-1 tornado 3 and G-2 tornado 3) to 110 mph (49 m s^{-1}) EF1, since both were listed with maximum winds of 111 mph (50 m s^{-1}). This adjustment also led to the downgrading of an EF1 tornado (G-1 tornado 7) to EF0 (leading to three total EF0s, since two tornadoes were rated EF0 in earlier drafts) and downward adjustments to the maximum wind gust estimates for several additional tornadoes, even if the EF ratings did not change. Furthermore, upon the reasoning presented by the reviewer as to why G-1 tornado 8 should be downgraded (presented later in this review), we have opted to shift the DOD for the house roof damage that gave the tornado an EF2 rating from its expected value to its lower-bound value, which leads to G-1 tornado 8 also being downgraded to a 110 mph (49 m s^{-1}) EF1.

These changes leave G-1 tornadoes 6 and 13 as the remaining EF2s in this reanalysis. We firmly believe that damage associated with both tornadoes was of EF2 intensity. Tornado 6 featured multiple instances of

EF2 damage, including the three-story barn that was destroyed, the house that was twisted on its foundation and had to be rebuilt, and a church that was also torqued on its foundation. Furthermore, contextual evidence along the path, including the severity of some of the hardwood tree damage observed both on the ground in aerial imagery, allows us to comfortably apply the EF2 rating to this tornado. Tornado 13's EF2 rating is maintained as we are leaving the snapped high-tension wooden power poles in the core damage track at the expected value of 118 mph (53 m s^{-1}). When averaged with snapped hardwood trees evident on satellite imagery (110 mph, 49 m s^{-1}), the wind speed estimate [rounds to] 115 mph (51-m s^{-1}) EF2.

One additional addition to the revised text is a reference to a paper published by the reviewer which supports the plausibility of EF2 tornadoes based on the very favorable environmental conditions present on the evening of 30 June 2014.

There is no radar data or numerical simulations the authors presented to support the idea of tornadogenesis at the rear of a mesovortex. KLOT WSR-88D imagery does not suffice. *"The proposed conceptual model is simply that: a proposal requiring further examination. Modeling studies certainly would shed light on the veracity of this proposal and therefore are encouraged, but are beyond the scope of this paper."* Proposing an idea is not in of itself unscientific. However, introducing a theory or conceptual model on mesovortex tornadogenesis does *require* some burden of supporting evidence. Because the radar data is unequivocally insufficient to support the proposed theory, providing some form of numerical simulation work is necessary, but the authors so far have declined. This lack of supporting evidence is my #1 concern. "We propose them forming in the back of the mesovortices and revolving counterclockwise until dissipation on the right side." Why would the tornadoes dissipate on the right side of the mesovortex and not continue to rotate cyclonically through the mesovortex to the front of the parent mesovortex? There is essentially no explanation offered.

We have removed the conceptual model section (section 7) and all references to the conceptual model in the paper. We have amended our focus in the operational considerations discussion to the development of numerous tornadoes in close proximity to each other within a single large mesovortex where we previously had discussed the conceptual model. Such cases are hardly unprecedented (one particularly similar case was observed in east-central Wisconsin on 28 August 2018: https://www.weather.gov/mkx/aug2818).

"We strongly disagree with this assertion…determine the cause of damage": I can't fundamentally disagree more. The consequences of confirmation bias (e.g., tornado warning issued, etc…), and the nonuniformity of the WSR-88D network's sampling of shallow mesovortices, to directly classify damage are immense and very troubling. Yes, I agree radar data can be used to help locate possible areas of damage and provide information to gain understanding of possible mechanisms or phenomena that led to the damage. Just like mesocyclones being capable of RFD-related straight-line wind damage, mesovortices and the RIJ surges on the south side of a mesovortex are capable of straight-line wind damage. It is my understanding based on the manuscript's language that the methods utilized to classify tornadoes used base-moment radar data to classify tornadoes, in addition to the ground survey/satellite data. And little to no description of uncertainty was articulated about the classification process or references provided to give the reader a measure of "gray area" associated with classification of weak EF-scale damage. Hence, "Other than dual-pol tornadic debris signature, radar should have *no* influence on the classification of a tornado. This can only be done *directly* via a post-event damage survey."

As we have stated in a previous response in this round of reviews, all but two of the tornadoes consisted of damage that was already declared tornadic during the first two ground surveys. Of the two remaining tornadoes, G-1 tornado 7 had damage witnessed but not thoroughly surveyed during the first ground survey, and G-1 tornado 9 was a clear, narrow track of damage resolved in satellite imagery. The tornado/nontornado calls made by the ground survey teams were based on the damage observed being cyclonic or convergent in tree fall or debris dispersal, having sharp gradients in inferred wind speeds through the damage patterns observed, and by having large length:width aspect ratio. The errors in the original survey results described in Section 3 resulted from a lack of information from areas that were either not assessed or were feasibly inaccessible during the ground survey process.

In order to address the uncertainty, we have added a new paragraph to Section 6 addressing the difficulty that can be faced in determining tornadic vs. nontornadic damage at low EF-ratings. This paragraph cites Forbes and Wakimoto (1983) which explicitly discusses this topic.

"While radar alone absolutely cannot be used to definitively determine the presence of a tornado without a TDS being present," Good! This clarifies the paper and I strongly urge the authors to include portions of the statements (see below) in the paper and articulate the message that radar data can't be used to determine tornado or wind damage (exception being a TDS). Radar data can only assist the damage classification process because the presence of a radar-resolvable mesovortex can result in straight-line wind damage or tornado.

We absolutely do not dispute this point. We never have intended to suggest that tornadoes are being directly detected by radar. We never used radar data as the sole source of declaring a tornado (i.e., without any evidence of damage witnessed in ground surveys, the aerial survey, or in satellite imagery). We have added some clarifying language across sections 4 and 5 that should serve to better explain exactly the role that radar data played in this analysis.

[Re: "We would like additional details on how the reviewer came to this conclusion."]
The roof is largely intact. The exposed gable did not subsequently cause the roof to blow away. OSB board is the exterior wall with weathering plastic on top and the wall did not fail, despite the lack of an exterior facade such as brick. There are a couple of heavily damaged trees but others immediately adjacent do not exhibit much damage. Again, I think there are a large number of sites through the paper that have been incorrectly rated on the EF-scale and assigned aggressive wind speed estimates.

We find the reviewer's assessment to be reasonable. Therefore, in this revision, we have amended the house DI to the lower bound of DI 1, DOD 4, which lowers the maximum damage rating of the tornado to a 110-mph (49 m s^{-1}) EF1 based off of snapping of numerous healthy hardwood and softwood trees along the track.

[Minor comments omitted...]

Third Review:

Reviewer recommendation: Revisions required.

General Comments: I request the Editor provide additional constructive criticism here forward. It is my opinion quite a few of the images and tables can be removed to help make the paper more concise. I think the paper has been improved because the authors have lowered an appreciable number of tornado EF-ratings, removed their proposed conceptual model, explicitly included potential sources of error or provided descriptions of uncertainty, and related this weak tornado cluster to a metric like DPI. Accept with major revisions is my final review assessment.

I think the burden of proof is still on the authors to convince the reading audience all or a large fraction of these "tornadoes" are in fact tornadoes and not squall line gust front eddies not typically considered tornadic but rather amplified speeds within the squall line gust front from a small-scale vortex not connected to cloud base. This study is eerily reminiscent of a central IA-based study's assertion/claim of several dozen tornadoes because of documented narrow paths of damage. Ultimately, it is a taxonomic exercise and "What is a tornado?" probably needs to be revisited in literature, to distinguish some of the tornado events in this study from more accepted QLCS tornado definitions/events. Obviously this is beyond the scope of a review and I invite the authors or the reading audience to pursue this work.

[Editor's note: I agree with the reviewer that a) the authors can cut a few figures, b) soften some overly certain language in the disputed cases, and c) the "taxonomic exercise" of defining QLCS tornadoes is beyond the scope of this case study. As such, in my letter to the authors, I have recommended (a) and (b), though they appear to me more "minor" than "major" changes.]

We have removed Figs. 4 (the composite sounding), 5, 11, and 19 from this draft, as well as Table 1, which featured specific variable values from the composite sounding. To further address taxonomic uncertainty, particularly in consideration of future potential work in defining QLCS tornadoes, the following footnote has been added near the beginning of Section 5 (the primary reanalysis summary section): "As stated previously, damage was declared tornadic in nature if the preponderance of the survey evidence supported a concentrated vortex of ≥EF0 damage intensity, including tree fall direction and debris dispersal, length-to-width aspect ratio, and eyewitness reports of pressure changes and/or very short damaging wind duration.

Furthermore, evidence of concentrated, enhanced azimuthal shear from the KLOT radar in close proximity to the damage was used to further bolster identification of a damage swath as being tornadic. Significant debate does exist in the meteorological community regarding the taxonomy of QLCS-generated vortices, and it is acknowledged that future definitions may exclude some of these tornadoes." Attempting to differentiate between "tornadoes" and "possible" tornadoes beyond this would risk evolving into an even more speculative/subjective exercise and strongly complicate presentation of these findings. Given that the gust front remained closely tied to the primary convective band through the duration of the lifespan of damage production during the second QLCS and the association of the damage tracks with radar-identifiable areas of shear/rotation, the likelihood of these circulations being "gust front eddies" or gustnadoes that we do agree would not be considered tornadic seems less than the likelihood that these vortices would qualify under the current definition of a tornado.

Major Comments: I've given more thought regarding the representativeness of this composite sounding approach and it is a misapplication of a proximity sounding. Please remove this sounding as it is argumentative at best and provides too much hand-waving to describe the vertical structure of the atmosphere at the tornado location. The authors are welcome to discuss details of the AMDAR sounding or ILX RAOB to try and relate some things in a general sense but this information is not acceptable in present form nor is Table 1. In the last paragraph of section 2, remove "extremely conducive" to tornadoes and instead mention "supportive of tornadoes and damaging gusts".

We have removed the composite sounding and softened the language away from "extremely conducive" to simply "conducive".

Your confidence [in crop type and damage intensity at original Fig. 5 damage site] is misplaced… If the authors are so adamant about their claim, I ask the Editor to examine this information independently. I included examples to illustrate the incorrect labeling of figures in previous versions of the paper and to provide another example of the over-estimation of wind speeds assigned damage. I am satisfied with the authors' removal of the image with annotated graphic and how the material is currently presented. …

If the authors determined there were two tornadoes that resulted in damage in the figure below, I'll defer to the authors on this assertion (current Fig. 18). Originally the only information provided in the paper was the "original" tornado isopleth included both the damage from the house at the north part of the figure to the grain silos on the southeast. Presented with this evidence, I was highly skeptical. Please reference previous correspondence between the authors and reviewer regarding the vegetation discrepancy and the wind speed assigned to broken power poles and how this was communicated to the authors in terms of attempting to communicate a high damage estimate bias and inconsistency with classification of tornado damage. The notion of one of the tornadoes only having two damage points with the beginning point being a snapped power pole with it "pointing" to the west or southwest and the end point being minor crop damage a considerable distance away is one more example.

References to the crop type of the damage observed at this disputed location were already removed from the body text in the previous round of revisions, and the one remaining reference to corn damage that had been described for tornado 13 in Appendix A has been generalized to crop damage.

[Minor comments omitted...]

REVIEWER C (Ian M. Giammanco):

Initial Review:

Recommendation: Revisions required.

General Comments: The paper represents a very detailed look back at an extremely complex damaging QLCS wind event, with a variety of features causing the observed damage. It does call into question the results of the operational National Weather Service damage survey and the associated *Storm Data* reports. It is clear the authors paid close attention to detail in a painstaking re-analysis. The work also highlights the difficulty in assessing wind damage mode and the need for improved damage assessment methods and multidisciplinary research to begin to solve the complexities of convectively-driven high wind events. In general, the manuscript is reasonably constructed; however, there are a few general issues that would improve readability, improve its clarity, and illustrate how complex these types of events are.

We thank the reviewer for his thorough and thoughtful review and hope that our responses address the reviewer's concerns.

Substantive Comments: The authors reference the Lyza et al. (2017) paper regarding this event and make assumptions that the reader is well versed in this paper. Given that it is not a true companion paper (i.e. Part I and II), the authors should provide a little more of the background details understanding that it could be repetitive between the two papers but help the readability and understanding of the event. On this note, a radar composite figure showing the evolution of the QLCS features would help greatly in understanding how this event unfolded.

We've added a new Section 2 to describe the background environment and overall QLCS evolution.

A larger question that is worth discussing is the issue of scales of features. The definition of what a "mesovortex" is in this context is not stated clearly. While we can assume it is an embedded feature within the QLCS, some distinction should be made to help with readability. The goal would be to distinguish these features from persistent supercell structures, especially for the two features of interest (G-1 and G-2). Readability in this manuscript is very important since it was such a complicated event.

In keeping with Lyza et al. (2017), we refer to G-1 and G-2 as mesovortices in order to maintain consistency with past work on these leading-edge circulations in QLCSs. G-1 may have attained supercellular characteristics. Lyza et al. (2017) shows the maximum depth of G-1 reaching 8.8 km ARL. G-2 only reached a depth of 3.6 km ARL. However, given that we are cognizant of the open debate regarding the existence of embedded supercells within QLCSs, we wish to not use this paper to open that debate and risk having it overshadow the important findings we are trying to convey from this event.

In general, the tracks of the identified features follow the mean propagation of the overall QLCS, is this common? Which it may be for tornado-producing QLCS features… A better radar-overview would be useful in showing the reader what this event looked like without having to return to the author's 2017 paper.

We have moved the three-panel radar overview of the entire double derecho evolution from Lyza et al. (2017) and added it here as Fig. 2, and we have also created a more zoomed-in loop of the second QLCS moving over the Kankakee Valley with the new tornado tracks overlaid (Fig. 13).

<u>Wind-damage commentary:</u> Given the gradients of damage discussed in the manuscript it is worth mentioning (while not in peer-review literature), full-scale testing at the Insurance Institute for Business & Home Safety of two identical residential structures under identical wind loading conditions produced two vastly different damage modes when the structure was internally pressurized (i.e. building envelope compromised): 1) Full roof system failure; 2) Garage door—exterior wall failure. While every attempt was made to ensure the two structures were constructed identically, even subtle differences can change the damage mode and potentially the degree of damage with no difference in the wind loads. This does call

into question the immediate assumption regarding gradients in damage. It is a true blend of both the physical phenomenon and these differences in building characteristics. This sentiment needs to be captured and is unfortunately excluded in many atmospheric science-centric papers. I would encourage the authors to include some of this discussion and to explore work in the Journal of Wind Engineering and Industrial Aerodynamics and Journal of Wind and Structures.

We are sympathetic to the point the reviewer makes above. We do make an attempt to address the nature of the damage gradient with the new tornado 3 of G-1. In that case, the assessment of the gradient of the wind speed across the property was largely based off how trees of same or similar species were impacted as the tornado moved across the property. We acknowledge that tree reaction can also very easily vary from tree to tree in a small area. In this particular case, the gradient in tree damage seemed rather dramatic across the property, going from partial snapping and snapping of large limbs at the northern end to snapping of all trees and flagging of westward-facing limbs at the southern end of the property, just west of where the shed was destroyed. Beyond this, we are hesitant to dive deeper into this subject in this paper. While we do reassess the ratings of several damage locations in this paper, it is not intended to be the primary focus of the paper. The primary [foci] of the paper are on how these tornadoes evolved within the mesovortices, how Google Earth satellite data was useful in identifying something closer to the truth of how the tornadoes evolved, how radar might be useful in identifying a prolifically tornadic mesovortex like these, and what operational lessons can be learned from this event.

In examining a conceptual model, the authors failed to recognize the work included of Shenkman et al. (2012; JAS) which models some of the features that are described here. The authors should also consider applying similar terminology to that used in the Shenkman et al. model-based study. This work was successful in simulating a dominant mesovortex feature with attendant vorticity couplets extending further southward along the leading edge of the reflectivity gradient/outflow/cold pool. I struggle to see the true value in relating the features described here to a mature 3 May 1999 tornado case. The authors should answer the following questions: 1) Is the observation of these features true vortex breakdown? 2) Is it provable? 3) Is this comparison of different scales suitable? 4) is it useful? The structure shown mimics more of what is described in the Shenkman paper.

We have removed the comparison to the multiple-vortex tornado structure that was previously included in this manuscript, primarily in response to question (2). With the dataset we have, this comparison was far too overly speculative to include in this paper, in retrospect. In reviewing the Schenkman et al. paper, we agree that this case may represent a more prolific example of their conceptual model and have added mention of the similarity to this section.

[Minor comments omitted...]

Second Review:

Reviewer recommendation: Accept with minor revisions.

General comment: The authors have completed the necessary revision requested and this reviewer commends them for making the manuscript easier to follow for such a complex case. The following are only minor wording suggestions and can be used or not.

[Minor comments omitted...]